

Symmetry-enforced Moiré Topology

Yunzhe Liu,¹ Kaijie Yang,² Chao-Xing Liu,^{1,*} and Jiabin Yu^{3,4,†}

¹*Department of Physics, The Pennsylvania State University, University Park, Pennsylvania 16802, USA*

²*Department of Materials Science and Engineering,*

University of Washington, Seattle, Washington 98195, USA

³*Department of Physics, University of Florida, Gainesville, FL, USA*

⁴*Quantum Theory Project, University of Florida, Gainesville, FL, USA*

(Dated: September 9, 2025)

Topological flat bands in two-dimensional (2D) moiré materials have emerged as promising platforms for exploring the interplay between topology and correlation effects. However, realistic calculations of moiré band topology using density functional theory (DFT) are computationally inefficient due to the large number of atoms in a single moiré unit cell. In this work, we propose a systematic scheme to predict the topology of moiré bands from atomic symmetry data and moiré symmetry group, both of which can be efficiently extracted from DFT. Specifically, for Γ -valley electron gases, we find that certain combinations of atomic symmetry data and moiré symmetry groups can enforce nontrivial band topology in the low-energy moiré bands, as long as the moiré band gap is smaller than the atomic band splitting at the moiré Brillouin zone boundary. This symmetry-enforced nontrivial moiré topology, including both topological insulators and topological semimetals, is robust against various material-specific details such as the precise form and strength of the moiré potential or the exact twist angle. By exhaustively scanning all 2D atomic symmetry data and moiré symmetry groups, we identify 197 combinations that can yield symmetry-enforced nontrivial moiré topology, and we verify one such combination using a moiré model with cubic Rashba spin-orbit coupling. Our approach is generalizable to other valleys and provides a useful guideline for experimental efforts to discover and design new topologically nontrivial moiré materials.

I. INTRODUCTION

Moiré materials [1, 2] have emerged as one of the most important platforms for exploring exotic strongly correlated physics, primarily because they host energy bands that are (nearly) flat and topological. The most recent prominent example is twisted bilayer MoTe_2 , which has been extensively studied both experimentally [3–17] and theoretically [18–58], where the flat bands with nonzero Chern numbers give rise to fractional Chern insulators [59–63] at fractional fillings. The small bandwidth of the moiré bands in moiré materials naturally arises from the large moiré unit cell, which folds the non-moiré bands (*i.e.*, atomic bands) hundreds of times, leading to energy bands that have bandwidths much smaller than their non-moiré counterparts. However, the nontrivial topology of the flat bands is not necessarily guaranteed. There is one known example of enforcing the nontrivial topology of the low-energy moiré bands based on the non-moiré band topology—twisted bilayer graphene (and related graphene-based systems) [1, 2, 64–70]. Yet, this case is quite special: one needs *both* the $C_2\mathcal{T}$ symmetry (*i.e.*, combination of two-fold rotation C_2 and time reversal (TR) symmetry \mathcal{T}) and an effective normal-state particle-hole symmetry [69], which, especially the latter, are not common beyond graphene-based systems. Indeed, the nontrivial topology of the flat bands in twisted bilayer MoTe_2 is not guaranteed—the Chern numbers of

the bands are sensitive to material parameters such as twisted angles [39, 42, 47, 55].

It would be transformative to develop general principles that can guarantee the nontrivial topology of Moiré flat bands based on ubiquitous symmetries, such as crystalline and TR symmetries. The reason is summarized in Fig. 1 and elaborated in the following. Given a realistic moiré system formed by 2D non-moiré layered materials, it is extremely time consuming to directly calculate the moiré bands and their band topology (the red box in Fig. 1), especially when the moiré unit cell becomes very large, *e.g.* twist bilayer MoTe_2 with a twist angle smaller than 2° . On the other hand, it is highly efficient to know the symmetry group (crystalline and TR) and symmetry representations of the non-moiré layered materials at high-symmetry momenta (which together we refer to as atomic symmetry data), and it takes no time to know the symmetry group of the moiré system (which we refer to as moiré symmetry group), as depicted by the green boxes in Fig. 1. Therefore, the principles that can derive moiré topology from atomic symmetry data and moiré symmetry group can dramatically advance our ability of numerically predicting new topological moiré platforms. They are also crucial for experimental studies, as those principles should be robust against sizable variations in material parameters that are often difficult to control in practice—such as the twist angle and moiré potential/tunneling strength.

In this work, we successfully establish such a principle. Specifically, for Γ -valley electron gas subject to weak moiré potential, we find that certain combinations of atomic symmetry group, atomic symmetry represen-

* cxl56@psu.edu

† yujiabin@ufl.edu

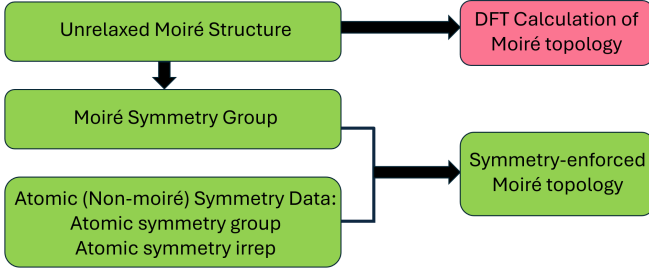


FIG. 1. **Theoretical Approaches to Identify Moiré Topology.** All green blocks are easily computationally accessible, while the red block is computationally inefficient. Our work provides an efficient way to indicate moiré topology from the moiré symmetry group and atomic symmetry data.

tation at Γ and moiré symmetry group can enforce nontrivial topology of the low-energy moiré bands, where nontrivial topology includes both topological insulator and topological semi-metal phases. Here the low-energy moiré bands refer to the moiré bands that are closest to the charge neutrality, *i.e.*, conduction bottom bands or valence top bands. We refer to such enforced nontrivial topology as symmetry-enforced moiré topology. Weak moiré potential means that the strength of the moiré potential is weaker than the atomic band splitting, which is a realistic condition at Γ valley satisfied by known examples such as twisted bilayer MoTe_2 , as discussed in Sec. V. In other words, for those combinations of atomic symmetry data and moiré symmetry group, the phase diagram of the low-energy bands of the moiré model only includes topological insulator and semi-metal phases—no topologically trivial phases. By systematically analyzing all possible combinations, we identify 197 combinations that can lead to symmetry-enforced nontrivial moiré topology, with 16 of them for the topological insulating phase in the phase diagram. The general principle is explicitly verified in a moiré model with cubic Rashba spin-orbit coupling (SOC). Clearly, our principle does not rely on precisely-tuned values of moiré parameters such as twist angle and moiré potential strength. It is also independent of the form of moiré potential, in contrast to Refs.[71, 72].

We note that the moiré topological semi-metal phases may also be a fertile ground for exotic strongly-correlated phases. It is because electron-electron interactions may open a gap between topological metallic bands and drive the system into topologically ordered states. A closely related example is the emergence of fractional Chern insulators in multilayer rhombohedral graphene/hexagonal boron nitride (hBN) heterostructures at various electron fillings [73–83], where the moiré bands are nearly gapless at the single-particle level [71, 84–104].

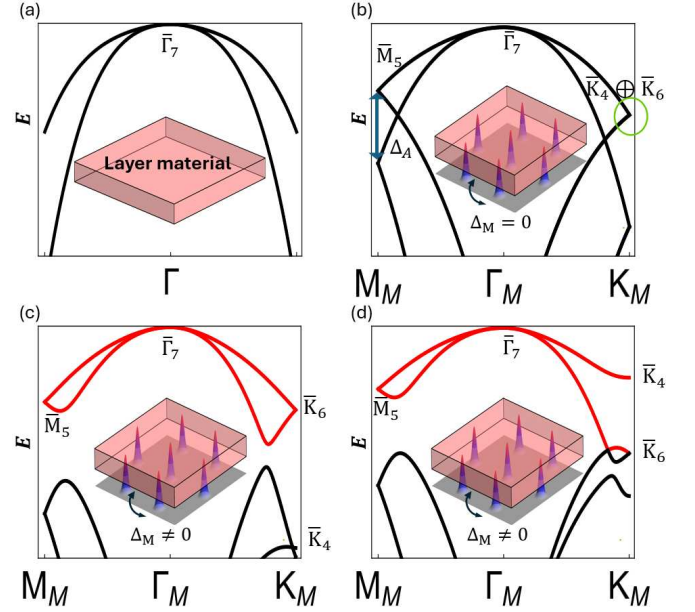


FIG. 2. **Schematics of Symmetry-Enforced Moiré Topology.** (a) The band structure around Γ point of a pristine layered material with point group C_{6v} . The low-energy band at Γ is described by the 2D $\bar{\Gamma}_7$ irrep. (b) Band folding at zero moiré potential. At K_M , the folded bands form a three-dimensional representation $\bar{K}_4 \oplus \bar{K}_6$, while at M_M they form a two-dimensional irrep \bar{M}_5 . Δ_A marks the energy scale of the atomic band splitting at the mBZ boundary. (c) One possible moiré band structure in the presence of weak moiré potential, *i.e.*, the energy splitting generated by Δ_M is smaller than Δ_A . Here the top two bands (red) carry the \bar{K}_6 irrep, while the third top band has the \bar{K}_4 irrep, resulting in nontrivial topology in the isolated top two bands. (d) The other possible moiré band structure in the presence of weak moiré potential. The \bar{K}_4 band has higher energy than the two \bar{K}_6 bands, resulting in a topological semi-metallic phase for the red bands due to the unavoidable touching between the second and third top bands at K_M .

II. ILLUSTRATION OF PRINCIPLE

We will first use a specific set of atomic symmetry data and moiré symmetry group to illustrate the underlying principle. Let us consider spin-orbit-coupled electrons around Γ point of a non-moiré layered material. Suppose the electrons carry total out-of-plane angular momentum $J_z = \pm 3/2$, and have the point group C_{6v} and TR symmetry. $J_z = \pm 3/2$ can be generated by the addition of atomic orbitals (p , d or higher) and electron spin. The C_{6v} group is generated by a six-fold rotation along the out-of-plane direction and a mirror reflection about the y -axis (M_y). Owing to the angular momentum, the electrons at Γ form a doublet, furnishing $\bar{\Gamma}_7$ irreducible representation (irrep) of C_{6v} . Without loss of generality, we choose both bands to bend downward, and the two bands naturally get split by the SOC away from Γ , as shown in Fig. 2(a).

Now we introduce the moiré potential that preserves

the point group C_{6v} and TR symmetry. In addition, the moiré potential would introduce the discrete moiré translation symmetry, leading to a plane group $P6mm$. In order to understand the generation of the moiré bands, let us first consider an artificial limit where the moiré potential strength Δ_M vanishes. In this case, the moiré bands simply come from the artificial band folding of the Γ -valley atomic bands (Fig. 2(a)) into the moiré Brillouin zone (mBZ), as shown in Fig. 2(b). The $\bar{\Gamma}_7$ irrep survives under the band folding and stays at the moiré Γ_M point, while the band folding generates a Kramers' pair among the top two bands at the M_M point, furnishing \bar{M}_5 irrep. Most importantly, the band folding gives rise to three accidentally degenerate states at K_M point. The degeneracy is accidental because they can be split into a one-dimensional (1D) irrep \bar{K}_4 and a two-dimensional (2D) irrep \bar{K}_6 according to the moiré symmetry group discussed below.

Now we resume the nonzero moiré strength Δ_M . We consider the weak moiré region where the energy splitting induced by the moiré potential is smaller than the atomic band splitting (Δ_A) at the mBZ boundary. The moiré potential will leave the $\bar{\Gamma}_7$ irrep at Γ_M and the \bar{M}_5 irrep at M_M intact, as protected by symmetry. Nevertheless, the moiré potential will split the \bar{K}_4 and \bar{K}_6 bands at K_M . Focusing on the top two bands, there are two possibilities. One is that the top two bands carry the 2D \bar{K}_6 irrep, and the third band possesses the \bar{K}_4 irrep, resulting in the top two bands being isolated (Fig. 2(c)). In this case, the top two bands have nontrivial topology as the irreps $\bar{\Gamma}_7$, \bar{M}_5 and \bar{K}_6 can never appear simultaneously for an isolated set of trivial bands according to topological quantum chemistry [105–107] and symmetry indicator theory [108–113]. The other possibility is that the top two bands are from one 1D \bar{K}_4 irrep and one component of the 2D \bar{K}_6 irrep. In this case, the top second band definitely touches the third band as they together form the \bar{K}_6 irrep at K_M . Therefore, regardless of which possibility, the low-energy moiré bands are either topologically insulating or topologically semi-metallic. Such nontrivial moiré topology is enforced by the atomic symmetry data and moiré symmetry group, as long as the moiré potential is weak compared to atomic band splitting.

III. MOIRÉ CUBIC RASHBA MODEL

We now use an specific example to verify the principle. We consider a model Hamiltonian describing a spin-orbit-coupled 2D electron gas around Γ point subject to a moiré superlattice potential. As discussed in Sec. II, we impose the point group C_{6v} and TR symmetry, and consider $J_z = \pm 3/2$ doublet at Γ . Then, the atomic part of the Hamiltonian up to the fourth order of the momentum

\mathbf{k} has the following general form

$$\hat{H}^A = \sum_{\mathbf{k}n\mathbf{m}} c_{n\mathbf{k}}^\dagger [H^A(\mathbf{k})]_{nm} c_{m\mathbf{k}},$$

$$H^A(\mathbf{k}) = \begin{pmatrix} \alpha k^2 + \beta k^4 & iR_3 k_-^3 \\ -iR_3 k_+^3 & \alpha k^2 + \beta k^4 \end{pmatrix}. \quad (1)$$

where $c_{n\mathbf{k}}$ is the fermion annihilation operator with $n = 1, 2$ indexing $J_z = \pm 3/2$. To ensure that both bands of \hat{H}^A bend down, we choose both α and β to be negative in the kinetic term $\alpha k^2 + \beta k^4$, where the k^4 term is necessary due to the cubic Rashba SOC term, *i.e.*, the R_3 term in Eq. (1).

We consider the moiré superlattice potential on a hexagonal moiré lattice, which reads

$$\hat{H}_M = \sum_{\alpha=1,2} \int d^2r c_{n\mathbf{r}}^\dagger H_M(\mathbf{r}) c_{n\mathbf{r}}, \quad (2)$$

with $c_{n\mathbf{r}} = \frac{1}{\sqrt{V}} \int_{\mathbb{R}^2} d^2k c_{n\mathbf{k}} e^{i\mathbf{k}\cdot\mathbf{r}}$ and V the system area. We include both the first and second harmonic moiré superlattice potential, namely, $H_M(\mathbf{r}) = \sum_{\mathbf{g} \in \mathbf{G}_M^1} \Delta_1 e^{i\mathbf{g}\cdot\mathbf{r}} + \sum_{\mathbf{g} \in \mathbf{G}_M^2} \Delta_2 e^{i\mathbf{g}\cdot\mathbf{r}}$, where \mathbf{G}_M^1 consists of \mathbf{b}_1^M and its partners under six-fold rotation symmetries, \mathbf{G}_M^2 consists of $\mathbf{b}_1^M + \mathbf{b}_2^M$ and its partners under six-fold rotation symmetries. $\mathbf{b}_1^M = 2\pi(1, -1/\sqrt{3})/a_M$ and $\mathbf{b}_2^M = 2\pi(1, 1/\sqrt{3})/a_M$ are primitive reciprocal lattice vectors, and a_M is the moiré lattice constant. The moiré potential in Eq. (2) has plane group $P6mm$, generated by the point group C_{6v} and the moiré lattice translation symmetry, and also preserves the TR symmetry. Those symmetries are preserved even after we incorporate the atomic Hamiltonian in Eq. (1), resulting in the total Hamiltonian

$$\hat{H} = \hat{H}^A + \hat{H}_M. \quad (3)$$

To illustrate our principle, we focus on the weak moiré region, where the moiré gap is smaller than the band splitting caused by Rashba SOC. By choosing reasonable parameter values (listed in supplementary material (SM) Sec.C1 [114].), we obtain the phase diagram as a function of Δ_1 and Δ_2 in Fig. 3(a). The color represents the direct band gap E_Δ between the second and third topmost moiré bands (see Fig. 3(b)) and the red dashed line separates the insulating region from the semi-metallic region for the top two moiré bands. (See more details in SM Sec.C1 [114].) We find that regardless of the value of the moiré parameter values, there are only two phases for the low-energy physics: (i) topological insulator phase where the top two bands are isolated with band irreps ($\bar{\Gamma}_7$, \bar{M}_5 , \bar{K}_6) and have $\mathbb{Z}_2 = 1$ in Fig. 3(b), and (ii) topological semi-metal phase where the top two bands are enforced to be connected to other bands in Fig. 3(c) as the irrep \bar{K}_4 for the topmost band is 1D, while \bar{M}_5 and $\bar{\Gamma}_7$ irreps are 2D. This is consistent with the principle that we discussed in Sec. II.

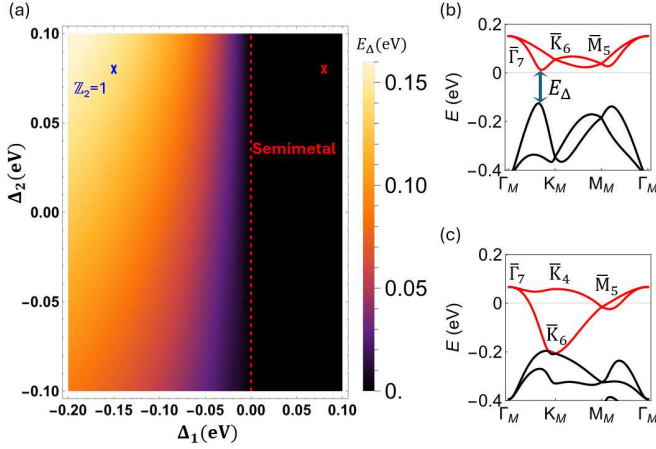


FIG. 3. **Cubic Rashba SOC model under moiré potential.** (a) Phase diagram of the topmost two bands of the moiré cubic Rashba model in Eq. (3). E_Δ denotes the band gap between the second and third topmost bands. The red dashed lines separate the insulator region and semimetal region. (b) The band dispersion and band irreps computed with the parameters labeled by the blue cross point in (a). The top two bands have $\mathbb{Z}_2 = 1$. (c) The band dispersion and band irreps computed with the parameters labeled by the red cross point in (a). The top two bands are connected to the top third band.

$G_0 \backslash G_0^A$	C_{6v}	C_{3v}	C_6	C_3	C_{4v}	C_{2v}	C_s
$P6mm$	$\bar{\Gamma}_7$						
$P3m1$	$\bar{\Gamma}_7$	$\bar{\Gamma}_4 \bar{\Gamma}_5$					
$P31m$	$\bar{\Gamma}_7$	$\bar{\Gamma}_4 \bar{\Gamma}_5$					
$P6$	$\bar{\Gamma}_7$		$\bar{\Gamma}_7 \bar{\Gamma}_8$				
$P3$	$\bar{\Gamma}_7$	$\bar{\Gamma}_4 \bar{\Gamma}_5$	$\bar{\Gamma}_7 \bar{\Gamma}_8$	$\bar{\Gamma}_4 \bar{\Gamma}_4$			
$P4bm$					$\bar{\Gamma}_6, \bar{\Gamma}_7$		
$Pba2$	$\bar{\Gamma}_7, \bar{\Gamma}_8, \bar{\Gamma}_9$				$\bar{\Gamma}_6, \bar{\Gamma}_7$	$\bar{\Gamma}_5$	
$Pma2$	$\bar{\Gamma}_7, \bar{\Gamma}_8, \bar{\Gamma}_9$				$\bar{\Gamma}_6, \bar{\Gamma}_7$	$\bar{\Gamma}_5$	
$Pb11$	$\bar{\Gamma}_7, \bar{\Gamma}_8, \bar{\Gamma}_9$	$\bar{\Gamma}_4 \bar{\Gamma}_5, \bar{\Gamma}_6$			$\bar{\Gamma}_6, \bar{\Gamma}_7$	$\bar{\Gamma}_5$	$\bar{\Gamma}_3 \bar{\Gamma}_4$

TABLE I. **Spinful TR-invariant Cases for Symmetry-enforced Moiré Topology.** List of combinations of atomic point group G_0^A , atomic Γ irrep, and moiré plane group G_0 that lead to symmetry-enforced nontrivial moiré topology, in the presence of both TR symmetry and SOC. For a given G_0^A and G_0 , the table entry indicates the required atomic Γ irrep to give symmetry-enforced topology. The irrep is highlighted by the red means the low-energy bands can be topological insulating.

IV. SYMMETRY-ENFORCED MOIRÉ TOPOLOGY IN 2D PLANE GROUP

The symmetry-enforced moiré topology is not limited to the symmetry data discussed in Sec. II. In this section, we will show that there are many other cases where nontrivial moiré topology can be enforced by the atomic symmetry data and the moiré symmetry group. We still

focus on the Γ -valley electron gas (both with and without SOC and TR) in the weak moiré region (*i.e.*, the moiré gap is weaker than atomic band splitting if present).

As discussed in Sec. II, atomic symmetry data includes the atomic symmetry group G^A , and its irrep Λ_Γ^A furnished by the considered states at Γ , and we use G to label the moiré symmetry group. Here G^A is simply the point group at Γ , G_0^A , if there is no TR symmetry, but also includes the TR symmetry, denoted as \mathcal{T} , if it appears. Similarly, G is simply the moiré plane group, G_0 , if there is no TR symmetry, but also includes the TR symmetry if it appears. We focus on the case that the moiré potential does not cause extra TR breaking. For the specific case in Sec. II, we have $G^A = G_0^A \rtimes \mathcal{T}$ with $G_0^A = C_{6v}$, the irrep $\Lambda_\Gamma^A = \bar{\Gamma}_7$, and $G = G_0 \rtimes \mathcal{T}$ with $G_0 = P6mm$. Although we have the atomic symmetry group to be included by the moiré symmetry group in Sec. II, we do not assume such a relation in the general study in this section. The detailed steps for this general search are illustrated in SM Sec.A [114].

We went through all possible combinations of G^A , the irrep Λ_Γ^A , G , and the presence/absence of SOC, as elaborated in SM Sec.B [114]. The results are summarized in Tab. I for the spinful case with TR and in Tab. II for the spinless case without TR, where spinful (spinless) simply refers to the case with (without) SOC as indicated by the irrep notation with (without) a bar [115–117]. (The results of spinless cases with TR and spinful cases without TR are summarized in Tab. SI(c) and SIV(b) in the SM Sec.B [114] respectively.) We find 58 combinations that lead to symmetry-enforced moiré topology in the spinful case, and 139 in the spinless case. Out of the 58 spinful combinations (139 spinless combinations), we find that there are 11 (5) combinations that allow for isolated topological bands at low-energy, while all other combinations only have topological semi-metal phases in the weak moiré potential limit. The symmetry-enforced gapped moiré topology has the following scenarios: (i) for the TR-preserving case, isolated topological moiré bands may carry nonzero \mathbb{Z}_2 index in addition to other possibilities such as fragile topology; (ii) for the TR-breaking case, the topological moiré bands always have nonzero Chern number.

From our results, we can immediately provide several guiding principles for finding moiré topological insulators in Γ -valley moiré systems. First, symmetry-enforced moiré gapped topology only happens for doublets at Γ for both the TR-preserving and TR-breaking cases. Second, almost all symmetry-enforced moiré topological insulators happen on a triangular/hexagonal lattice, with only three combinations as exceptions. Therefore, to look for moiré topological insulators in Γ -valley moiré systems, it is favorable to look for low-energy 2D irreps at Γ valley subject to triangular/hexagonal moiré potential. Finally, symmetry-enforced moiré topological insulators only happen when SOC and TR symmetry are simultaneously present or simultaneously absent, meaning that the simultaneous presence and absence of TR symmetry

$G_0 \backslash G_0^A$	C_{6v}	C_{4v}	C_{3v}	C_{2v}	C_s
$P6$	Γ_5, Γ_6				
$P2$	Γ_5, Γ_6	Γ_5			
$P6mm$	Γ_5, Γ_6				
$P4mm$		Γ_5			
$P4bm$		$\Gamma_1, \Gamma_2, \Gamma_3, \Gamma_4$			
$P3m1$	Γ_5, Γ_6				
$Pmm2$	Γ_5, Γ_6	Γ_5			
$Cmm2$	Γ_5, Γ_6	Γ_5			
$Pba2$	$\Gamma_1, \Gamma_2, \Gamma_3, \Gamma_4$	$\Gamma_1, \Gamma_2, \Gamma_3, \Gamma_4$		$\Gamma_1, \Gamma_2, \Gamma_3, \Gamma_4$	
$Pma2$	$\Gamma_1, \Gamma_2, \Gamma_3, \Gamma_4, \Gamma_5, \Gamma_6$	$\Gamma_1, \Gamma_2, \Gamma_3, \Gamma_4, \Gamma_5$		$\Gamma_1, \Gamma_2, \Gamma_3, \Gamma_4$	
$Pm11$	Γ_5, Γ_6	Γ_5			
$Pb11$	$\Gamma_1, \Gamma_2, \Gamma_3, \Gamma_4$	$\Gamma_1, \Gamma_2, \Gamma_3, \Gamma_4$	Γ_1, Γ_2	$\Gamma_1, \Gamma_2, \Gamma_3, \Gamma_4$	Γ_1, Γ_2

TABLE II. **Spinless TR-breaking Cases for Symmetry-enforced Moiré Topology.** List of combinations of atomic point group G_0^A , atomic Γ irrep, and moiré plane group G_0 that lead to symmetry-enforced nontrivial moiré topology, without TR symmetry and without SOC. The meaning of the table entries is the same as that in Tab. I.

and SOC is also favorable for moiré topological insulators in Γ -valley moiré systems.

On the other hand, symmetry-enforced moiré topological semimetals are much easier to be realized than symmetry-enforced moiré topological insulators. There are no particular constraints on the lattice type, or the simultaneous presence/absence of TR symmetry and SOC. Nevertheless, doublets at Γ are still required to realize symmetry-enforced moiré topological semimetal, unless the moiré plane group is non-symmorphic [118–122].

V. CONCLUSION AND DISCUSSION

We have proposed the concept of symmetry-enforced moiré topology, and list all combinations of atomic symmetry data and moiré symmetry group to realize it for Γ -valley electron gas subject to a weak moiré potential. We note that although the SOC term may have a high power of momentum, such as the k^3 term in Eq. (3), the weak moiré condition is still realistic. To show its realistic nature in our consideration, we consider the bands of twisted bilayer MoTe_2 near Γ valley. In monolayer MoTe_2 , the low-energy $\bar{\Gamma}_4\bar{\Gamma}_5$ doublet at Γ (included in Tab. I) also has a k^3 band splitting term to the leading order. Yet, its atomic band splitting is around 7–11 meV at the edge of the mBZ of twisted bilayer MoTe_2 with twist angle from 3.5° to 4° , whereas the moiré band gap is about 3 meV [40], naturally satisfying the weak moiré condition. (See SM Sec.D [114] for details.) Moreover, the TR-breaking cases with the spinless models in Sec.C2 of SM [114] can also be applied to topological

moiré magnon systems [123–125].

The generation of the moiré potential is not limited to twisting two homobilayers—it can also be done (i) by forming hetero-structure with insulating materials such as boron nitride or transition metal dichalcogenides (TMD) [126–129] and (ii) by fabricating patterned hole arrays in dielectric substrate materials [130, 131]. We note that although the homobilayer structure contains two copies of the Γ -valley modes from each layer, the low-energy physics can only involve either the bonding combination or the anti-bonding combination between these two copies, owing to the strong uniform interlayer coupling [21, 40, 132, 133]. As a result, at low energies, homobilayer twist structure effectively has only one set of the Γ -valley modes. This is exactly the case in twisted homobilayer TMD at Γ valley [21, 40, 132]. While our current study focuses on layered materials with low-energy Γ -valley modes, the methodology should be generalizable to other valleys, such as K or M valleys [134], which we leave for the future work.

VI. ACKNOWLEDGMENT

We acknowledge the helpful discussion with Jennifer Cano and Lei Chen. J. Y.’s work is supported by startup funds at University of Florida. Y.L. and C.L. acknowledge the support from the Penn State Materials Research Science and Engineering Center for Nanoscale Science under National Science Foundation award DMR-2011839. This work was performed in part at Aspen Center for Physics, which is supported by National Science Foundation grant PHY-2210452.

[1] Y. Cao, V. Fatemi, S. Fang, K. Watanabe, T. Taniguchi, E. Kaxiras, and P. Jarillo-Herrero, Unconventional superconductivity in magic-angle graphene superlattices,

Nature **556**, 43 (2018).

[2] R. Bistritzer and A. H. MacDonald, Moiré bands in twisted double-layer graphene, Proceedings of the Na-

- tional Academy of Sciences **108**, 12233 (2011).
- [3] J. Cai, E. Anderson, C. Wang, X. Zhang, X. Liu, W. Holtzmann, Y. Zhang, F. Fan, T. Taniguchi, K. Watanabe, *et al.*, Signatures of fractional quantum anomalous hall states in twisted mote2, *Nature* **622**, 63 (2023).
 - [4] Y. Zeng, Z. Xia, K. Kang, J. Zhu, P. Knüppel, C. Vaswani, K. Watanabe, T. Taniguchi, K. F. Mak, and J. Shan, Thermodynamic evidence of fractional chern insulator in moiré mote2, *Nature* **622**, 69 (2023).
 - [5] H. Park, J. Cai, E. Anderson, Y. Zhang, J. Zhu, X. Liu, C. Wang, W. Holtzmann, C. Hu, Z. Liu, *et al.*, Observation of fractionally quantized anomalous hall effect, *Nature* **622**, 74 (2023).
 - [6] F. Xu, Z. Sun, T. Jia, C. Liu, C. Xu, C. Li, Y. Gu, K. Watanabe, T. Taniguchi, B. Tong, *et al.*, Observation of integer and fractional quantum anomalous hall effects in twisted bilayer mote 2, *Physical Review X* **13**, 031037 (2023).
 - [7] Z. Ji, H. Park, M. E. Barber, C. Hu, K. Watanabe, T. Taniguchi, J.-H. Chu, X. Xu, and Z.-X. Shen, Local probe of bulk and edge states in a fractional chern insulator, *Nature* **635**, 578 (2024).
 - [8] E. Redekop, C. Zhang, H. Park, J. Cai, E. Anderson, O. Sheekey, T. Arp, G. Babikyan, S. Salters, K. Watanabe, *et al.*, Direct magnetic imaging of fractional chern insulators in twisted mote2, *Nature* **635**, 584 (2024).
 - [9] K. Kang, B. Shen, Y. Qiu, Y. Zeng, Z. Xia, K. Watanabe, T. Taniguchi, J. Shan, and K. F. Mak, Evidence of the fractional quantum spin hall effect in moiré mote2, *Nature* **628**, 522 (2024).
 - [10] H. Park, J. Cai, E. Anderson, X.-W. Zhang, X. Liu, W. Holtzmann, W. Li, C. Wang, C. Hu, Y. Zhao, *et al.*, Ferromagnetism and topology of the higher flat band in a fractional chern insulator, *Nature Physics*, 1 (2025).
 - [11] L. An, H. Pan, W.-X. Qiu, N. Wang, S. Ru, Q. Tan, X. Dai, X. Cai, Q. Shang, X. Lu, *et al.*, Observation of ferromagnetic phase in the second moiré band of twisted mote2, *Nature Communications* **16**, 5131 (2025).
 - [12] Y. Jia, T. Song, Z. J. Zheng, G. Cheng, A. J. Uzan, G. Yu, Y. Tang, C. J. Pollak, F. Yuan, M. Onyszczak, *et al.*, Anomalous superconductivity in twisted mote2 nanojunctions, *Science Advances* **11**, eadq5712 (2025).
 - [13] F. Xu, X. Chang, J. Xiao, Y. Zhang, F. Liu, Z. Sun, N. Mao, N. Peshcherenko, J. Li, K. Watanabe, *et al.*, Interplay between topology and correlations in the second moiré band of twisted bilayer mote2, *Nature Physics*, 1 (2025).
 - [14] K. Kang, Y. Qiu, B. Shen, K. Lee, Z. Xia, Y. Zeng, K. Watanabe, T. Taniguchi, J. Shan, and K. F. Mak, Time-reversal symmetry breaking fractional quantum spin hall insulator in moiré mote2, *arXiv preprint arXiv:2501.02525* (2025).
 - [15] H. Park, W. Li, C. Hu, C. Beach, M. Gonçalves, J. F. Mendez-Valderrama, J. Herzog-Arbeitman, T. Taniguchi, K. Watanabe, D. Cobden, *et al.*, Observation of high-temperature dissipationless fractional chern insulator, *arXiv preprint arXiv:2503.10989* (2025).
 - [16] F. Xu, Z. Sun, J. Li, C. Zheng, C. Xu, J. Gao, T. Jia, K. Watanabe, T. Taniguchi, B. Tong, *et al.*, Signatures of unconventional superconductivity near reentrant and fractional quantum anomalous hall insulators, *arXiv preprint arXiv:2504.06972* (2025).
 - [17] Y. Xia, Z. Han, J. Zhu, Y. Zhang, P. Knüppel, K. Watanabe, T. Taniguchi, K. F. Mak, and J. Shan, Simulating high-temperature superconductivity in moiré wse2, *arXiv preprint arXiv:2508.02662* (2025).
 - [18] F. Wu, T. Lovorn, E. Tutuc, I. Martin, and A. MacDonald, Topological insulators in twisted transition metal dichalcogenide homobilayers, *Physical review letters* **122**, 086402 (2019).
 - [19] H. Yu, M. Chen, and W. Yao, Giant magnetic field from moiré induced berry phase in homobilayer semiconductors, *National Science Review* **7**, 12 (2020).
 - [20] H. Pan, F. Wu, and S. Das Sarma, Band topology, hubbard model, heisenberg model, and dzyaloshinskii-moriya interaction in twisted bilayer wse 2, *Physical Review Research* **2**, 033087 (2020).
 - [21] Y. Zhang, T. Liu, and L. Fu, Electronic structures, charge transfer, and charge order in twisted transition metal dichalcogenide bilayers, *Physical Review B* **103**, 155142 (2021).
 - [22] H. Li, U. Kumar, K. Sun, and S.-Z. Lin, Spontaneous fractional chern insulators in transition metal dichalcogenide moiré superlattices, *Physical Review Research* **3**, L032070 (2021).
 - [23] T. Devakul, V. Crépel, Y. Zhang, and L. Fu, Magic in twisted transition metal dichalcogenide bilayers, *Nature communications* **12**, 6730 (2021).
 - [24] N. Morales-Durán, J. Wang, G. R. Schleder, M. Angeli, Z. Zhu, E. Kaxiras, C. Repellin, and J. Cano, Pressure-enhanced fractional chern insulators in moiré transition metal dichalcogenides along a magic line, *arXiv preprint arXiv:2304.06669* (2023).
 - [25] C. Wang, X.-W. Zhang, X. Liu, Y. He, X. Xu, Y. Ran, T. Cao, and D. Xiao, Fractional chern insulator in twisted bilayer mote 2, *Physical Review Letters* **132**, 036501 (2024).
 - [26] A. P. Reddy, F. Alsallom, Y. Zhang, T. Devakul, and L. Fu, Fractional quantum anomalous hall states in twisted bilayer mote 2 and wse 2, *Physical Review B* **108**, 085117 (2023).
 - [27] W.-X. Qiu, B. Li, X.-J. Luo, and F. Wu, Interaction-driven topological phase diagram of twisted bilayer mote 2, *Physical Review X* **13**, 041026 (2023).
 - [28] J. Dong, J. Wang, P. J. Ledwith, A. Vishwanath, and D. E. Parker, Composite fermi liquid at zero magnetic field in twisted mote 2, *Physical Review Letters* **131**, 136502 (2023).
 - [29] T. Wang, T. Devakul, M. P. Zaletel, and L. Fu, Diverse magnetic orders and quantum anomalous hall effect in twisted bilayer mote2 and wse2, *arXiv preprint arXiv:2306.02501* (2023).
 - [30] H. Goldman, A. P. Reddy, N. Paul, and L. Fu, Zero-field composite fermi liquid in twisted semiconductor bilayers, *Physical review letters* **131**, 136501 (2023).
 - [31] N. Morales-Durán, N. Wei, J. Shi, and A. H. MacDonald, Magic angles and fractional chern insulators in twisted homobilayer transition metal dichalcogenides, *Physical Review Letters* **132**, 096602 (2024).
 - [32] X. Liu, Y. He, C. Wang, X.-W. Zhang, T. Cao, and D. Xiao, Gate-tunable antiferromagnetic chern insulator in twisted bilayer transition metal dichalcogenides, *Physical Review Letters* **132**, 146401 (2024).
 - [33] C. Xu, J. Li, Y. Xu, Z. Bi, and Y. Zhang, Maximally localized wannier functions, interaction models, and frac-

- tional quantum anomalous hall effect in twisted bilayer mote2, *Proceedings of the National Academy of Sciences* **121**, e2316749121 (2024).
- [34] A. P. Reddy and L. Fu, Toward a global phase diagram of the fractional quantum anomalous hall effect, *Physical Review B* **108**, 245159 (2023).
- [35] X.-Y. Song, Y.-H. Zhang, and T. Senthil, Phase transitions out of quantum hall states in moiré materials, *Physical Review B* **109**, 085143 (2024).
- [36] Y.-M. Wu, D. Shaffer, Z. Wu, and L. H. Santos, Time-reversal invariant topological moiré flat band: A platform for the fractional quantum spin hall effect, *Physical Review B* **109**, 115111 (2024).
- [37] J. Yu, J. Herzog-Arbeitman, M. Wang, O. Vafek, B. A. Bernevig, and N. Regnault, Fractional chern insulators versus nonmagnetic states in twisted bilayer mote 2, *Physical Review B* **109**, 045147 (2024).
- [38] A. Abouelkomsan, A. P. Reddy, L. Fu, and E. J. Bergholtz, Band mixing in the quantum anomalous hall regime of twisted semiconductor bilayers, *Physical Review B* **109**, L121107 (2024).
- [39] B. Li, W.-X. Qiu, and F. Wu, Electrically tuned topology and magnetism in twisted bilayer mote 2 at $\nu = 1$, *Physical Review B* **109**, L041106 (2024).
- [40] Y. Jia, J. Yu, J. Liu, J. Herzog-Arbeitman, Z. Qi, H. Pi, N. Regnault, H. Weng, B. A. Bernevig, and Q. Wu, Moiré fractional chern insulators. i. first-principles calculations and continuum models of twisted bilayer mote 2, *Physical Review B* **109**, 205121 (2024).
- [41] N. Mao, C. Xu, J. Li, T. Bao, P. Liu, Y. Xu, C. Felser, L. Fu, and Y. Zhang, Transfer learning relaxation, electronic structure and continuum model for twisted bilayer mote2, *Communications Physics* **7**, 262 (2024).
- [42] X.-W. Zhang, C. Wang, X. Liu, Y. Fan, T. Cao, and D. Xiao, Polarization-driven band topology evolution in twisted mote2 and wse2, *Nature Communications* **15**, 4223 (2024).
- [43] T. Wang, M. Wang, W. Kim, S. G. Louie, L. Fu, and M. P. Zaletel, Topology, magnetism and charge order in twisted mote2 at higher integer hole fillings, *arXiv preprint arXiv:2312.12531* (2023).
- [44] H. Li, Y. Su, Y. B. Kim, H.-Y. Kee, K. Sun, and S.-Z. Lin, Contrasting twisted bilayer graphene and transition metal dichalcogenides for fractional chern insulators: An emergent gauge picture, *Physical Review B* **109**, 245131 (2024).
- [45] D. Sheng, A. P. Reddy, A. Abouelkomsan, E. J. Bergholtz, and L. Fu, Quantum anomalous hall crystal at fractional filling of moiré superlattices, *Physical Review Letters* **133**, 066601 (2024).
- [46] A. P. Reddy, N. Paul, A. Abouelkomsan, and L. Fu, Non-abelian fractionalization in topological minibands, *Physical review letters* **133**, 166503 (2024).
- [47] C. Xu, N. Mao, T. Zeng, and Y. Zhang, Multiple chern bands in twisted mote 2 and possible non-abelian states, *Physical Review Letters* **134**, 066601 (2025).
- [48] C.-E. Ahn, W. Lee, K. Yananose, Y. Kim, and G. Y. Cho, Non-abelian fractional quantum anomalous hall states and first landau level physics of the second moiré band of twisted bilayer mote 2, *Physical Review B* **110**, L161109 (2024).
- [49] C. Wang, X.-W. Zhang, X. Liu, J. Wang, T. Cao, and D. Xiao, Higher landau-level analogs and signatures of non-abelian states in twisted bilayer mote 2, *Physical Review Letters* **134**, 076503 (2025).
- [50] X. Shen, C. Wang, R. Guo, Z. Xu, W. Duan, and Y. Xu, Stabilizing fractional chern insulators via exchange interaction in moiré systems, *arXiv preprint arXiv:2405.12294* (2024).
- [51] M. Wang, X. Wang, and O. Vafek, Phase diagram of twisted bilayer mote 2 in a magnetic field with an account for the electron-electron interaction, *Physical Review B* **110**, L201107 (2024).
- [52] Y. H. Kwan, G. Wagner, J. Yu, A. K. Dagnino, Y. Jiang, X. Xu, B. A. Bernevig, T. Neupert, and N. Regnault, When could abelian fractional topological insulators exist in twisted mote 2 (and other systems), *arXiv preprint arXiv:2407.02560* (2024).
- [53] A.-K. Wu, S. Sarkar, X. Wan, K. Sun, and S.-Z. Lin, Quantum-metric-induced quantum hall conductance inversion and reentrant transition in fractional chern insulators, *Physical Review Research* **6**, L032063 (2024).
- [54] T. Zaklaman, D. Luo, and L. Fu, Structure factor and topological bound of twisted bilayer semiconductors at fractional fillings, *Physical Review B* **112**, L041115 (2025).
- [55] Y. Zhang, H. Pi, J. Liu, W. Miao, Z. Qi, N. Regnault, H. Weng, X. Dai, B. A. Bernevig, Q. Wu, *et al.*, Universal moiré-model-building method without fitting: Application to twisted mote 2 and wse 2, *arXiv preprint arXiv:2411.08108* (2024).
- [56] W.-X. Qiu and F. Wu, Topological magnons and domain walls in twisted bilayer mote 2, *Physical Review B* **112**, 085132 (2025).
- [57] M. Gonçalves, J. F. Mendez-Valderrama, J. Herzog-Arbeitman, J. Yu, X. Xu, D. Xiao, B. A. Bernevig, and N. Regnault, Spinless and spinful charge excitations in moiré fractional chern insulators, *arXiv preprint arXiv:2506.05330* (2025).
- [58] Z. Liu, B. Li, Y. Shi, and F. Wu, Characterization of fractional chern insulator quasiparticles in moiré transition metal dichalcogenides, *arXiv preprint arXiv:2507.04056* (2025).
- [59] T. Neupert, L. Santos, C. Chamon, and C. Mudry, Fractional quantum hall states at zero magnetic field, *Physical review letters* **106**, 236804 (2011).
- [60] D. Sheng, Z.-C. Gu, K. Sun, and L. Sheng, Fractional quantum hall effect in the absence of landau levels, *Nature communications* **2**, 389 (2011).
- [61] N. Regnault and B. A. Bernevig, Fractional chern insulator, *Physical Review X* **1**, 021014 (2011).
- [62] E. Tang, J.-W. Mei, and X.-G. Wen, High-temperature fractional quantum hall states, *Physical review letters* **106**, 236802 (2011).
- [63] K. Sun, Z. Gu, H. Katsura, and S. Das Sarma, Nearly flatbands with nontrivial topology, *Physical review letters* **106**, 236803 (2011).
- [64] Y. Cao, V. Fatemi, A. Demir, S. Fang, S. L. Tomarken, J. Y. Luo, J. D. Sanchez-Yamagishi, K. Watanabe, T. Taniguchi, E. Kaxiras, *et al.*, Correlated insulator behaviour at half-filling in magic-angle graphene superlattices, *Nature* **556**, 80 (2018).
- [65] Z. Song, Z. Wang, W. Shi, G. Li, C. Fang, and B. A. Bernevig, All magic angles in twisted bilayer graphene are topological, *Physical review letters* **123**, 036401 (2019).
- [66] H. C. Po, L. Zou, T. Senthil, and A. Vishwanath, Faithful tight-binding models and fragile topology of magic-

- angle bilayer graphene, *Physical Review B* **99**, 195455 (2019).
- [67] J. Ahn, S. Park, and B.-J. Yang, Failure of nielsen-ninomiya theorem and fragile topology in two-dimensional systems with space-time inversion symmetry: application to twisted bilayer graphene at magic angle, *Physical Review X* **9**, 021013 (2019).
- [68] G. Tarnopolsky, A. J. Kruchkov, and A. Vishwanath, Origin of magic angles in twisted bilayer graphene, *Physical review letters* **122**, 106405 (2019).
- [69] Z.-D. Song, B. Lian, N. Regnault, and B. A. Bernevig, Twisted bilayer graphene. ii. stable symmetry anomaly, *Physical Review B* **103**, 205412 (2021).
- [70] Z.-D. Song and B. A. Bernevig, Magic-angle twisted bilayer graphene as a topological heavy fermion problem, *Physical review letters* **129**, 047601 (2022).
- [71] V. Cr  pel and J. Cano, Efficient prediction of superlattice and anomalous miniband topology from quantum geometry, *Physical Review X* **15**, 011004 (2025).
- [72] N. Lhachemi, V. Cr  pel, and J. Cano, in preparation.
- [73] Z. Lu, T. Han, Y. Yao, A. P. Reddy, J. Yang, J. Seo, K. Watanabe, T. Taniguchi, L. Fu, and L. Ju, Fractional quantum anomalous hall effect in multilayer graphene, *Nature* **626**, 759 (2024).
- [74] J. Xie, Z. Huo, X. Lu, Z. Feng, Z. Zhang, W. Wang, Q. Yang, K. Watanabe, T. Taniguchi, K. Liu, *et al.*, Tunable fractional chern insulators in rhombohedral graphene superlattices, *Nature Materials* , 1 (2025).
- [75] D. Waters, A. Okounkova, R. Su, B. Zhou, J. Yao, K. Watanabe, T. Taniguchi, X. Xu, Y.-H. Zhang, J. Folk, *et al.*, Chern insulators at integer and fractional filling in moir   pentalayer graphene, *Physical Review X* **15**, 011045 (2025).
- [76] Z. Lu, T. Han, Y. Yao, Z. Hadjri, J. Yang, J. Seo, L. Shi, S. Ye, K. Watanabe, T. Taniguchi, *et al.*, Extended quantum anomalous hall states in graphene/hbn moir   superlattices, *Nature* **637**, 1090 (2025).
- [77] S. H. Aronson, T. Han, Z. Lu, Y. Yao, J. P. Butler, K. Watanabe, T. Taniguchi, L. Ju, and R. C. Ashoori, Displacement field-controlled fractional chern insulators and charge density waves in a graphene/hbn moir   superlattice, *Physical Review X* **15**, 031026 (2025).
- [78] W. Zhou, J. Ding, J. Hua, L. Zhang, K. Watanabe, T. Taniguchi, W. Zhu, and S. Xu, Layer-polarized ferromagnetism in rhombohedral multilayer graphene, *Nature Communications* **15**, 2597 (2024).
- [79] X. Han, Q. Liu, Y. Wang, R. Niu, Z. Qu, Z. Wang, Z. Li, C. Han, K. Watanabe, T. Taniguchi, *et al.*, Engineering the band topology in a rhombohedral trilayer graphene moir   superlattice, *Nano Letters* **24**, 6286 (2024).
- [80] H. Xiang, J. Ding, J. Hua, N. Liu, W. Zhou, Q. Chen, K. Watanabe, T. Taniguchi, N. Xin, W. Zhu, *et al.*, Continuously tunable anomalous hall crystals in rhombohedral heptalayer graphene, *arXiv preprint arXiv:2502.18031* (2025).
- [81] Z. Wang, Q. Liu, X. Han, Z. Li, W. Zhao, Z. Qu, C. Han, K. Watanabe, T. Taniguchi, Z. V. Han, *et al.*, Electrical switching of chern insulators in moir   rhombohedral heptalayer graphene, *arXiv preprint arXiv:2503.00837* (2025).
- [82] C. Li, Z. Sun, K. Liu, L. Qiao, Y. Wei, C. Zheng, C. Zhang, K. Watanabe, T. Taniguchi, H. Yang, *et al.*, Tunable chern insulators in moir  -e-distant and moir  -e-proximal rhombohedral pentalayer graphene, *arXiv preprint arXiv:2505.01767* (2025).
- [83] J. Xie, Z. Zhang, X. Chen, Y. H. Kwan, Z. Huo, J. Herzog-Arbeitman, L. Guo, K. Watanabe, T. Taniguchi, K. Liu, *et al.*, Unconventional orbital magnetism in graphene-based fractional chern insulators, *arXiv preprint arXiv:2506.01485* (2025).
- [84] Y. Park, Y. Kim, B. L. Chittari, and J. Jung, Topological flat bands in rhombohedral tetralayer and multilayer graphene on hexagonal boron nitride moir   superlattices, *Physical Review B* **108**, 155406 (2023).
- [85] Z. Dong, A. S. Patri, and T. Senthil, Theory of quantum anomalous hall phases in pentalayer rhombohedral graphene moir   structures, *Physical Review Letters* **133**, 206502 (2024).
- [86] B. Zhou, H. Yang, and Y.-H. Zhang, Fractional quantum anomalous hall effect in rhombohedral multilayer graphene in the moir  less limit, *Physical Review Letters* **133**, 206504 (2024).
- [87] J. Dong, T. Wang, T. Wang, T. Soejima, M. P. Zaletel, A. Vishwanath, and D. E. Parker, Anomalous hall crystals in rhombohedral multilayer graphene. i. interaction-driven chern bands and fractional quantum hall states at zero magnetic field, *Physical Review Letters* **133**, 206503 (2024).
- [88] J. Herzog-Arbeitman, Y. Wang, J. Liu, P. M. Tam, Z. Qi, Y. Jia, D. K. Efetov, O. Vafeek, N. Regnault, H. Weng, *et al.*, Moir   fractional chern insulators. ii. first-principles calculations and continuum models of rhombohedral graphene superlattices, *Physical Review B* **109**, 205122 (2024).
- [89] Z. Guo, X. Lu, B. Xie, and J. Liu, Fractional chern insulator states in multilayer graphene moir   superlattices, *Physical Review B* **110**, 075109 (2024).
- [90] Y. H. Kwan, J. Yu, J. Herzog-Arbeitman, D. K. Efetov, N. Regnault, and B. A. Bernevig, Moir   fractional chern insulators. iii. hartree-fock phase diagram, magic angle regime for chern insulator states, role of moir   potential, and goldstone gaps in rhombohedral graphene superlattices, *Physical Review B* **112**, 075109 (2025).
- [91] T. Soejima, J. Dong, T. Wang, T. Wang, M. P. Zaletel, A. Vishwanath, and D. E. Parker, Anomalous hall crystals in rhombohedral multilayer graphene. ii. general mechanism and a minimal model, *Physical Review B* **110**, 205124 (2024).
- [92] Z. Dong, A. S. Patri, and T. Senthil, Stability of anomalous hall crystals in multilayer rhombohedral graphene, *Physical Review B* **110**, 205130 (2024).
- [93] M. Xie and S. Das Sarma, Integer and fractional quantum anomalous hall effects in pentalayer graphene, *Physical Review B* **109**, L241115 (2024).
- [94] K. Kudo, R. Nakai, and K. Nomura, Quantum anomalous, spin, and valley hall effects in pentalayer rhombohedral graphene moir   superlattices, *Physical Review B* **110**, 245135 (2024).
- [95] K. Huang, X. Li, S. Das Sarma, and F. Zhang, Self-consistent theory of fractional quantum anomalous hall states in rhombohedral graphene, *Physical Review B* **110**, 115146 (2024).
- [96] J. Yu, J. Herzog-Arbeitman, Y. H. Kwan, N. Regnault, and B. A. Bernevig, Moir   fractional chern insulators iv: Fluctuation-driven collapse of fcis in multiband exact diagonalization calculations on rhombohedral graphene, *arXiv preprint arXiv:2407.13770* (2024).

- [97] K. Huang, S. Das Sarma, and X. Li, Fractional quantum anomalous hall effect in rhombohedral multilayer graphene with a strong displacement field, *Physical Review B* **111**, 075130 (2025).
- [98] S. Das Sarma and M. Xie, Thermal crossover from a chern insulator to a fractional chern insulator in pentilayer graphene, *Physical Review B* **110**, 155148 (2024).
- [99] Z. Wei, A.-K. Wu, M. Gonçalves, and S.-Z. Lin, Edge-driven transition between extended quantum anomalous hall crystal and fractional chern insulator in rhombohedral graphene multilayers, *Physical Review B* **111**, 035116 (2025).
- [100] B. Zhou and Y.-H. Zhang, New classes of quantum anomalous hall crystals in multilayer graphene, *Physical Review Letters* **135**, 036501 (2025).
- [101] Y. Zeng and A. J. Millis, Berry phase dynamics of sliding electron crystals, *Physical Review X* **15**, 031059 (2025).
- [102] B. A. Bernevig and Y. H. Kwan, "berry trashcan" model of interacting electrons in rhombohedral graphene, *arXiv preprint arXiv:2503.09692* (2025).
- [103] H. Li, B. A. Bernevig, and N. Regnault, Multiband exact diagonalization and an iteration approach to search for fractional chern insulators in rhombohedral multilayer graphene, *Physical Review B* **112**, 075130 (2025).
- [104] T. Uchida, T. Kawakami, and M. Koshino, Non-abelian chern band in rhombohedral graphene multilayers, *arXiv preprint arXiv:2508.07366* (2025).
- [105] B. Bradlyn, L. Elcoro, J. Cano, M. G. Vergniory, Z. Wang, C. Felser, M. I. Aroyo, and B. A. Bernevig, Topological quantum chemistry, *Nature* **547**, 298 (2017).
- [106] J. Cano and B. Bradlyn, Band representations and topological quantum chemistry, *Annual Review of Condensed Matter Physics* **12**, 225 (2021).
- [107] L. Elcoro, B. J. Wieder, Z. Song, Y. Xu, B. Bradlyn, and B. A. Bernevig, Magnetic topological quantum chemistry, *Nature communications* **12**, 5965 (2021).
- [108] H. C. Po, A. Vishwanath, and H. Watanabe, Symmetry-based indicators of band topology in the 230 space groups, *Nature communications* **8**, 50 (2017).
- [109] J. Kruthoff, J. De Boer, J. Van Wezel, C. L. Kane, and R.-J. Slager, Topological classification of crystalline insulators through band structure combinatorics, *Physical Review X* **7**, 041069 (2017).
- [110] L. Fu and C. L. Kane, Topological insulators with inversion symmetry, *Physical Review B—Condensed Matter and Materials Physics* **76**, 045302 (2007).
- [111] C. Fang, M. J. Gilbert, and B. A. Bernevig, Bulk topological invariants in noninteracting point group symmetric insulators, *Physical Review B—Condensed Matter and Materials Physics* **86**, 115112 (2012).
- [112] H. C. Po, Symmetry indicators of band topology, *Journal of Physics: Condensed Matter* **32**, 263001 (2020).
- [113] P. M. Lenggenhager, X. Liu, T. Neupert, and T. Bzdušek, Universal higher-order bulk-boundary correspondence of triple nodal points, *Physical Review B* **106**, 085129 (2022).
- [114] Y. Liu, K. Yang, C.-X. Liu, and J. Yu, Supplementary materials for "symmetry-enforced topological moiré mini-bands".
- [115] M. I. Aroyo, J. M. Perez-Mato, D. Orobengoa, E. Tasci, G. de la Flor, and A. Kirov, Crystallography online: Bilbao crystallographic server, *Bulg. Chem. Commun* **43**, 183 (2011).
- [116] M. I. Aroyo, A. Kirov, C. Capillas, J. Perez-Mato, and H. Wondratschek, Bilbao crystallographic server. ii. representations of crystallographic point groups and space groups, *Acta Crystallographica Section A: Foundations of Crystallography* **62**, 115 (2006).
- [117] M. I. Aroyo, J. M. Perez-Mato, C. Capillas, E. Kroumova, S. Ivantchev, G. Madariaga, A. Kirov, and H. Wondratschek, Bilbao crystallographic server: I. databases and crystallographic computing programs, *Zeitschrift für Kristallographie-Crystalline Materials* **221**, 15 (2006).
- [118] L. Michel and J. Zak, Connectivity of energy bands in crystals, *Physical Review B* **59**, 5998 (1999).
- [119] L. Michel and J. Zak, Elementary energy bands in crystals are connected, *Physics Reports* **341**, 377 (2001).
- [120] H. Watanabe, H. C. Po, A. Vishwanath, and M. Zaletel, Filling constraints for spin-orbit coupled insulators in symmorphic and nonsymmorphic crystals, *Proceedings of the National Academy of Sciences* **112**, 14551 (2015).
- [121] H. Watanabe, H. C. Po, M. P. Zaletel, and A. Vishwanath, Filling-enforced gaplessness in band structures of the 230 space groups, *Physical review letters* **117**, 096404 (2016).
- [122] M. Vergniory, L. Elcoro, Z. Wang, J. Cano, C. Felser, M. Aroyo, B. A. Bernevig, and B. Bradlyn, Graph theory data for topological quantum chemistry, *Physical Review E* **96**, 023310 (2017).
- [123] Y.-H. Li and R. Cheng, Moiré magnons in twisted bilayer magnets with collinear order, *Physical Review B* **102**, 094404 (2020).
- [124] C. Wang, Y. Gao, H. Lv, X. Xu, and D. Xiao, Stacking domain wall magnons in twisted van der waals magnets, *Physical Review Letters* **125**, 247201 (2020).
- [125] S. C. Ganguli, M. Aapro, S. Kezilebieke, M. Amini, J. L. Lado, and P. Liljeroth, Visualization of moiré magnons in monolayer ferromagnet, *Nano Letters* **23**, 3412 (2023).
- [126] K. Yasuda, X. Wang, K. Watanabe, T. Taniguchi, and P. Jilario-Herrero, Stacking-engineered ferroelectricity in bilayer boron nitride, *Science* **372**, 1458 (2021).
- [127] C. Woods, P. Ares, H. Nevison-Andrews, M. Holwill, R. Fabregas, F. Guinea, A. Geim, K. Novoselov, N. Walet, and L. Fumagalli, Charge-polarized interfacial superlattices in marginally twisted hexagonal boron nitride, *Nature communications* **12**, 347 (2021).
- [128] P. Zhao, C. Xiao, and W. Yao, Universal superlattice potential for 2d materials from twisted interface inside h-bn substrate, *npj 2D Materials and Applications* **5**, 38 (2021).
- [129] D. S. Kim, R. C. Dominguez, R. Mayorga-Luna, D. Ye, J. Embley, T. Tan, Y. Ni, Z. Liu, M. Ford, F. Y. Gao, *et al.*, Electrostatic moiré potential from twisted hexagonal boron nitride layers, *Nature materials* **23**, 65 (2024).
- [130] C. Forsythe, X. Zhou, K. Watanabe, T. Taniguchi, A. Pasupathy, P. Moon, M. Koshino, P. Kim, and C. R. Dean, Band structure engineering of 2d materials using patterned dielectric superlattices, *Nature nanotechnology* **13**, 566 (2018).
- [131] D. Barcons Ruiz, H. Herzig Sheinflux, R. Hoffmann, I. Torre, H. Agarwal, R. K. Kumar, L. Vistoli, T. Taniguchi, K. Watanabe, A. Bachtold, *et al.*, Engineering high quality graphene superlattices via ion

- milled ultra-thin etching masks, *Nature communications* **13**, 6926 (2022).
- [132] M. Angeli and A. H. MacDonald, γ valley transition metal dichalcogenide moiré bands, *Proceedings of the National Academy of Sciences* **118**, e2021826118 (2021).
- [133] Y. Liu, A. Aryal, D. Calugaru, Z. Fang, K. Yang, H. Hu, Q. Yan, B. A. Bernevig, and C.-x. Liu, "ideal" topological heavy fermion model in two-dimensional moiré heterostructures with type-II band alignment, arXiv preprint arXiv:2507.06168 (2025).
- [134] D. Călugăru, Y. Jiang, H. Hu, H. Pi, J. Yu, M. G. Vergniory, J. Shan, C. Felser, L. M. Schoop, D. K. Efetov, *et al.*, Moiré materials based on m-point twisting, *Nature* **643**, 376 (2025).

Supplemental Materials for "Symmetry-enforced Moiré Topology"

Yunzhe Liu¹, Kaijie Yang², Chao-Xing Liu^{1,*}, and Jiabin Yu^{3,†}

¹*Department of Physics, The Pennsylvania State University, University Park, Pennsylvania 16802, USA*

²*Department of Materials Science and Engineering,*

University of Washington, Seattle, Washington 98195, USA and

³*Department of Physics, University of Florida, Gainesville, FL, USA*

(Dated: September 9, 2025)

A. GENERAL FORMALISM FOR TOPOLOGICAL PROPERTIES OF MOIRÉ SYSTEMS BASED ON TOPOLOGICAL QUANTUM CHEMISTRY

We consider a two-dimensional (2D) layered material, in which the conduction band minimum (CBM) or valence band maximum (VBM) is near the Γ point in the atomic Brillouin zone (ABZ). We assume the low-energy physics of this 2D material occurs around Γ and can be described by an effective Hamiltonian \hat{H}^A . We further introduce a moiré superlattice potential, leading to the following full Hamiltonian

$$\hat{H} = \hat{H}^A + \hat{H}_M, \quad (\text{S.A1})$$

where \hat{H}_M describes the weak moiré superlattice potential. The low-energy moiré bands refer to conduction bottom bands or valence top bands, as they are closest to charge neutrality. Here we will show how the low-energy moiré bands can be guaranteed to be topologically non-trivial by atomic symmetry data and moiré symmetry group (G), as long as the moiré potential is weaker than the atomic band splitting—the weak moiré condition is satisfied. The atomic symmetry data include the atomic symmetry group of \hat{H}^A , labeled as G^A , and the symmetry representation of G^A , denoted as Λ_{Γ}^A , furnished by the basis of \hat{H}^A at Γ . Throughout the paper, we always make sure the basis of \hat{H}^A at Γ furnishes an irreducible representation (irrep).

To address this question, the key step is to determine all the possible symmetry representations of the low-energy moiré bands at high symmetry momenta in the moiré Brillouin zone (mBZ) given a fixed combination of atomic symmetry data and moiré symmetry group. Once the moiré symmetry representations are obtained, we can directly use the theoretical formalism of topological quantum chemistry (TQC) [1–3] and symmetry indicators [4–9] to determine the moiré topology.

We first consider the case where the full Hamiltonian \hat{H} does not have time reversal (TR) symmetry. In this case, the atomic symmetry group $G^A = G_0^A$ is a point group. The effective atomic model also has the continuous translation T , in addition to $G^A = G_0^A$. Let us denote the plane group of the moiré potential \hat{H}_M as G_0^M , which contains the moiré translations T_M . Then, the symmetry group of the full Hamiltonian \hat{H} is $G = G_0 = G_0^M \cap (G_0^A \rtimes T)$. Below we always use \mathbf{k}_0 to denote the momentum in the ABZ and \mathbf{k}_M to denote the momentum in the mBZ, e.g. $\mathbf{k}_0 = \mathbf{k}_M + \mathbf{g}$ for a certain moiré reciprocal lattice vector \mathbf{g} . Given a moiré momentum \mathbf{k}_M , the group of operations in $G_0^A \rtimes T$ and G_0 that leaves \mathbf{k}_M invariant are denoted as

$$G_{\mathbf{k}_M}^A = \{\mathcal{S} | \mathcal{S} \in G_0^A \rtimes T \ \& \ \mathcal{S}\mathbf{k}_M = \mathbf{k}_M + \exists \mathbf{g}\}, \quad (\text{S.A2})$$

$$G_{\mathbf{k}_M} = \{\mathcal{S} | \mathcal{S} \in G_0 \ \& \ \mathcal{S}\mathbf{k}_M = \mathbf{k}_M + \exists \mathbf{g}\}, \quad (\text{S.A3})$$

respectively, where \mathbf{g} is a moiré reciprocal lattice vector. $G_{\mathbf{k}_M}$ is a subgroup of $G_{\mathbf{k}_M}^A$, because G_0 is a subgroup of $G_0^A \rtimes T$. We note that as T is the group of continuous translation, G is allowed to be nonsymmorphic.

We label the dimension of the irrep Λ_{Γ}^A as n_d . Owing to the irreducible nature, all eigen-states of \hat{H}^A are degenerate at Γ with the degeneracy n_d for $n_d > 1$. The highest dimension of Λ_{Γ}^A for all possible G^A for 2D materials is two [10], so that we only need to consider $n_d \leq 2$. We refer to Λ_{Γ}^A together with G^A as atomic symmetry data. For the momentum \mathbf{k} away from Γ , the band splitting of these n_d -fold degenerate states will follow the compatibility relations [1–3, 7, 8, 11, 12]. The moiré potential \hat{H}_M can further lower the space group symmetry, thus inducing additional band splitting. Here we focus on the *weak moiré potential limit*, which means the band splitting induced by the moiré potential \hat{H}_M is smaller than the intrinsic band splitting of \hat{H}^A at the mBZ boundary.

[*] cx156@psu.edu

[†] yujiabin@ufl.edu

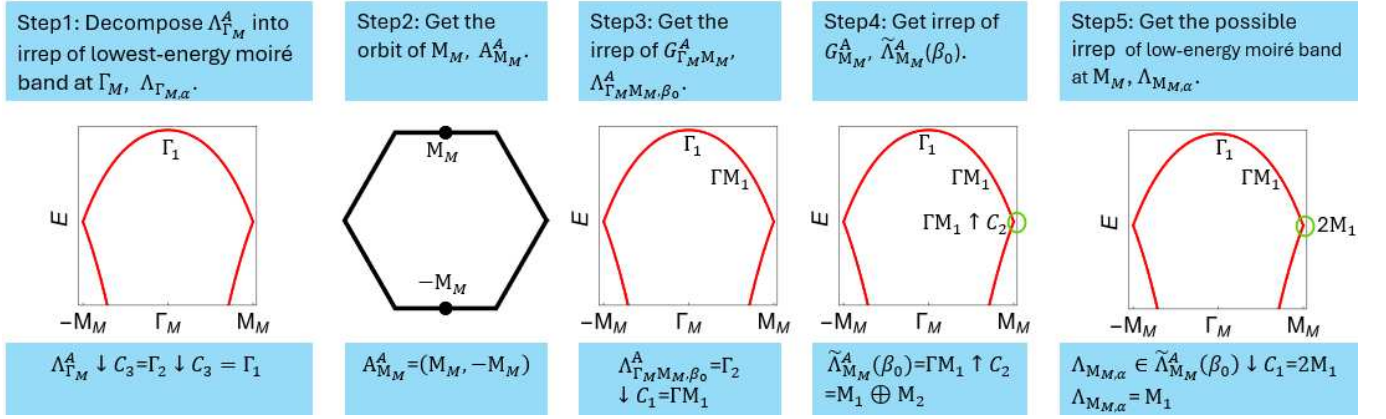


FIG. S1: The workflow chart illustrating how to determine the irreps at high-symmetry points in the MBZ. We take the combination of $G_0^A = C_6$, $\Lambda_{\Gamma}^A = \Gamma_2$ and $G_0 = P3$ as an example. In this example, $G_{\Gamma_M \mathbf{M}_M}^A = C_1$, $G_{\mathbf{M}_M}^A = C_2$, $G_{\Gamma_M} = C_3$, and $G_{\mathbf{M}_M} = C_1$. We get the irrep of G_{Γ_M} at Γ in the step 1, which is Γ_1 . We obtain the representation of $G_{\mathbf{M}_M}^A$, and subsequently that of $G_{\mathbf{M}_M}$, for the folded bands through Steps 2 to 5. Specifically, $\mathbf{M}_1 \oplus \mathbf{M}_2$ denotes the representation of $G_{\mathbf{M}_M}^A$ for the folded bands, whereas $2\mathbf{M}_1$ denotes the representation of $G_{\mathbf{M}_M}$ for the folded bands. Therefore, when moiré potential is included, the irrep $\Lambda_{\mathbf{M}_M,\alpha}$ of topmost band at \mathbf{M}_M is \mathbf{M}_1 .

Based on the above notation, we next will identify all the possible symmetry irreps of the low-energy moiré bands in the mBZ, namely, the moiré symmetry data. The moiré symmetry data allow us to straightforwardly extract the topological information of these moiré bands according to the TQC [1–3] and symmetry indicator [4–9]. Given the atomic symmetry data and moiré symmetry group, the moiré symmetry data can be obtained in five steps, as illustrated in the Fig. S1. In the following, we consider the case where the atomic Hamiltonian comes from VBM, without loss of generality. We focus on the n_d lowest energy moiré bands of \hat{H} , and discuss these five steps in detail.

Step 1: The irrep of the n_d moiré bands at Γ_M in the mBZ is inherited directly from the irrep Λ_{Γ}^A of G^A for \hat{H}^A as $\Gamma_M = \Gamma$ in the ABZ. In particular, Λ_{Γ}^A can be decomposed into the irreps of the little group G_{Γ_M} at Γ_M in the mBZ as

$$\Lambda_{\Gamma}^A \downarrow G_{\Gamma_M} = \oplus_{\alpha} c_{\alpha} \Lambda_{\Gamma_M,\alpha}, \quad (\text{S.A4})$$

where $\Lambda_{\Gamma_M,\alpha}$ is the α th irrep of G_{Γ_M} that is contained in Λ_{Γ}^A (i.e., restricted irrep of Λ_{Γ}^A), c_{α} is the multiplicity of this decomposition, and \downarrow means the restricted representation of G_{Γ_M} . Eq.(S.A4) determines the band splitting and band irreps of n_d moiré bands at Γ_M in the mBZ from the atomic irrep Λ_{Γ}^A .

Step 2: We now start addressing the possible irreps at other high symmetry points at the mBZ boundary, which come from the band folding. In this step, we list the atomic momenta that fold into the same moiré momentum. For a high symmetry momentum \mathbf{k}_M , we label the set of the momenta in the ABZ that are folded into \mathbf{k}_M as

$$A_{\mathbf{k}_M} = \{\mathbf{k}_0 | \mathbf{k}_0 = \mathbf{k}_M + \mathbf{g}\} \quad (\text{S.A5})$$

with the moiré reciprocal lattice vector \mathbf{g} . Any element of $G_{\mathbf{k}_M}^A$, defined in Eq. (S.A2), leaves $A_{\mathbf{k}_M}$ invariant. The orbit of \mathbf{k}_M , labelled as $A_{\mathbf{k}_M}^A$, is particularly important and defined by applying all symmetry operators in $G_{\mathbf{k}_M}^A$ to \mathbf{k}_M , namely,

$$A_{\mathbf{k}_M}^A = \{S\mathbf{k}_M | S \in G_{\mathbf{k}_M}^A\}, \quad (\text{S.A6})$$

where all elements are guaranteed to lie within the first mBZ or on the boundary of the first mBZ.

As any two momenta in $A_{\mathbf{k}_M}^A$ are related by symmetry, the eigen-energy spectrum of $\hat{H}^A(\mathbf{k})$ is the same for any $\mathbf{k} \in A_{\mathbf{k}_M}^A$. With a zero moiré potential, all the non-moiré (i.e., atomic) bands at $\mathbf{k} \in A_{\mathbf{k}_M}^A$ will be folded into \mathbf{k}_M .

Step 3: Clearly, the n_d atomic bands at \mathbf{k}_M may not have the same energy, leading to different sets of moiré bands at \mathbf{k}_M with different energies. It comes from the fact that the symmetry along the path from Γ_M to \mathbf{k}_M , which we label as $\Gamma_M \mathbf{k}_M$, can be lower than that at Γ_M , leading to the atomic band splitting. To account for this, we use $G_{\Gamma_M \mathbf{k}_M}^A$ to label the little group of $G^A \rtimes T$ at any momentum on $\Gamma_M \mathbf{k}_M$, which is given by the union of all $G_{\mathbf{k}}^A$ with \mathbf{k} ranging over $\Gamma_M \mathbf{k}_M$. (Here, $G_{\mathbf{k}}^A$ is simply given by replacing \mathbf{k}_M in Eq. (S.A2) by \mathbf{k} .) Since there are momenta on $\Gamma_M \mathbf{k}_M$ that are not on the mBZ boundary, all elements of $G_{\Gamma_M \mathbf{k}_M}^A$ simply leave $\Gamma_M \mathbf{k}_M$ invariant without being up to moiré reciprocal lattice vectors.

Naturally, $G_{\Gamma_M \mathbf{k}_M}^A$ is a subgroup of $G_{\Gamma_M}^A$, and thus we can decompose Λ_{Γ}^A into the irreps $\Lambda_{\Gamma_M \mathbf{k}_M}^A$ of the little group $G_{\Gamma_M \mathbf{k}_M}^A$ as

$$\Lambda_{\Gamma_M}^A \downarrow G_{\Gamma_M \mathbf{k}_M}^A = \oplus_{\beta} \Lambda_{\Gamma_M \mathbf{k}_M, \beta}^A, \quad (\text{S.A7})$$

where $\beta = (\alpha, \mu)$, α labels the type of irrep, and μ labels the copies of the same irrep—different copies are furnished by different physical states. Clearly, it is possible that $\Lambda_{\Gamma_M \mathbf{k}_M, \beta}^A$ and $\Lambda_{\Gamma_M \mathbf{k}_M, \beta'}^A$ are the same irreps for $\beta \neq \beta'$, but they are always furnished by different physical states. There are no symmetries that relate states that belong to different β , and thus it is natural to expect different $\Lambda_{\Gamma_M \mathbf{k}_M, \beta}^A$ correspond to different energies.

Step 4: For each copy of irrep $\Lambda_{\Gamma_M \mathbf{k}_M, \beta}^A$, we can construct the corresponding induced representation $\tilde{\Lambda}_{\mathbf{k}_M}^A(\beta)$ of $G_{\mathbf{k}_M}^A$ as

$$\tilde{\Lambda}_{\mathbf{k}_M}^A(\beta) = \Lambda_{\Gamma_M \mathbf{k}_M, \beta}^A \uparrow G_{\mathbf{k}_M}^A \quad (\text{S.A8})$$

where \uparrow denotes the induction of the representation $\Lambda_{\Gamma_M \mathbf{k}_M, \beta}^A$ in the little group $G_{\mathbf{k}_M}^A$ defined in Eq.(S.A2). This induction process is nothing but the band folding—all moiré bands that belong to $\tilde{\Lambda}_{\mathbf{k}_M}^A(\beta)$ have the same energy as the $\Lambda_{\Gamma_M \mathbf{k}_M, \beta}^A$ atomic band at \mathbf{k}_M . For any β and any high symmetry \mathbf{k}_M , the dimension of $\tilde{\Lambda}_{\mathbf{k}_M}^A(\beta)$ is

$$N[\tilde{\Lambda}_{\mathbf{k}_M, \beta}^A] = N[\Lambda_{\Gamma_M \mathbf{k}_M, \beta}^A] \times N[A_{\mathbf{k}_M}^A], \quad (\text{S.A9})$$

where $N[\dots]$ is the dimension if “...” is a representation or the number of elements if “...” is a set. If $N[\tilde{\Lambda}_{\mathbf{k}_M, \beta}^A] \geq n_d$, we can just choose $\tilde{\Lambda}_{\mathbf{k}_M, \beta}^A$ that corresponds to the lowest energy, which we labeled as β_0 . Here the lowest energy refers to the energy of the topmost valence band or the bottommost conduction band. If $N[\tilde{\Lambda}_{\mathbf{k}_M, \beta}^A] < n_d$, we just should choose the lowest energy two irreps, β_0 and β_1 .

Step 5: At last, the possible irreps of the low-energy n_d moiré bands at \mathbf{k}_M are contained in

$$\oplus_{\beta} (\tilde{\Lambda}_{\mathbf{k}_M}^A(\beta) \downarrow G_{\mathbf{k}_M}) = \oplus_{\beta} \oplus_{\alpha} c_{\mathbf{k}_M, \beta \alpha} \Lambda_{\mathbf{k}_M, \alpha}, \quad (\text{S.A10})$$

where β only ranges over β_0 if $N[\tilde{\Lambda}_{\mathbf{k}_M, \beta}^A] \geq n_d$ or β_0 and β_1 if $N[\tilde{\Lambda}_{\mathbf{k}_M, \beta}^A] < n_d$. Here, $\Lambda_{\mathbf{k}_M, \alpha}$ is the α th irrep of $G_{\mathbf{k}_M}$, and $c_{\mathbf{k}_M, \alpha}$ is the multiplicity.

Here, we need to emphasize one more point that the irreps at two *different* high symmetry momenta \mathbf{k}_M and \mathbf{k}'_M may be related by G^A . If there is a symmetry operator $\mathcal{S}_{\mathbf{k}_M} \in G^A$ such that $\mathcal{S}_{\mathbf{k}_M} \mathbf{k}_M = \mathbf{k}'_M$, the bands of \hat{H}^A at \mathbf{k}_M and \mathbf{k}'_M have the same energy under zero moiré potential and are related by symmetry. This leads to a relationship for the representations of folding bands at \mathbf{k}_M and \mathbf{k}'_M , given by

$$\chi_{\tilde{\Lambda}_{\mathbf{k}_M}^A(\beta)}(\mathcal{G}_{\mathbf{k}_M}) = \chi_{\tilde{\Lambda}_{\mathbf{k}'_M}^A(\beta)}(\mathcal{S}_{\mathbf{k}_M} \mathcal{G}_{\mathbf{k}_M} \mathcal{S}_{\mathbf{k}_M}^{-1}), \quad (\text{S.A11})$$

where $\mathcal{G}_{\mathbf{k}_M}$ and $\mathcal{S}_{\mathbf{k}_M} \mathcal{G}_{\mathbf{k}_M} \mathcal{S}_{\mathbf{k}_M}^{-1}$ are symmetry operators in group $G_{\mathbf{k}_M}$ and $G_{\mathbf{k}'_M}$, respectively. One example is the combination of $G_0^A = C_6$ and $G_0 = P3$, two distinct high symmetry points \mathbf{K}_M and \mathbf{KA}_M ($-\mathbf{K}_M$) are related by the symmetry C_{2z} in G_0^A . The representation formed by the folded band at \mathbf{KA}_M , $\tilde{\Lambda}_{\mathbf{KA}_M}^A(\beta)$, is related to the representation at \mathbf{K}_M , $\tilde{\Lambda}_{\mathbf{K}_M}^A(\beta)$, by the Eq.(S.A11).

With the above steps, we can derive all possible moiré symmetry data of the low-energy n_d moiré bands, as long as the moiré potential strength is weaker than the atomic band splitting. We can then compare the moiré symmetry data to the EBR tables in Bilbao Crystallographic Server [13–15] and indicate the topology of the low-energy n_d moiré bands, based on the TQC [1–3] and symmetry indicator [4–9].

In the above, we only focus on the space group symmetry and assume \hat{H}^A has no TR symmetry. In a TR invariant system, $G^A = \mathcal{T} \rtimes G_0^A$ and $G = \mathcal{T} \rtimes G_0$, where \mathcal{T} represents TR symmetry and G_0 represents plane group symmetry of \hat{H} . With TR, we can still follow exactly step 1 to step 5 to determine the moiré symmetry data of the low-energy n_d moiré bands. Of course, the extra TR symmetry can enlarge the irreps.

B. SYMMETRY-ENFORCED MOIRÉ TOPOLOGY

In this section, we list all combinations of atomic symmetry data and moiré symmetry group that enforce nontrivial topology of low-energy moiré bands, using the method developed in Sec.A.

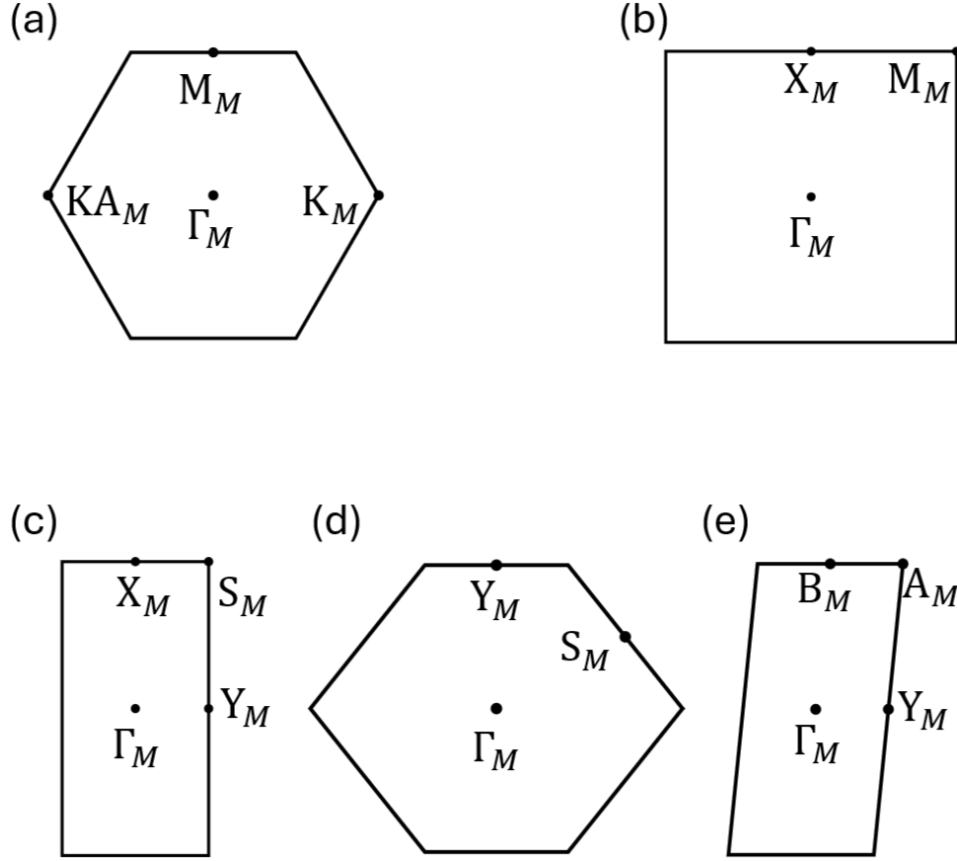


FIG. S2: The mBZs for different plane groups and high symmetry momenta. (a) shows the mBZs for plane group $P3$, $P3m1$, $P31m$, $P6$ and $P6mm$. The Bravais lattices are hexagonal. (b) shows the mBZs for plane group $P4$, $P4mm$ and $P4bm$. Bravais lattices of these groups are square (c) shows the mBZ for plane group $pm2$, $pma2$, $pmb2$, $pb11$ and $pm11$. Bravais lattices of these groups are rectangular. (d) shows the mBZs for plane group $Cmm2$ and $Cmm1$. Bravais lattices of these groups are centered rectangular (e) shows the mBZ for plane group $P2$ and $P1$.

1. Cases with TR symmetry

We start with the cases with TR symmetry. Table I in the main text summarizes all the combinations of G_0^A , Λ_F^A and G_0 that lead to symmetry-enforced moiré topology in a spinful TR-invariant system. Table SI summarizes all the combinations of G_0^A , Λ_F^A and G_0 that lead to symmetry-enforced moiré topology in a spinless TR-invariant system. In spinless systems, all symmetry-enforced topological moiré bands are semimetallic. We find 34 combinations that lead to symmetry-enforced moiré topology in the spinful case, and 73 in the spinless case, when there is TR symmetry. Among the 34 spinful cases, we find that there are 11 cases that allow the existence of low-energy isolated topological moiré bands in the phase diagram, while all other cases are completely semimetallic. We notice that most non-trivial cases are for 2D irreps. For a 1D spinless irrep Λ_F^A , we can only get a symmetry-enforced topological semimetal when G_0 is a nonsymmorphic plane group, in which a single isolated moiré band is not allowed [16–20].

Tables SII-SXV show all the representations at high-symmetry momenta in the mBZ for a certain Λ_F^A , which are constructed by applying the general approach developed in Sec. A to all combinations of G_0^A and G_0 listed in Table I in the main text and Table SI. We organize these tables according to G_0^A , namely, Tables SII-SV are for $G_0^A = C_{6v}$, Tables SVI-SVIII are for $G_0^A = C_{3v}$, Tables SIX-SX are for $G_0^A = C_{4v}$, Table SXI is for $G_0^A = C_{2v}$, Table SXII is for $G_0^A = C_s$, Table SXIII is for $G_0^A = C_6$, Table SXIV is for $G_0^A = C_4$ and Table SXV is for $G_0^A = C_3$. The character tables for above G_0^A are shown in Tables SXVI and SXVII.

As an example to illustrate how to identify the nontrivial cases from these tables, let us look at Table SII(a), where $G_0^A = C_{6v}$ and $G_0 = P6mm$, and the corresponding character tables for all high-symmetry points are shown in Table SXVIII. In the first row of Table SII(a), the first and second entries show the symmetry groups of G_0^A and G_0 , respectively. One should note that TR also exists for this table, so $G^A = \mathcal{T} \rtimes G_0^A$. Starting from the second row, the first column lists the irreps Λ_F^A . The irreps with a bar correspond to spinful systems, while those without a bar

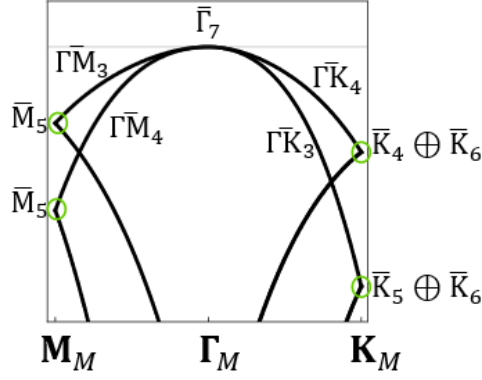


FIG. S3: (a) The schematic figure of band folding, and band irreps are labeled.

represent spinless systems [13–15]. For irreps with dimension greater than one, we explicitly label their dimension in the bracket. The second column shows the irrep of G_{Γ_M} in a TR-invariant system after taking into account the moiré potential, following **Step 1** in Sec. A. The third and fourth columns show the possible representations of the folded bands at the high-symmetry momenta \mathbf{M}_M and \mathbf{K}_M on the mBZ boundary, respectively, obtained by following **Steps 2–4** in Sec. A. The locations of high-symmetry momenta \mathbf{M}_M and \mathbf{K}_M in the mBZ are shown in Fig. S2(a). The irrep Λ_{Γ}^A labeled with a star (\star) indicates the case with isolated symmetry-enforced topological moiré bands, while the irreps Λ_{Γ}^A labeled with a triangle (\blacktriangle) indicate the cases where the symmetry-enforced topological moiré bands must be semimetallic.

To be more specific, we examine the case with $\Lambda_{\Gamma}^A = \bar{\Gamma}_7$, which corresponds to the basis functions with the out-of-plane total angular momentum $J_z = \pm \frac{3}{2}$. The irrep $\Lambda_{\Gamma_M, \alpha}^A$ of low-energy moiré bands for the little group G_{Γ} at Γ_M only takes one value for α and directly equals to $\Lambda_{\Gamma}^A = \bar{\Gamma}_7$ in the second column of Table SII(a). Along the $\Gamma_M \mathbf{M}_M$ line (with the little group $G_{\Gamma_M \mathbf{M}_M}^A = C_s$ and character table in Table SXIX), the two-fold degenerate $\bar{\Gamma}_7$ bands are split into two bands, which belong to irreps $\bar{\Gamma}_M3$ and $\bar{\Gamma}_M4$ with opposite mirror M_x (flipping x) eigenvalues. Therefore $\Lambda_{\Gamma_M \mathbf{M}_M, \beta_0}^A$ and $\Lambda_{\Gamma_M \mathbf{M}_M, \beta_1}^A$ take values from $\bar{\Gamma}_M3$ and $\bar{\Gamma}_M4$. The bands of \hat{H}^A at $\mathbf{k}_0 = \mathbf{M}_M$ and $-\mathbf{M}_M$ in the ABZ are folded into \mathbf{M}_M in the mBZ. According to Eqs. (S.A8) and (S.A10), regardless of $\Lambda_{\Gamma_M \mathbf{M}_M, \beta_0}^A$, the irrep formed by the folded band is the 2D irrep $\bar{\mathbf{M}}_5$, as shown in the third column of Table SII(a). Therefore, we don't need to consider $\Lambda_{\Gamma_M \mathbf{M}_M, \beta_1}^A$. Similarly, along the $\Gamma_M \mathbf{K}_M$ line (with the little group again $G_{\Gamma_M \mathbf{K}_M}^A = C_s$), these two bands belong to irreps $\bar{\Gamma}_M3$ and $\bar{\Gamma}_M4$ with opposite mirror M_y (flipping y) values. Therefore, $\Lambda_{\Gamma_M \mathbf{K}_M, \beta_0}^A$ and $\Lambda_{\Gamma_M \mathbf{K}_M, \beta_1}^A$ take values from $\bar{\Gamma}_M3$ and $\bar{\Gamma}_M4$. There are three equivalent \mathbf{K}_M , denoted as $\mathbf{k}_0 = \mathbf{K}_M$, $C_{3z}\mathbf{K}_M$, and $C_{3z}^{-1}\mathbf{K}_M$ in the ABZ, related by the three-fold rotation C_{3z} around the out-of-plane axis. The bands of \hat{H}^A at these three momenta are folded into \mathbf{K}_M in the mBZ and form a three dimensional (3D) representation. Thus, again we don't need to consider $\Lambda_{\Gamma_M \mathbf{K}_M, \beta_1}^A$. The 3D representation can be decomposed into one 1D irrep and one 2D irrep. According to Eqs. (S.A8) and (S.A10), the decomposition gives rise to $\bar{\mathbf{K}}_4 \oplus \bar{\mathbf{K}}_6$ when $\Lambda_{\Gamma_M \mathbf{K}_M, \beta_0}^A = \bar{\Gamma}_M4$, and yields $\bar{\mathbf{K}}_5 \oplus \bar{\mathbf{K}}_6$ when $\Lambda_{\Gamma_M \mathbf{K}_M, \beta_0}^A = \bar{\Gamma}_M3$, where $\bar{\mathbf{K}}_4$ and $\bar{\mathbf{K}}_5$ are 1D irreps, while $\bar{\mathbf{K}}_6$ is a 2D irrep. No matter which case, $\bar{\mathbf{K}}_5 \oplus \bar{\mathbf{K}}_6$ and $\bar{\mathbf{K}}_4 \oplus \bar{\mathbf{K}}_6$ have different energies caused by the atomic band splitting, even if there is no moiré potential. The moiré potential will further split the three-fold degenerate states of $\bar{\mathbf{K}}_5 \oplus \bar{\mathbf{K}}_6$ ($\bar{\mathbf{K}}_4 \oplus \bar{\mathbf{K}}_6$), but this moiré energy scale splitting is smaller than the atomic energy scale. Thus, the low-energy two bands should be from either $\bar{\mathbf{K}}_5 \oplus \bar{\mathbf{K}}_6$ or $\bar{\mathbf{K}}_4 \oplus \bar{\mathbf{K}}_6$.

Without loss of generality, we consider the low-energy moiré bands to be from the $\bar{\mathbf{K}}_4 \oplus \bar{\mathbf{K}}_6$ bands, as schematically shown in Fig. S3 for zero moiré potential after band folding. In Section II of the main text, we demonstrated that under the weak moiré condition, the low-energy two bands must be topological. Indeed, if the $\bar{\mathbf{K}}_6$ irrep is kept for the low-energy two bands, we can find they form a topological insulator by comparing with all the 2D EBRs in Table SXX [13–15], according to the theory of topological quantum chemistry [1–3] and symmetry indicator [6–8]. In contrast, if the energy of $\bar{\mathbf{K}}_4$ band is closer to the band gap, two low-energy bands are from one 1D $\bar{\mathbf{K}}_4$ irrep and one component of the 2D $\bar{\mathbf{K}}_6$ irrep. In this case, the second low-energy band must connect to another band at \mathbf{K}_M , resulting in a topological semimetal. We can reach the exactly same conclusion if the low-energy moiré bands are from the $\bar{\mathbf{K}}_5 \oplus \bar{\mathbf{K}}_6$ bands. In conclusion, when incorporating TR with the combination $G_0^A = C_{6v}$, $\Lambda_{\Gamma}^A = \bar{\Gamma}_7$, and $G_0 = P6mm$, the low-energy two moiré bands in this case must be symmetry-enforced topological under the weak moiré condition.

From Table SI(a), all isolated symmetry-enforced topological moiré bands exhibit two common characteristics. Firstly, the basis states of \hat{H}^A carry the total out-of-plane angular momentum $J_z = \pm \frac{3}{2}$. Secondly, the moiré

potential maintains C_{3z} symmetry, so that the mBZ is hexagonal.

$G_0 \backslash G_0^A$	C_{6v}	C_{4v}	C_{3v}	C_{2v}	C_s	C_6	C_4
$P6mm$	Γ_5, Γ_6						
$P4mm$		Γ_5					
$P4bm$		$\Gamma_1, \Gamma_2, \Gamma_3, \Gamma_4$					
$P3m1$	Γ_5, Γ_6		Γ_3				
$Pmm2$	Γ_5, Γ_6	Γ_5					
$Cmm2$	Γ_5, Γ_6	Γ_5					
$Pba2$	$\Gamma_1, \Gamma_2, \Gamma_3, \Gamma_4$	$\Gamma_1, \Gamma_2, \Gamma_3, \Gamma_4$		$\Gamma_1, \Gamma_2, \Gamma_3, \Gamma_4$			
$Pma2$	$\Gamma_1, \Gamma_2, \Gamma_3, \Gamma_4, \Gamma_5, \Gamma_6$	$\Gamma_1, \Gamma_2, \Gamma_3, \Gamma_4, \Gamma_5$		$\Gamma_1, \Gamma_2, \Gamma_3, \Gamma_4$			
$Pm11$	Γ_5, Γ_6	Γ_5	Γ_3				
$Pb11$	$\Gamma_1, \Gamma_2, \Gamma_3, \Gamma_4$	$\Gamma_1, \Gamma_2, \Gamma_3, \Gamma_4$	Γ_1, Γ_2	$\Gamma_1, \Gamma_2, \Gamma_3, \Gamma_4$	Γ_1, Γ_2		
$P6$	Γ_5, Γ_6					$\Gamma_3\Gamma_5, \Gamma_4\Gamma_6$	
$P2$	Γ_5, Γ_6	Γ_5				$\Gamma_3\Gamma_5, \Gamma_4\Gamma_6$	$\Gamma_3\Gamma_4$

TABLE SI: **Spinless TR-invariant cases for symmetry-enforced moiré topology.** List of combinations of atomic point group G_0^A , atomic Γ irrep, and moiré plane group G_0 that lead to symmetry-enforced nontrivial moiré topology, in the presence of TR symmetry and without SOC. For a given G_0^A and G_0 , the table entry indicates the required atomic Γ irrep to give symmetry-enforced topology. The low-energy bands are all semimetallic in this case.

$G_0^A = C_{6v}$	$G_0 = P6mm$		
Γ	Γ_M	M_M	K_M
Γ_1	Γ_1	$M_1 \oplus M_4$	$K_1 \oplus K_3(2)$
Γ_2	Γ_2	$M_2 \oplus M_3$	$K_2 \oplus K_3(2)$
Γ_3	Γ_3	$M_2 \oplus M_3$	$K_1 \oplus K_3(2)$
Γ_4	Γ_4	$M_1 \oplus M_4$	$K_2 \oplus K_3(2)$
$\blacktriangle \Gamma_5(2)$	$\Gamma_5(2)$	$M_1 \oplus M_4$	$K_1 \oplus K_3(2)$
		$M_2 \oplus M_3$	$K_2 \oplus K_3(2)$
$\blacktriangle \Gamma_6(2)$	$\Gamma_6(2)$	$M_1 \oplus M_4$	$K_1 \oplus K_3(2)$
		$M_2 \oplus M_3$	$K_2 \oplus K_3(2)$
$\star \bar{\Gamma}_7(2)$	$\bar{\Gamma}_7(2)$	$\bar{M}_5(2)$	$\bar{K}_4 \oplus \bar{K}_6(2)$
			$\bar{K}_5 \oplus \bar{K}_6(2)$
$\bar{\Gamma}_8(2)$	$\bar{\Gamma}_8(2)$	$\bar{M}_5(2)$	$\bar{K}_4 \oplus \bar{K}_6(2)$
			$\bar{K}_5 \oplus \bar{K}_6(2)$
$\bar{\Gamma}_9(2)$	$\bar{\Gamma}_9(2)$	$\bar{M}_5(2)$	$\bar{K}_4 \oplus \bar{K}_6(2)$
			$\bar{K}_5 \oplus \bar{K}_6(2)$

(a) $G_0^A = C_{6v}$ and $G_0 = P6mm$

$G_0^A = C_{6v}$	$G_0 = P6$		
Γ	Γ_M	M_M	K_M
Γ_1	Γ_1	$M_1 \oplus M_2$	$K_1 \oplus K_2 \oplus K_3$
Γ_2	Γ_1	$M_1 \oplus M_2$	$K_1 \oplus K_2 \oplus K_3$
Γ_3	Γ_2	$M_1 \oplus M_2$	$K_1 \oplus K_2 \oplus K_3$
Γ_4	Γ_2	$M_1 \oplus M_2$	$K_1 \oplus K_2 \oplus K_3$
$\blacktriangle \Gamma_5(2)$	$\Gamma_3 \Gamma_5(2)$	$M_1 \oplus M_2$	$K_1 \oplus K_2 \oplus K_3$
$\blacktriangle \Gamma_6(2)$	$\Gamma_4 \Gamma_6(2)$	$M_1 \oplus M_2$	$K_1 \oplus K_2 \oplus K_3$
$\star \bar{\Gamma}_7(2)$	$\bar{\Gamma}_7 \bar{\Gamma}_8(2)$	$\bar{M}_3 \bar{M}_4(2)$	$\bar{K}_4 \oplus \bar{K}_5 \oplus \bar{K}_6$
$\bar{\Gamma}_8(2)$	$\bar{\Gamma}_9 \bar{\Gamma}_{12}(2)$	$\bar{M}_3 \bar{M}_4(2)$	$\bar{K}_4 \oplus \bar{K}_5 \oplus \bar{K}_6$
$\bar{\Gamma}_9(2)$	$\bar{\Gamma}_{10} \bar{\Gamma}_{11}(2)$	$\bar{M}_3 \bar{M}_4(2)$	$\bar{K}_4 \oplus \bar{K}_5 \oplus \bar{K}_6$

(c) $G_0^A = C_{6v}$ and $G_0 = P6$

$G_0^A = C_{6v}$	$G_0 = P3m1$		
Γ	Γ_M	M_M	K_M
Γ_1	Γ_1	$2M_1$	$K_1 \oplus K_2 \oplus K_3$
Γ_2	Γ_2	$2M_2$	$K_1 \oplus K_2 \oplus K_3$
Γ_3	Γ_2	$2M_2$	$K_1 \oplus K_2 \oplus K_3$
Γ_4	Γ_1	$2M_1$	$K_1 \oplus K_2 \oplus K_3$
$\blacktriangle \Gamma_5(2)$	$\Gamma_3(2)$	$2M_1$	$K_1 \oplus K_2 \oplus K_3$
		$2M_2$	
$\blacktriangle \Gamma_6(2)$	$\Gamma_3(2)$	$2M_1$	$K_1 \oplus K_2 \oplus K_3$
		$2M_2$	
$\star \bar{\Gamma}_7(2)$	$\bar{\Gamma}_4 \bar{\Gamma}_5(2)$	$\bar{M}_3 \bar{M}_4(2)$	$\bar{K}_4 \oplus \bar{K}_5 \oplus \bar{K}_6$
$\bar{\Gamma}_8(2)$	$\bar{\Gamma}_6(2)$	$\bar{M}_3 \bar{M}_4(2)$	$\bar{K}_4 \oplus \bar{K}_5 \oplus \bar{K}_6$
$\bar{\Gamma}_9(2)$	$\bar{\Gamma}_6(2)$	$\bar{M}_3 \bar{M}_4(2)$	$\bar{K}_4 \oplus \bar{K}_5 \oplus \bar{K}_6$

(b) $G_0^A = C_{6v}$ and $G_0 = P3m1$

TABLE SII: With TR and $G_0^A = C_{6v}$, for the space groups G_0 of the moiré system listed above, there are two possible situations with nontrivial moiré topology: (i) for a certain irrep of G_0^A , symmetry-enforced moiré topology must occur and the low-energy moiré bands can be topologically insulating; (ii) for a certain irrep, the low-energy n_d moiré bands are necessarily symmetry-enforced semimetallic. Irreps denoted with a bar (e.g., $\bar{\Gamma}_7$) are spinful, while those without a bar are spinless. The number 2 in the bracket after the irrep indicates the dimension of 2 for the irrep, otherwise they are 1D. The first column lists the irreps of the atomic symmetry group G^A at the Γ point. The corresponding entries show the possible representation from band folding at high-symmetry momenta of space group G_0 with TR. If a cell contains multiple rows, it indicates that multiple representations are allowed for the folded bands at that high-symmetry momentum. For example, for the irrep $\bar{\Gamma}_7$ of G^A and $G_0 = P6mm$, the representation of folded bands at the K_M point can be $\bar{K}_5 \oplus \bar{K}_6(2)$ or $\bar{K}_4 \oplus \bar{K}_6(2)$. The star (\star) label indicates the topologically insulating low-energy moiré bands, while the triangle (\blacktriangle) label indicates guaranteed semi-metallic low-energy moiré bands.

$G_0^A = C_{6v}$	$G_0 = P31m$		
Γ	Γ_M	M_M	$K_M(KA_M)$
Γ_1	Γ_1	$M_1 \oplus M_2$	$K_1 \oplus K_3(2) (KA_1 \oplus KA_3(2))$
Γ_2	Γ_2	$M_1 \oplus M_2$	$K_2 \oplus K_3(2) (KA_2 \oplus KA_3(2))$
Γ_3	Γ_1	$M_1 \oplus M_2$	$K_1 \oplus K_3(2) (KA_1 \oplus KA_3(2))$
Γ_4	Γ_2	$M_1 \oplus M_2$	$K_2 \oplus K_3(2) (KA_2 \oplus KA_3(2))$
$\Gamma_5(2)$	$\Gamma_3(2)$	$M_1 \oplus M_2$	$K_1 \oplus K_3(2) (KA_1 \oplus KA_3(2))$ $K_2 \oplus K_3(2) (KA_2 \oplus KA_3(2))$
$\Gamma_6(2)$	$\Gamma_3(2)$	$M_1 \oplus M_2$	$K_1 \oplus K_3(2) (KA_1 \oplus KA_3(2))$ $K_2 \oplus K_3(2) (KA_2 \oplus KA_3(2))$
$\star\bar{\Gamma}_7(2)$	$\bar{\Gamma}_4\bar{\Gamma}_5(2)$	$\bar{M}_3\bar{M}_4(2)$	$\bar{K}_4 \oplus \bar{K}_6(2) (\bar{KA}_4 \oplus \bar{KA}_6(2))$ $\bar{K}_5 \oplus \bar{K}_6(2) (\bar{KA}_5 \oplus \bar{KA}_6(2))$
$\bar{\Gamma}_8(2)$	$\bar{\Gamma}_6(2)$	$\bar{M}_3\bar{M}_4(2)$	$\bar{K}_4 \oplus \bar{K}_6(2) (\bar{KA}_4 \oplus \bar{KA}_6(2))$ $\bar{K}_5 \oplus \bar{K}_6(2) (\bar{KA}_5 \oplus \bar{KA}_6(2))$
$\bar{\Gamma}_9(2)$	$\bar{\Gamma}_6(2)$	$\bar{M}_3\bar{M}_4(2)$	$\bar{K}_4 \oplus \bar{K}_6(2) (\bar{KA}_4 \oplus \bar{KA}_6(2))$ $\bar{K}_5 \oplus \bar{K}_6(2) (\bar{KA}_5 \oplus \bar{KA}_6(2))$

(a) $G_0^A = C_{6v}$ and $G_0 = P31m$

$G_0^A = C_{6v}$	$G_0 = P3$		
Γ	Γ_M	M_M	$K_M(KA_M)$
Γ_1	Γ_1	$2M_1$	$K_1 \oplus K_2 \oplus K_3 (KA_1 \oplus KA_2 \oplus KA_3)$
Γ_2	Γ_1	$2M_1$	$K_1 \oplus K_2 \oplus K_3 (KA_1 \oplus KA_2 \oplus KA_3)$
Γ_3	Γ_1	$2M_1$	$K_1 \oplus K_2 \oplus K_3 (KA_1 \oplus KA_2 \oplus KA_3)$
Γ_4	Γ_1	$2M_1$	$K_1 \oplus K_2 \oplus K_3 (KA_1 \oplus KA_2 \oplus KA_3)$
$\Gamma_5(2)$	$\Gamma_2\Gamma_3(2)$	$2M_1$	$K_1 \oplus K_2 \oplus K_3 (KA_1 \oplus KA_2 \oplus KA_3)$
$\Gamma_6(2)$	$\Gamma_2\Gamma_3(2)$	$2M_1$	$K_1 \oplus K_2 \oplus K_3 (KA_1 \oplus KA_2 \oplus KA_3)$
$\star\bar{\Gamma}_7(2)$	$\bar{\Gamma}_4\bar{\Gamma}_4(2)$	$\bar{M}_2\bar{M}_2(2)$	$\bar{K}_4 \oplus \bar{K}_5 \oplus \bar{K}_6 (\bar{KA}_4 \oplus \bar{KA}_5 \oplus \bar{KA}_6)$
$\bar{\Gamma}_8(2)$	$\bar{\Gamma}_5\bar{\Gamma}_6(2)$	$\bar{M}_2\bar{M}_2(2)$	$\bar{K}_4 \oplus \bar{K}_5 \oplus \bar{K}_6 (\bar{KA}_4 \oplus \bar{KA}_5 \oplus \bar{KA}_6)$
$\bar{\Gamma}_9(2)$	$\bar{\Gamma}_5\bar{\Gamma}_6(2)$	$\bar{M}_2\bar{M}_2(2)$	$\bar{K}_4 \oplus \bar{K}_5 \oplus \bar{K}_6 (\bar{KA}_4 \oplus \bar{KA}_5 \oplus \bar{KA}_6)$

(b) $G_0^A = C_{6v}$ and $G_0 = P3$

TABLE III: With TR and $G_0^A = C_{6v}$, for the space groups G_0 listed above, there exists at least one irrep for symmetry-enforced topologically insulating moiré bands. In the last columns of panels (a) and (b), we indicate KA_M in parentheses after K_M to highlight that the K_M and KA_M points are related by symmetry. For example, for the irrep $\bar{\Gamma}_7$ of G^A and $G_0 = P31m$, if the representation of folded bands at K_M is $\bar{K}_5 \oplus \bar{K}_6(2)$, the representation at KA_M is $\bar{KA}_5 \oplus \bar{KA}_6(2)$.

$G_0^A = C_{6v}$	$G_0 = Pmm2$			
Γ	Γ_M	\mathbf{Y}_M	\mathbf{X}_M	\mathbf{S}_M
Γ_1	Γ_1	$\mathbf{Y}_1 \oplus \mathbf{Y}_3$	$\mathbf{X}_1 \oplus \mathbf{X}_4$	$\mathbf{S}_1 \oplus \mathbf{S}_2 \oplus \mathbf{S}_3 \oplus \mathbf{S}_4$
Γ_2	Γ_2	$\mathbf{Y}_2 \oplus \mathbf{Y}_4$	$\mathbf{X}_2 \oplus \mathbf{X}_3$	$\mathbf{S}_1 \oplus \mathbf{S}_2 \oplus \mathbf{S}_3 \oplus \mathbf{S}_4$
Γ_3	Γ_3	$\mathbf{Y}_1 \oplus \mathbf{Y}_3$	$\mathbf{X}_1 \oplus \mathbf{X}_4$	$\mathbf{S}_1 \oplus \mathbf{S}_2 \oplus \mathbf{S}_3 \oplus \mathbf{S}_4$
Γ_4	Γ_4	$\mathbf{Y}_2 \oplus \mathbf{Y}_4$	$\mathbf{X}_2 \oplus \mathbf{X}_3$	$\mathbf{S}_1 \oplus \mathbf{S}_2 \oplus \mathbf{S}_3 \oplus \mathbf{S}_4$
$\Delta\Gamma_5(2)$	$\Gamma_1 \oplus \Gamma_2$	$\mathbf{Y}_1 \oplus \mathbf{Y}_3$ $\mathbf{Y}_2 \oplus \mathbf{Y}_4$	$\mathbf{X}_1 \oplus \mathbf{X}_4$ $\mathbf{X}_2 \oplus \mathbf{X}_3$	$\mathbf{S}_1 \oplus \mathbf{S}_2 \oplus \mathbf{S}_3 \oplus \mathbf{S}_4$
$\Delta\Gamma_6(2)$	$\Gamma_3 \oplus \Gamma_4$	$\mathbf{Y}_1 \oplus \mathbf{Y}_3$ $\mathbf{Y}_2 \oplus \mathbf{Y}_4$	$\mathbf{X}_2 \oplus \mathbf{X}_3$ $\mathbf{X}_1 \oplus \mathbf{X}_4$	$\mathbf{S}_1 \oplus \mathbf{S}_2 \oplus \mathbf{S}_3 \oplus \mathbf{S}_4$
$\bar{\Gamma}_7(2)$	$\bar{\Gamma}_5(2)$	$\bar{\mathbf{Y}}_5(2)$	$\bar{\mathbf{X}}_5(2)$	$\bar{\mathbf{S}}_5(2) \oplus \bar{\mathbf{S}}_5(2)$
$\bar{\Gamma}_8(2)$	$\bar{\Gamma}_5(2)$	$\bar{\mathbf{Y}}_5(2)$	$\bar{\mathbf{X}}_5(2)$	$\bar{\mathbf{S}}_5(2) \oplus \bar{\mathbf{S}}_5(2)$
$\bar{\Gamma}_9(2)$	$\bar{\Gamma}_5(2)$	$\bar{\mathbf{Y}}_5(2)$	$\bar{\mathbf{X}}_5(2)$	$\bar{\mathbf{S}}_5(2) \oplus \bar{\mathbf{S}}_5(2)$

(a) $G_0^A = C_{6v}$ and $G_0 = Pmm2$

$G_0^A = C_{6v}$	$G = C2mm$		
Γ	Γ_M	\mathbf{Y}_M	\mathbf{S}_M
Γ_1	Γ_1	$\mathbf{Y}_1 \oplus \mathbf{Y}_4$	$\mathbf{S}_1 \oplus \mathbf{S}_2$
Γ_2	Γ_2	$\mathbf{Y}_2 \oplus \mathbf{Y}_3$	$\mathbf{S}_1 \oplus \mathbf{S}_2$
Γ_3	Γ_3	$\mathbf{Y}_2 \oplus \mathbf{Y}_3$	$\mathbf{S}_1 \oplus \mathbf{S}_2$
Γ_4	Γ_4	$\mathbf{Y}_1 \oplus \mathbf{Y}_4$	$\mathbf{S}_1 \oplus \mathbf{S}_2$
$\Delta\Gamma_5(2)$	$\Gamma_1 \oplus \Gamma_2$	$\mathbf{Y}_1 \oplus \mathbf{Y}_4$ $\mathbf{Y}_2 \oplus \mathbf{Y}_3$	$\mathbf{S}_1 \oplus \mathbf{S}_2$
$\Delta\Gamma_6(2)$	$\Gamma_3 \oplus \Gamma_4$	$\mathbf{Y}_2 \oplus \mathbf{Y}_3$ $\mathbf{Y}_1 \oplus \mathbf{Y}_4$	$\mathbf{S}_1 \oplus \mathbf{S}_2$
$\bar{\Gamma}_7(2)$	$\bar{\Gamma}_5(2)$	$\bar{\mathbf{Y}}_5(2)$	$\bar{\mathbf{S}}_3\bar{\mathbf{S}}_4(2)$
$\bar{\Gamma}_8(2)$	$\bar{\Gamma}_5(2)$	$\bar{\mathbf{Y}}_5(2)$	$\bar{\mathbf{S}}_3\bar{\mathbf{S}}_4(2)$
$\bar{\Gamma}_9(2)$	$\bar{\Gamma}_5(2)$	$\bar{\mathbf{Y}}_5(2)$	$\bar{\mathbf{S}}_3\bar{\mathbf{S}}_4(2)$

(c) $G_0^A = C_{6v}$ and $G_0 = C2mm$

$G_0^A = C_{6v}$	$G_0 = Pm11$			
Γ	Γ_M	\mathbf{Y}_M	\mathbf{X}_M	\mathbf{S}_M
Γ_1	Γ_1	$\mathbf{Y}_1 \oplus \mathbf{Y}_2$	$2\mathbf{X}_1$	$2\mathbf{S}_1 \oplus 2\mathbf{S}_2$
Γ_2	Γ_2	$\mathbf{Y}_1 \oplus \mathbf{Y}_2$	$2\mathbf{X}_2$	$2\mathbf{S}_1 \oplus 2\mathbf{S}_2$
Γ_3	Γ_1	$\mathbf{Y}_1 \oplus \mathbf{Y}_2$	$2\mathbf{X}_1$	$2\mathbf{S}_1 \oplus 2\mathbf{S}_2$
Γ_4	Γ_2	$\mathbf{Y}_1 \oplus \mathbf{Y}_2$	$2\mathbf{X}_2$	$2\mathbf{S}_1 \oplus 2\mathbf{S}_2$
$\Delta\Gamma_5(2)$	$\Gamma_1 \oplus \Gamma_2$	$\mathbf{Y}_1 \oplus \mathbf{Y}_2$	$2\mathbf{X}_1$ $2\mathbf{X}_2$	$2\mathbf{S}_1 \oplus 2\mathbf{S}_2$
$\Delta\Gamma_6(2)$	$\Gamma_1 \oplus \Gamma_2$	$\mathbf{Y}_1 \oplus \mathbf{Y}_2$	$2\mathbf{X}_1$ $2\mathbf{X}_2$	$2\mathbf{S}_1 \oplus 2\mathbf{S}_2$
$\bar{\Gamma}_7(2)$	$\bar{\Gamma}_3\bar{\Gamma}_4(2)$	$\bar{\mathbf{Y}}_3\bar{\mathbf{Y}}_4(2)$	$\bar{\mathbf{X}}_3\bar{\mathbf{X}}_4(2)$	$\bar{\mathbf{S}}_3\bar{\mathbf{S}}_4(2) \oplus \bar{\mathbf{S}}_3\bar{\mathbf{S}}_4(2)$
$\bar{\Gamma}_8(2)$	$\bar{\Gamma}_3\bar{\Gamma}_4(2)$	$\bar{\mathbf{Y}}_3\bar{\mathbf{Y}}_4(2)$	$\bar{\mathbf{X}}_3\bar{\mathbf{X}}_4(2)$	$\bar{\mathbf{S}}_3\bar{\mathbf{S}}_4(2) \oplus \bar{\mathbf{S}}_3\bar{\mathbf{S}}_4(2)$
$\bar{\Gamma}_9(2)$	$\bar{\Gamma}_3\bar{\Gamma}_4(2)$	$\bar{\mathbf{Y}}_3\bar{\mathbf{Y}}_4(2)$	$\bar{\mathbf{X}}_3\bar{\mathbf{X}}_4(2)$	$\bar{\mathbf{S}}_3\bar{\mathbf{S}}_4(2) \oplus \bar{\mathbf{S}}_3\bar{\mathbf{S}}_4(2)$

(b) $G_0^A = C_{6v}$ and $G_0 = Pm11$

$G_0^A = C_{6v}$	$G_0 = P2$			
Γ	Γ_M	\mathbf{Y}_M	\mathbf{A}_M	\mathbf{B}_M
Γ_1	Γ_1	$\mathbf{Y}_1 \oplus \mathbf{Y}_2$	$\mathbf{A}_1 \oplus \mathbf{A}_2$	$\mathbf{B}_1 \oplus \mathbf{B}_2$
Γ_2	Γ_1	$\mathbf{Y}_1 \oplus \mathbf{Y}_2$	$\mathbf{A}_1 \oplus \mathbf{A}_2$	$\mathbf{B}_1 \oplus \mathbf{B}_2$
Γ_3	Γ_2	$\mathbf{Y}_1 \oplus \mathbf{Y}_2$	$\mathbf{A}_1 \oplus \mathbf{A}_2$	$\mathbf{B}_1 \oplus \mathbf{B}_2$
Γ_4	Γ_2	$\mathbf{Y}_1 \oplus \mathbf{Y}_2$	$\mathbf{A}_1 \oplus \mathbf{A}_2$	$\mathbf{B}_1 \oplus \mathbf{B}_2$
$\Delta\Gamma_5(2)$	$2\Gamma_1$	$\mathbf{Y}_1 \oplus \mathbf{Y}_2$	$\mathbf{A}_1 \oplus \mathbf{A}_2$	$\mathbf{B}_1 \oplus \mathbf{B}_2$
$\Delta\Gamma_6(2)$	$2\Gamma_2$	$\mathbf{Y}_1 \oplus \mathbf{Y}_2$	$\mathbf{A}_1 \oplus \mathbf{A}_2$	$\mathbf{B}_1 \oplus \mathbf{B}_2$
$\bar{\Gamma}_7(2)$	$\bar{\Gamma}_3 \oplus \bar{\Gamma}_4$	$\bar{\mathbf{Y}}_3 \oplus \bar{\mathbf{Y}}_4$	$\bar{\mathbf{A}}_3 \oplus \bar{\mathbf{A}}_4$	$\bar{\mathbf{B}}_3 \oplus \bar{\mathbf{B}}_4$
$\bar{\Gamma}_8(2)$	$\bar{\Gamma}_3 \oplus \bar{\Gamma}_4$	$\bar{\mathbf{Y}}_3 \oplus \bar{\mathbf{Y}}_4$	$\bar{\mathbf{A}}_3 \oplus \bar{\mathbf{A}}_4$	$\bar{\mathbf{B}}_3 \oplus \bar{\mathbf{B}}_4$
$\bar{\Gamma}_9(2)$	$\bar{\Gamma}_3 \oplus \bar{\Gamma}_4$	$\bar{\mathbf{Y}}_3 \oplus \bar{\mathbf{Y}}_4$	$\bar{\mathbf{A}}_3 \oplus \bar{\mathbf{A}}_4$	$\bar{\mathbf{B}}_3 \oplus \bar{\mathbf{B}}_4$

(d) $G_0^A = C_{6v}$ and $G_0 = P2$

TABLE SIV: With TR and $G_0^A = C_{6v}$, for the symmorphic space groups G_0 listed above, there exists at least one irrep for which the low-energy moiré bands are necessarily symmetry-enforced semimetallic.

$G_0^A = C_{6v}$					$G_0 = Pba2$				
$G_0^A = C_{6v}$					$G_0 = Pba2$				
Γ	Γ_M	Y_M	X_M	S_M	Γ	Γ_M	Y_M	X_M	S_M
$\Delta\Gamma_1$	Γ_1	$Y_1(2)$	$X_1(2)$	$S_1S_2(2) \oplus S_3S_4(2)$	$\Delta\Gamma_1$	Γ_1	$Y_1 \oplus Y_3$	$X_1(2)$	$2S_1(2)$
$\Delta\Gamma_2$	Γ_2	$Y_1(2)$	$X_1(2)$	$S_1S_2(2) \oplus S_3S_4(2)$	$\Delta\Gamma_2$	Γ_2	$Y_2 \oplus Y_4$	$X_1(2)$	$2S_1(2)$
$\Delta\Gamma_3$	Γ_3	$Y_1(2)$	$X_1(2)$	$S_1S_2(2) \oplus S_3S_4(2)$	$\Delta\Gamma_3$	Γ_3	$Y_1 \oplus Y_3$	$X_1(2)$	$2S_1(2)$
$\Delta\Gamma_4$	Γ_4	$Y_1(2)$	$X_1(2)$	$S_1S_2(2) \oplus S_3S_4(2)$	$\Delta\Gamma_4$	Γ_4	$Y_2 \oplus Y_4$	$X_1(2)$	$2S_1(2)$
$\Gamma_5(2)$	$\Gamma_1 \oplus \Gamma_2$	$Y_1(2)$	$X_1(2)$	$S_1S_2(2) \oplus S_3S_4(2)$	$\Delta\Gamma_5(2)$	$\Gamma_1 \oplus \Gamma_2$	$Y_1 \oplus Y_3$	$X_1(2)$	$2S_1(2)$
$\Gamma_6(2)$	$\Gamma_3 \oplus \Gamma_4$	$Y_1(2)$	$X_1(2)$	$S_1S_2(2) \oplus S_3S_4(2)$	$\Delta\Gamma_6(2)$	$\Gamma_3 \oplus \Gamma_4$	$Y_1 \oplus Y_3$	$X_1(2)$	$2S_1(2)$
$\Delta\bar{\Gamma}_7(2)$	$\bar{\Gamma}_5(2)$	$\bar{Y}_2\bar{Y}_3(2)$ $\bar{Y}_4\bar{Y}_5(2)$	$\bar{X}_2\bar{X}_5(2)$ $\bar{X}_3\bar{X}_4(2)$	$\bar{S}_5\bar{S}_5(4)$	$\Delta\bar{\Gamma}_7(2)$	$\bar{\Gamma}_5(2)$	$\bar{Y}_5(2)$	$\bar{X}_2\bar{X}_5(2)$ $\bar{X}_3\bar{X}_4(2)$	$\bar{S}_2\bar{S}_5(2) \oplus \bar{S}_3\bar{S}_4(2)$
$\Delta\bar{\Gamma}_8(2)$	$\bar{\Gamma}_5(2)$	$\bar{Y}_2\bar{Y}_3(2)$ $\bar{Y}_4\bar{Y}_5(2)$	$\bar{X}_2\bar{X}_5(2)$ $\bar{X}_3\bar{X}_4(2)$	$\bar{S}_5\bar{S}_5(4)$	$\Delta\bar{\Gamma}_8(2)$	$\bar{\Gamma}_5(2)$	$\bar{Y}_5(2)$	$\bar{X}_2\bar{X}_5(2)$ $\bar{X}_3\bar{X}_4(2)$	$\bar{S}_2\bar{S}_5(2) \oplus \bar{S}_3\bar{S}_4(2)$
$\Delta\bar{\Gamma}_9(2)$	$\bar{\Gamma}_5(2)$	$\bar{Y}_2\bar{Y}_3(2)$ $\bar{Y}_4\bar{Y}_5(2)$	$\bar{X}_2\bar{X}_5(2)$ $\bar{X}_3\bar{X}_4(2)$	$\bar{S}_5\bar{S}_5(4)$	$\Delta\bar{\Gamma}_9(2)$	$\bar{\Gamma}_5(2)$	$\bar{Y}_5(2)$	$\bar{X}_2\bar{X}_5(2)$ $\bar{X}_3\bar{X}_4(2)$	$\bar{S}_2\bar{S}_5(2) \oplus \bar{S}_3\bar{S}_4(2)$

(a) $G_0^A = C_{6v}$ and $G_0 = Pba2$

$G_0^A = C_{6v}$					$G_0 = Pma2$				
$G_0^A = C_{6v}$					$G_0 = Pma2$				
Γ	Γ_M	Y_M	X_M	S_M	Γ	Γ_M	Y_M	X_M	S_M
$\Delta\Gamma_1$	Γ_1	$Y_1 \oplus Y_2$	$X_1X_2(2)$	$2S_1S_2(2)$	$\Delta\Gamma_1$	Γ_1	$Y_1 \oplus Y_3$	$X_1(2)$	$2S_1(2)$
$\Delta\Gamma_2$	Γ_2	$Y_1 \oplus Y_2$	$X_1X_2(2)$	$2S_1S_2(2)$	$\Delta\Gamma_2$	Γ_2	$Y_2 \oplus Y_4$	$X_1(2)$	$2S_1(2)$
$\Delta\Gamma_3$	Γ_1	$Y_1 \oplus Y_2$	$X_1X_2(2)$	$2S_1S_2(2)$	$\Delta\Gamma_3$	Γ_3	$Y_1 \oplus Y_3$	$X_1(2)$	$2S_1(2)$
$\Delta\Gamma_4$	Γ_2	$Y_1 \oplus Y_2$	$X_1X_2(2)$	$2S_1S_2(2)$	$\Delta\Gamma_4$	Γ_4	$Y_2 \oplus Y_4$	$X_1(2)$	$2S_1(2)$
$\Gamma_5(2)$	$\Gamma_1 \oplus \Gamma_2$	$Y_1 \oplus Y_2$	$X_1X_2(2)$	$2S_1S_2(2)$	$\Delta\Gamma_5(2)$	$\Gamma_1 \oplus \Gamma_2$	$Y_1 \oplus Y_3$	$X_1(2)$	$2S_1(2)$
$\Gamma_6(2)$	$\Gamma_1 \oplus \Gamma_2$	$Y_1 \oplus Y_2$	$X_1X_2(2)$	$2S_1S_2(2)$	$\Delta\Gamma_6(2)$	$\Gamma_3 \oplus \Gamma_4$	$Y_1 \oplus Y_3$	$X_1(2)$	$2S_1(2)$
$\Delta\bar{\Gamma}_7(2)$	$\bar{\Gamma}_3\bar{\Gamma}_4(2)$	$\bar{Y}_3\bar{Y}_4(2)$	$\bar{X}_3\bar{X}_3(2)$ $\bar{X}_4\bar{X}_4(2)$	$\bar{S}_3\bar{S}_3(2) \oplus \bar{S}_4\bar{S}_4(2)$	$\Delta\bar{\Gamma}_7(2)$	$\bar{\Gamma}_5(2)$	$\bar{Y}_5(2)$	$\bar{X}_2\bar{X}_5(2)$ $\bar{X}_3\bar{X}_4(2)$	$\bar{S}_2\bar{S}_5(2) \oplus \bar{S}_3\bar{S}_4(2)$
$\Delta\bar{\Gamma}_8$	$\bar{\Gamma}_3\bar{\Gamma}_4(2)$	$\bar{Y}_3\bar{Y}_4(2)$	$\bar{X}_3\bar{X}_3(2)$ $\bar{X}_4\bar{X}_4(2)$	$\bar{S}_3\bar{S}_3(2) \oplus \bar{S}_4\bar{S}_4(2)$	$\Delta\bar{\Gamma}_8(2)$	$\bar{\Gamma}_5(2)$	$\bar{Y}_5(2)$	$\bar{X}_2\bar{X}_5(2)$ $\bar{X}_3\bar{X}_4(2)$	$\bar{S}_2\bar{S}_5(2) \oplus \bar{S}_3\bar{S}_4(2)$
$\Delta\bar{\Gamma}_9$	$\bar{\Gamma}_3\bar{\Gamma}_4(2)$	$\bar{Y}_3\bar{Y}_4(2)$	$\bar{X}_3\bar{X}_3(2)$ $\bar{X}_4\bar{X}_4(2)$	$\bar{S}_3\bar{S}_3(2) \oplus \bar{S}_4\bar{S}_4(2)$	$\Delta\bar{\Gamma}_9(2)$	$\bar{\Gamma}_5(2)$	$\bar{Y}_5(2)$	$\bar{X}_2\bar{X}_5(2)$ $\bar{X}_3\bar{X}_4(2)$	$\bar{S}_2\bar{S}_5(2) \oplus \bar{S}_3\bar{S}_4(2)$

(b) $G_0^A = C_{6v}$ and $G_0 = Pma2$

$G_0^A = C_{6v}$					$G_0 = Pb11$				
$G_0^A = C_{6v}$					$G_0 = Pb11$				
Γ	Γ_M	Y_M	X_M	S_M	Γ	Γ_M	Y_M	X_M	S_M
$\Delta\Gamma_1$	Γ_1	$Y_1 \oplus Y_2$	$X_1X_2(2)$	$2S_1S_2(2)$	$\Delta\Gamma_1$	Γ_1	$Y_1 \oplus Y_2$	$X_1X_2(2)$	$2S_1S_2(2)$
$\Delta\Gamma_2$	Γ_2	$Y_1 \oplus Y_2$	$X_1X_2(2)$	$2S_1S_2(2)$	$\Delta\Gamma_2$	Γ_2	$Y_1 \oplus Y_2$	$X_1X_2(2)$	$2S_1S_2(2)$
$\Delta\Gamma_3$	Γ_1	$Y_1 \oplus Y_2$	$X_1X_2(2)$	$2S_1S_2(2)$	$\Delta\Gamma_3$	Γ_1	$Y_1 \oplus Y_2$	$X_1X_2(2)$	$2S_1S_2(2)$
$\Delta\Gamma_4$	Γ_2	$Y_1 \oplus Y_2$	$X_1X_2(2)$	$2S_1S_2(2)$	$\Delta\Gamma_4$	Γ_2	$Y_1 \oplus Y_2$	$X_1X_2(2)$	$2S_1S_2(2)$
$\Gamma_5(2)$	$\Gamma_1 \oplus \Gamma_2$	$Y_1 \oplus Y_2$	$X_1X_2(2)$	$2S_1S_2(2)$	$\Gamma_5(2)$	$\Gamma_1 \oplus \Gamma_2$	$Y_1 \oplus Y_2$	$X_1X_2(2)$	$2S_1S_2(2)$
$\Gamma_6(2)$	$\Gamma_1 \oplus \Gamma_2$	$Y_1 \oplus Y_2$	$X_1X_2(2)$	$2S_1S_2(2)$	$\Gamma_6(2)$	$\Gamma_1 \oplus \Gamma_2$	$Y_1 \oplus Y_2$	$X_1X_2(2)$	$2S_1S_2(2)$
$\Delta\bar{\Gamma}_7(2)$	$\bar{\Gamma}_3\bar{\Gamma}_4(2)$	$\bar{Y}_3\bar{Y}_4(2)$	$\bar{X}_3\bar{X}_3(2)$ $\bar{X}_4\bar{X}_4(2)$	$\bar{S}_3\bar{S}_3(2) \oplus \bar{S}_4\bar{S}_4(2)$	$\Delta\bar{\Gamma}_7(2)$	$\bar{\Gamma}_3\bar{\Gamma}_4(2)$	$\bar{Y}_3\bar{Y}_4(2)$	$\bar{X}_3\bar{X}_3(2)$ $\bar{X}_4\bar{X}_4(2)$	$\bar{S}_3\bar{S}_3(2) \oplus \bar{S}_4\bar{S}_4(2)$
$\Delta\bar{\Gamma}_8$	$\bar{\Gamma}_3\bar{\Gamma}_4(2)$	$\bar{Y}_3\bar{Y}_4(2)$	$\bar{X}_3\bar{X}_3(2)$ $\bar{X}_4\bar{X}_4(2)$	$\bar{S}_3\bar{S}_3(2) \oplus \bar{S}_4\bar{S}_4(2)$	$\Delta\bar{\Gamma}_8$	$\bar{\Gamma}_3\bar{\Gamma}_4(2)$	$\bar{Y}_3\bar{Y}_4(2)$	$\bar{X}_3\bar{X}_3(2)$ $\bar{X}_4\bar{X}_4(2)$	$\bar{S}_3\bar{S}_3(2) \oplus \bar{S}_4\bar{S}_4(2)$
$\Delta\bar{\Gamma}_9$	$\bar{\Gamma}_3\bar{\Gamma}_4(2)$	$\bar{Y}_3\bar{Y}_4(2)$	$\bar{X}_3\bar{X}_3(2)$ $\bar{X}_4\bar{X}_4(2)$	$\bar{S}_3\bar{S}_3(2) \oplus \bar{S}_4\bar{S}_4(2)$	$\Delta\bar{\Gamma}_9$	$\bar{\Gamma}_3\bar{\Gamma}_4(2)$	$\bar{Y}_3\bar{Y}_4(2)$	$\bar{X}_3\bar{X}_3(2)$ $\bar{X}_4\bar{X}_4(2)$	$\bar{S}_3\bar{S}_3(2) \oplus \bar{S}_4\bar{S}_4(2)$

(c) $G_0^A = C_{6v}$ and $G_0 = Pb11$

TABLE SV: With TR and $G_0^A = C_{6v}$, for the nonsymmorphic space groups G_0 listed above, there exists at least one irrep for which the low-energy moiré bands are necessarily symmetry-enforced semimetallic. Irreps with (2) are 2D, those with (4) are 4 dimensional (4D), and otherwise they are 1D.

$G_0^A = C_{3v}$		$G = P3m1$		
Γ	Γ_M	M_M	K_M	
Γ_1	Γ_1	$2M_1$	$K_1 \oplus K_2 \oplus K_3$	
Γ_2	Γ_2	$2M_2$	$K_1 \oplus K_2 \oplus K_3$	
$\Delta\Gamma_3$	Γ_3	$2M_1$ $2M_2$	$K_1 \oplus K_2 \oplus K_3$	
$\star\bar{\Gamma}_4\bar{\Gamma}_5(2)$	$\bar{\Gamma}_4\bar{\Gamma}_5(2)$	$\bar{M}_3\bar{M}_4(2)$	$\bar{K}_4 \oplus \bar{K}_5 \oplus \bar{K}_6$	
$\bar{\Gamma}_6(2)$	$\bar{\Gamma}_6(2)$	$\bar{M}_3\bar{M}_4(2)$	$\bar{K}_4 \oplus \bar{K}_5 \oplus \bar{K}_6$	

TABLE SVI: With TR and $G_0^A = C_{3v}$, for the space group G_0 listed above, there are two possible situations: (i) for a certain irrep of G_0^A , the symmetry-enforced nontrivial moiré topology occur and low-energy moiré bands can be topologically insulating; (ii) for a certain irrep, the low-energy n_d moiré bands are necessarily symmetry-enforced semimetallic.

$G_0^A = C_{3v}$	$G = P31m$		
Γ	Γ_M	\mathbf{M}_M	$\mathbf{K}_M(\mathbf{KA})_M$
Γ_1	Γ_1	$\mathbf{M}_1 \oplus \mathbf{M}_2$	$\mathbf{K}_1 \oplus \mathbf{K}_3(2) (\mathbf{KA}_1 \oplus \mathbf{KA}_3(2))$
Γ_2	Γ_2	$\mathbf{M}_1 \oplus \mathbf{M}_2$	$\mathbf{K}_2 \oplus \mathbf{K}_3(2) (\mathbf{KA}_2 \oplus \mathbf{KA}_3(2))$
$\Gamma_3(2)$	$\Gamma_3(2)$	$\mathbf{M}_1 \oplus \mathbf{M}_2$	$\mathbf{K}_1 \oplus \mathbf{K}_3(2) (\mathbf{KA}_1 \oplus \mathbf{KA}_3(2))$ $\mathbf{K}_2 \oplus \mathbf{K}_3(2) (\mathbf{KA}_2 \oplus \mathbf{KA}_3(2))$
$\star \bar{\Gamma}_4 \bar{\Gamma}_5(2)$	$\bar{\Gamma}_4 \bar{\Gamma}_5(2)$	$\bar{\mathbf{M}}_3 \bar{\mathbf{M}}_4(2)$	$\bar{\mathbf{K}}_4 \oplus \bar{\mathbf{K}}_6(2) (\bar{\mathbf{KA}}_4 \oplus \bar{\mathbf{KA}}_6(2))$ $\bar{\mathbf{K}}_5 \oplus \bar{\mathbf{K}}_6(2) (\bar{\mathbf{KA}}_5 \oplus \bar{\mathbf{KA}}_6(2))$
$\bar{\Gamma}_6(2)$	$\bar{\Gamma}_6(2)$	$\bar{\mathbf{M}}_3 \bar{\mathbf{M}}_4(2)$	$\bar{\mathbf{K}}_4 \oplus \bar{\mathbf{K}}_6(2) (\bar{\mathbf{KA}}_4 \oplus \bar{\mathbf{KA}}_6(2))$ $\bar{\mathbf{K}}_5 \oplus \bar{\mathbf{K}}_6(2) (\bar{\mathbf{KA}}_5 \oplus \bar{\mathbf{KA}}_6(2))$

(a) $G_0^A = C_{3v}$ and $G_0 = P31m$

$G_0^A = C_{3v}$	$G = P3$		
Γ	Γ_M	\mathbf{M}_M	$\mathbf{K}_M(\mathbf{KA})_M$
Γ_1	Γ_1	$2\mathbf{M}_1$	$\mathbf{K}_1 \oplus \mathbf{K}_2 \oplus \mathbf{K}_3 (\mathbf{KA}_1 \oplus \mathbf{KA}_2 \oplus \mathbf{KA}_3)$
Γ_2	Γ_1	$2\mathbf{M}_1$	$\mathbf{K}_1 \oplus \mathbf{K}_2 \oplus \mathbf{K}_3 (\mathbf{KA}_1 \oplus \mathbf{KA}_2 \oplus \mathbf{KA}_3)$
$\Gamma_3(2)$	$\Gamma_2 \Gamma_3(2)$	$2\mathbf{M}_1$	$\mathbf{K}_1 \oplus \mathbf{K}_2 \oplus \mathbf{K}_3 (\mathbf{KA}_1 \oplus \mathbf{KA}_2 \oplus \mathbf{KA}_3)$
$\star \bar{\Gamma}_4 \bar{\Gamma}_5(2)$	$\bar{\Gamma}_4 \bar{\Gamma}_5(2)$	$\bar{\mathbf{M}}_2 \bar{\mathbf{M}}_2(2)$	$\bar{\mathbf{K}}_4 \oplus \bar{\mathbf{K}}_5 \oplus \bar{\mathbf{K}}_6 (\bar{\mathbf{KA}}_4 \oplus \bar{\mathbf{KA}}_5 \oplus \bar{\mathbf{KA}}_6)$
$\bar{\Gamma}_6(2)$	$\bar{\Gamma}_5 \bar{\Gamma}_6(2)$	$\bar{\mathbf{M}}_2 \bar{\mathbf{M}}_2(2)$	$\bar{\mathbf{K}}_4 \oplus \bar{\mathbf{K}}_5 \oplus \bar{\mathbf{K}}_6 (\bar{\mathbf{KA}}_4 \oplus \bar{\mathbf{KA}}_5 \oplus \bar{\mathbf{KA}}_6)$

(b) $G_0^A = C_{3v}$ and $G_0 = P3$ TABLE SVII: With TR and $G_0^A = C_{3v}$, for the space groups G_0 listed above, there exists at least one irrep for symmetry-enforced topologically insulating moiré bands.

$G_0^A = C_{3v}$	$G_0 = Pb11$			
Γ	Γ_M	\mathbf{Y}_M	\mathbf{X}_M	\mathbf{S}_M
$\blacktriangle \Gamma_1$	Γ_1	$\mathbf{Y}_1 \oplus \mathbf{Y}_2$	$\mathbf{X}_1 \mathbf{X}_2(2)$	$2\mathbf{S}_1 \mathbf{S}_2(2)$
$\blacktriangle \Gamma_2$	Γ_2	$\mathbf{Y}_1 \oplus \mathbf{Y}_2$	$\mathbf{X}_1 \mathbf{X}_2(2)$	$2\mathbf{S}_1 \mathbf{S}_2(2)$
$\Gamma_3(2)$	$\Gamma_1 \oplus \Gamma_2$	$\mathbf{Y}_1 \oplus \mathbf{Y}_2$	$\mathbf{X}_1 \mathbf{X}_2(2)$	$2\mathbf{S}_1 \mathbf{S}_2(2)$
$\blacktriangle \bar{\Gamma}_4 \bar{\Gamma}_5(2)$	$\bar{\Gamma}_3 \bar{\Gamma}_4(2)$	$\bar{\mathbf{Y}}_3 \bar{\mathbf{Y}}_4(2)$	$\bar{\mathbf{X}}_3 \bar{\mathbf{X}}_3(2)$ $\bar{\mathbf{X}}_4 \bar{\mathbf{X}}_4(2)$	$\bar{\mathbf{S}}_3 \bar{\mathbf{S}}_3(2) \oplus \bar{\mathbf{S}}_4 \bar{\mathbf{S}}_4(2)$
$\blacktriangle \bar{\Gamma}_6(2)$	$\bar{\Gamma}_3 \bar{\Gamma}_4(2)$	$\bar{\mathbf{Y}}_3 \bar{\mathbf{Y}}_4(2)$	$\bar{\mathbf{X}}_3 \bar{\mathbf{X}}_3(2)$ $\bar{\mathbf{X}}_4 \bar{\mathbf{X}}_4(2)$	$\bar{\mathbf{S}}_3 \bar{\mathbf{S}}_3(2) \oplus \bar{\mathbf{S}}_4 \bar{\mathbf{S}}_4(2)$

(a) $G_0^A = C_{3v}$ and $G_0 = Pb11$

$G_0^A = C_{3v}$	$G_0 = Pm11$			
Γ	Γ_M	\mathbf{Y}_M	\mathbf{X}_M	\mathbf{S}_M
Γ_1	Γ_1	$\mathbf{Y}_1 \oplus \mathbf{Y}_2$	$2\mathbf{X}_1$	$2\mathbf{S}_1 \oplus 2\mathbf{S}_2$
Γ_2	Γ_2	$\mathbf{Y}_1 \oplus \mathbf{Y}_2$	$2\mathbf{X}_2$	$2\mathbf{S}_1 \oplus 2\mathbf{S}_2$
$\blacktriangle \Gamma_3(2)$	$\Gamma_1 \oplus \Gamma_2$	$\mathbf{Y}_1 \oplus \mathbf{Y}_2$	$2\mathbf{X}_1$ $2\mathbf{X}_2$	$2\mathbf{S}_1 \oplus 2\mathbf{S}_2$
$\bar{\Gamma}_4 \bar{\Gamma}_5(2)$	$\bar{\Gamma}_3 \bar{\Gamma}_4(2)$	$\bar{\mathbf{Y}}_3 \bar{\mathbf{Y}}_4(2)$	$\bar{\mathbf{X}}_3 \bar{\mathbf{X}}_4(2)$	$\bar{\mathbf{S}}_3 \bar{\mathbf{S}}_4(2) \oplus \bar{\mathbf{S}}_3 \bar{\mathbf{S}}_4(2)$
$\bar{\Gamma}_6(2)$	$\bar{\Gamma}_3 \bar{\Gamma}_4(2)$	$\bar{\mathbf{Y}}_3 \bar{\mathbf{Y}}_4(2)$	$\bar{\mathbf{X}}_3 \bar{\mathbf{X}}_4(2)$	$\bar{\mathbf{S}}_3 \bar{\mathbf{S}}_4(2) \oplus \bar{\mathbf{S}}_3 \bar{\mathbf{S}}_4(2)$

(b) $G_0^A = C_{3v}$ and $G_0 = Pm11$ TABLE SVIII: With TR and $G_0^A = C_{3v}$, for the space groups G_0 listed above, there exists at least one irrep for which the low-energy n_d moiré bands are necessarily symmetry-enforced semimetallic.

$G_0^A = C_{4v}$	$G_0 = P4mm$		
Γ	Γ_M	\mathbf{M}_M	\mathbf{X}_M
Γ_1	Γ_1	$\mathbf{M}_1 \oplus \mathbf{M}_3 \oplus \mathbf{M}_5(2)$	$\mathbf{X}_1 \oplus \mathbf{X}_3$
Γ_2	Γ_2	$\mathbf{M}_2 \oplus \mathbf{M}_4 \oplus \mathbf{M}_5(2)$	$\mathbf{X}_1 \oplus \mathbf{X}_3$
Γ_3	Γ_3	$\mathbf{M}_1 \oplus \mathbf{M}_3 \oplus \mathbf{M}_5(2)$	$\mathbf{X}_2 \oplus \mathbf{X}_4$
Γ_4	Γ_4	$\mathbf{M}_2 \oplus \mathbf{M}_4 \oplus \mathbf{M}_5(2)$	$\mathbf{X}_2 \oplus \mathbf{X}_4$
$\Delta\Gamma_5(2)$	$\Gamma_5(2)$	$\mathbf{M}_1 \oplus \mathbf{M}_3 \oplus \mathbf{M}_5(2)$ $\mathbf{M}_2 \oplus \mathbf{M}_4 \oplus \mathbf{M}_5(2)$	$\mathbf{X}_1 \oplus \mathbf{X}_3$ $\mathbf{X}_2 \oplus \mathbf{X}_4$
$\bar{\Gamma}_6(2)$	$\bar{\Gamma}_6(2)$	$\mathbf{M}_6(2) \oplus \mathbf{M}_7(2)$	$\bar{\mathbf{X}}_5(2)$
$\bar{\Gamma}_7(2)$	$\bar{\Gamma}_7(2)$	$\mathbf{M}_6(2) \oplus \mathbf{M}_7(2)$	$\bar{\mathbf{X}}_5(2)$

(a) $G_0^A = C_{4v}$ and $G_0 = P4mm$

$G_0^A = C_{4v}$	$G_0 = Pm11$			
Γ	Γ	\mathbf{Y}	\mathbf{X}	\mathbf{S}
Γ_1	Γ_1	$\mathbf{Y}_1 \oplus \mathbf{Y}_2$	$2\mathbf{X}_1$	$2\mathbf{S}_1 \oplus 2\mathbf{S}_2$
Γ_2	Γ_1	$\mathbf{Y}_1 \oplus \mathbf{Y}_2$	$2\mathbf{X}_2$	$2\mathbf{S}_1 \oplus 2\mathbf{S}_2$
Γ_3	Γ_2	$\mathbf{Y}_1 \oplus \mathbf{Y}_2$	$2\mathbf{X}_1$	$2\mathbf{S}_1 \oplus 2\mathbf{S}_2$
Γ_4	Γ_2	$\mathbf{Y}_1 \oplus \mathbf{Y}_2$	$2\mathbf{X}_2$	$2\mathbf{S}_1 \oplus 2\mathbf{S}_2$
$\Delta\Gamma_5(2)$	$\Gamma_1 \oplus \Gamma_2$	$\mathbf{Y}_1 \oplus \mathbf{Y}_2$ $\mathbf{Y}_1 \oplus \mathbf{Y}_2$	$2\mathbf{X}_1$ $2\mathbf{X}_2$	$2\mathbf{S}_1 \oplus 2\mathbf{S}_2$
$\bar{\Gamma}_6(2)$	$\bar{\Gamma}_3\bar{\Gamma}_4(2)$	$\bar{\mathbf{Y}}_3\bar{\mathbf{Y}}_4(2)$	$\bar{\mathbf{X}}_3\bar{\mathbf{X}}_4(2)$	$\bar{\mathbf{S}}_3\bar{\mathbf{S}}_4(2) \oplus \bar{\mathbf{S}}_3\bar{\mathbf{S}}_4(2)$
$\bar{\Gamma}_7(2)$	$\bar{\Gamma}_3\bar{\Gamma}_4(2)$	$\bar{\mathbf{Y}}_3\bar{\mathbf{Y}}_4(2)$	$\bar{\mathbf{X}}_3\bar{\mathbf{X}}_4(2)$	$\bar{\mathbf{S}}_3\bar{\mathbf{S}}_4(2) \oplus \bar{\mathbf{S}}_3\bar{\mathbf{S}}_4(2)$

(c) $G_0^A = C_{4v}$ and $G_0 = Pm11$

$G_0^A = C_{4v}$	$G_0 = P2$			
Γ	Γ_M	\mathbf{Y}_M	\mathbf{A}_M	\mathbf{B}_M
Γ_1	Γ_1	$\mathbf{Y}_1 \oplus \mathbf{Y}_2$	$\mathbf{A}_1 \oplus \mathbf{A}_2$	$\mathbf{B}_1 \oplus \mathbf{B}_2$
Γ_2	Γ_1	$\mathbf{Y}_1 \oplus \mathbf{Y}_2$	$\mathbf{A}_1 \oplus \mathbf{A}_2$	$\mathbf{B}_1 \oplus \mathbf{B}_2$
Γ_3	Γ_2	$\mathbf{Y}_1 \oplus \mathbf{Y}_2$	$\mathbf{A}_1 \oplus \mathbf{A}_2$	$\mathbf{B}_1 \oplus \mathbf{B}_2$
Γ_4	Γ_2	$\mathbf{Y}_1 \oplus \mathbf{Y}_2$	$\mathbf{A}_1 \oplus \mathbf{A}_2$	$\mathbf{B}_1 \oplus \mathbf{B}_2$
$\Delta\Gamma_5(2)$	$2\Gamma_2$	$\mathbf{Y}_1 \oplus \mathbf{Y}_2$	$\mathbf{A}_1 \oplus \mathbf{A}_2$	$\mathbf{B}_1 \oplus \mathbf{B}_2$
$\bar{\Gamma}_6(2)$	$\bar{\Gamma}_3 \oplus \bar{\Gamma}_4$	$\bar{\mathbf{Y}}_3 \oplus \bar{\mathbf{Y}}_4$	$\bar{\mathbf{A}}_3 \oplus \bar{\mathbf{A}}_4$	$\bar{\mathbf{B}}_3 \oplus \bar{\mathbf{B}}_4$
$\bar{\Gamma}_7(2)$	$\bar{\Gamma}_3 \oplus \bar{\Gamma}_4$	$\bar{\mathbf{Y}}_3 \oplus \bar{\mathbf{Y}}_4$	$\bar{\mathbf{A}}_3 \oplus \bar{\mathbf{A}}_4$	$\bar{\mathbf{B}}_3 \oplus \bar{\mathbf{B}}_4$

(e) $G_0^A = C_{4v}$ and $G_0 = P2$

$G_0^A = C_{4v}$	$G_0 = Pmm2$			
Γ	Γ_M	\mathbf{Y}_M	\mathbf{X}_M	\mathbf{S}_M
Γ_1	Γ_1	$\mathbf{Y}_1 \oplus \mathbf{Y}_3$	$\mathbf{X}_1 \oplus \mathbf{X}_4$	$\mathbf{S}_1 \oplus \mathbf{S}_2 \oplus \mathbf{S}_3 \oplus \mathbf{S}_4$
Γ_2	Γ_1	$\mathbf{Y}_1 \oplus \mathbf{Y}_3$	$\mathbf{X}_2 \oplus \mathbf{X}_3$	$\mathbf{S}_1 \oplus \mathbf{S}_2 \oplus \mathbf{S}_3 \oplus \mathbf{S}_4$
Γ_3	Γ_2	$\mathbf{Y}_2 \oplus \mathbf{Y}_4$	$\mathbf{X}_2 \oplus \mathbf{X}_3$	$\mathbf{S}_1 \oplus \mathbf{S}_2 \oplus \mathbf{S}_3 \oplus \mathbf{S}_4$
Γ_4	Γ_2	$\mathbf{Y}_2 \oplus \mathbf{Y}_4$	$\mathbf{X}_1 \oplus \mathbf{X}_4$	$\mathbf{S}_1 \oplus \mathbf{S}_2 \oplus \mathbf{S}_3 \oplus \mathbf{S}_4$
$\Delta\Gamma_5(2)$	$\Gamma_3 \oplus \Gamma_4$	$\mathbf{Y}_1 \oplus \mathbf{Y}_3$ $\mathbf{Y}_2 \oplus \mathbf{Y}_4$	$\mathbf{X}_1 \oplus \mathbf{X}_4$ $\mathbf{X}_2 \oplus \mathbf{X}_3$	$\mathbf{S}_1 \oplus \mathbf{S}_2 \oplus \mathbf{S}_3 \oplus \mathbf{S}_4$
$\bar{\Gamma}_6(2)$	$\bar{\Gamma}_5(2)$	$\bar{\mathbf{Y}}_5(2)$	$\bar{\mathbf{X}}_5(2)$	$\bar{\mathbf{S}}_5(2) \oplus \bar{\mathbf{S}}_5(2)$
$\bar{\Gamma}_7(2)$	$\bar{\Gamma}_5(2)$	$\bar{\mathbf{Y}}_5(2)$	$\bar{\mathbf{X}}_5(2)$	$\bar{\mathbf{S}}_5(2) \oplus \bar{\mathbf{S}}_5(2)$

(b) $G_0^A = C_{4v}$ and $G_0 = Pmm2$

$G_0^A = C_{4v}$	$G_0 = C2mm$		
Γ	Γ_M	\mathbf{Y}_M	\mathbf{S}_M
Γ_1	Γ_1	$\mathbf{Y}_1 \oplus \mathbf{Y}_4$	$\mathbf{S}_1 \oplus \mathbf{S}_2$
Γ_2	Γ_1	$\mathbf{Y}_1 \oplus \mathbf{Y}_4$	$\mathbf{S}_1 \oplus \mathbf{S}_2$
Γ_3	Γ_2	$\mathbf{Y}_2 \oplus \mathbf{Y}_3$	$\mathbf{S}_1 \oplus \mathbf{S}_2$
Γ_4	Γ_2	$\mathbf{Y}_2 \oplus \mathbf{Y}_3$	$\mathbf{S}_1 \oplus \mathbf{S}_2$
$\Delta\Gamma_5(2)$	$\Gamma_3 \oplus \Gamma_4$	$\mathbf{Y}_2 \oplus \mathbf{Y}_3$ $\mathbf{Y}_1 \oplus \mathbf{Y}_4$	$\mathbf{S}_1 \oplus \mathbf{S}_2$
$\bar{\Gamma}_6(2)$	$\bar{\Gamma}_5(2)$	$\bar{\mathbf{Y}}_5(2)$	$\bar{\mathbf{S}}_3\bar{\mathbf{S}}_4(2)$
$\bar{\Gamma}_7(2)$	$\bar{\Gamma}_5(2)$	$\bar{\mathbf{Y}}_5(2)$	$\bar{\mathbf{S}}_3\bar{\mathbf{S}}_4(2)$

(d) $G_0^A = C_{4v}$ and $G_0 = C2mm$ TABLE SIX: With TR and $G_0^A = C_{4v}$, for the symmorphic space groups G_0 listed above, there exists at least one irrep for which the low-energy n_d moiré bands are necessarily symmetry-enforced semimetallic.

$G_0^A = C_{4v}$	$G_0 = P4bm$		
Γ	Γ_M	M_M	X_M
$\blacktriangle \Gamma_1$	Γ_1	$M_1 \oplus M_3 \oplus M_5(2)$	$X_1(2)$
$\blacktriangle \Gamma_2$	Γ_2	$M_2 \oplus M_4 \oplus M_5(2)$	$X_1(2)$
$\blacktriangle \Gamma_3$	Γ_3	$M_1 \oplus M_3 \oplus M_5(2)$	$X_1(2)$
$\blacktriangle \Gamma_4$	Γ_4	$M_2 \oplus M_4 \oplus M_5(2)$	$X_1(2)$
$\Gamma_5(2)$	$\Gamma_5(2)$	$M_1 \oplus M_3 \oplus M_5(2)$ $M_2 \oplus M_4 \oplus M_5(2)$	$X_1(2)$
$\blacktriangle \bar{\Gamma}_6(2)$	$\bar{\Gamma}_6(2)$	$\bar{M}_6(2) \oplus \bar{M}_7(2)$	$\bar{X}_2 \bar{X}_3(2)$ $\bar{X}_4 \bar{X}_5(2)$
$\blacktriangle \bar{\Gamma}_7(2)$	$\bar{\Gamma}_7(2)$	$\bar{M}_6(2) \oplus \bar{M}_7(2)$	$\bar{X}_2 \bar{X}_3(2)$ $\bar{X}_4 \bar{X}_5(2)$

(a) $G_0^A = C_{4v}$ and $G_0 = P4bm$

$G_0^A = C_{4v}$	$G_0 = Pma2$			
Γ	Γ	Y	X	S
$\blacktriangle \Gamma_1$	Γ_1	$Y_1 \oplus Y_3$	$X_1(2)$	$2S_1(2)$
$\blacktriangle \Gamma_2$	Γ_1	$Y_1 \oplus Y_3$	$X_1(2)$	$2S_1(2)$
$\blacktriangle \Gamma_3$	Γ_2	$Y_2 \oplus Y_4$	$X_1(2)$	$2S_1(2)$
$\blacktriangle \Gamma_4$	Γ_2	$Y_2 \oplus Y_4$	$X_1(2)$	$2S_1(2)$
$\blacktriangle \Gamma_5(2)$	$\Gamma_3 \oplus \Gamma_4$	$Y_1 \oplus Y_3$ $Y_2 \oplus Y_4$	$X_1(2)$	$2S_1(2)$
$\blacktriangle \bar{\Gamma}_6(2)$	$\bar{\Gamma}_5(2)$	$\bar{Y}_5(2)$ $\bar{Y}_5(2)$	$\bar{X}_2 \bar{X}_5(2)$ $\bar{X}_3 \bar{X}_4(2)$	$\bar{S}_2 \bar{S}_5(2) \oplus \bar{S}_3 \bar{S}_4(2)$
$\blacktriangle \bar{\Gamma}_7(2)$	$\bar{\Gamma}_5(2)$	$\bar{Y}_5(2)$ $\bar{Y}_5(2)$	$\bar{X}_2 \bar{X}_5(2)$ $\bar{X}_3 \bar{X}_4(2)$	$\bar{S}_2 \bar{S}_5(2) \oplus \bar{S}_3 \bar{S}_4(2)$

(c) $G_0^A = C_{4v}$ and $G_0 = Pma2$

$G_0^A = C_{4v}$	$G_0 = Pba2$			
Γ	Γ	Y	X	S
$\blacktriangle \Gamma_1$	Γ_1	$Y_1(2)$	$X_1(2)$	$S_1 S_2(2) \oplus S_3 S_4(2)$
$\blacktriangle \Gamma_2$	Γ_1	$Y_1(2)$	$X_1(2)$	$S_1 S_2(2) \oplus S_3 S_4(2)$
$\blacktriangle \Gamma_3$	Γ_2	$Y_1(2)$	$X_1(2)$	$S_1 S_2(2) \oplus S_3 S_4(2)$
$\blacktriangle \Gamma_4$	Γ_2	$Y_1(2)$	$X_1(2)$	$S_1 S_2(2) \oplus S_3 S_4(2)$
$\Gamma_5(2)$	$\Gamma_3 \oplus \Gamma_4$	$Y_1(2)$	$X_1(2)$	$S_1 S_2(2) \oplus S_3 S_4(2)$
$\blacktriangle \bar{\Gamma}_6(2)$	$\bar{\Gamma}_5(2)$	$\bar{Y}_2 \bar{Y}_3(2)$ $\bar{Y}_4 \bar{Y}_5(2)$	$\bar{X}_2 \bar{X}_5(2)$ $\bar{X}_3 \bar{X}_4(2)$	$\bar{S}_5 \bar{S}_5(4)$
$\blacktriangle \bar{\Gamma}_7(2)$	$\bar{\Gamma}_5(2)$	$\bar{Y}_2 \bar{Y}_3(2)$ $\bar{Y}_4 \bar{Y}_5(2)$	$\bar{X}_2 \bar{X}_5(2)$ $\bar{X}_3 \bar{X}_4(2)$	$\bar{S}_5 \bar{S}_5(4)$

(b) $G_0^A = C_{4v}$ and $G_0 = Pba2$

$G_0^A = C_{4v}$	$G_0 = Pb11$			
Γ	Γ_M	Y_M	X_M	S_M
$\blacktriangle \Gamma_1$	Γ_1	$Y_1 \oplus Y_2$	$X_1 X_2(2)$	$2S_1 S_2(2)$
$\blacktriangle \Gamma_2$	Γ_1	$Y_1 \oplus Y_2$	$X_1 X_2(2)$	$2S_1 S_2(2)$
$\blacktriangle \Gamma_3$	Γ_2	$Y_1 \oplus Y_2$	$X_1 X_2(2)$	$2S_1 S_2(2)$
$\blacktriangle \Gamma_4$	Γ_2	$Y_1 \oplus Y_2$	$X_1 X_2(2)$	$2S_1 S_2(2)$
$\Gamma_5(2)$	$\Gamma_1 \oplus \Gamma_2$	$Y_1 \oplus Y_2$	$X_1 X_2(2)$	$2S_1 S_2(2)$
$\blacktriangle \bar{\Gamma}_6(2)$	$\bar{\Gamma}_3 \bar{\Gamma}_4(2)$	$\bar{Y}_3 \bar{Y}_4(2)$ $\bar{Y}_3 \bar{Y}_4(2)$	$\bar{X}_3 \bar{X}_3(2)$ $\bar{X}_4 \bar{X}_4(2)$	$\bar{S}_3 \bar{S}_3(2) \oplus \bar{S}_4 \bar{S}_4(2)$
$\blacktriangle \bar{\Gamma}_7(2)$	$\bar{\Gamma}_3 \bar{\Gamma}_4(2)$	$\bar{Y}_3 \bar{Y}_4(2)$ $\bar{Y}_3 \bar{Y}_4(2)$	$\bar{X}_3 \bar{X}_3(2)$ $\bar{X}_4 \bar{X}_4(2)$	$\bar{S}_3 \bar{S}_3(2) \oplus \bar{S}_4 \bar{S}_4(2)$

(d) $G_0^A = C_{4v}$ and $G_0 = Pb11$

TABLE SX: With TR and $G_0^A = C_{4v}$, for the nonsymmorphic space groups G_0 listed above, there exists at least one irrep for which the low-energy n_d moiré bands are necessarily symmetry-enforced semimetallic.

$G_0^A = C_{2v}$	$G_0 = Pba2$			
Γ	Γ_M	\mathbf{Y}_M	\mathbf{X}_M	\mathbf{S}_M
$\mathbf{\Delta}\Gamma_1$	Γ_1	$\mathbf{Y}_1(2)$	$\mathbf{X}_1(2)$	$\mathbf{S}_1\mathbf{S}_2(2) \oplus \mathbf{S}_3\mathbf{S}_4(2)$
$\mathbf{\Delta}\Gamma_2$	Γ_2	$\mathbf{Y}_1(2)$	$\mathbf{X}_1(2)$	$\mathbf{S}_1\mathbf{S}_2(2) \oplus \mathbf{S}_3\mathbf{S}_4(2)$
$\mathbf{\Delta}\Gamma_3$	Γ_3	$\mathbf{Y}_1(2)$	$\mathbf{X}_1(2)$	$\mathbf{S}_1\mathbf{S}_2(2) \oplus \mathbf{S}_3\mathbf{S}_4(2)$
$\mathbf{\Delta}\Gamma_4$	Γ_4	$\mathbf{Y}_1(2)$	$\mathbf{X}_1(2)$	$\mathbf{S}_1\mathbf{S}_2(2) \oplus \mathbf{S}_3\mathbf{S}_4(2)$
$\mathbf{\Delta}\bar{\Gamma}_5(2)$	$\bar{\Gamma}_5(2)$	$\bar{\mathbf{Y}}_2\bar{\mathbf{Y}}_3(2)$ $\bar{\mathbf{Y}}_4\bar{\mathbf{Y}}_5(2)$	$\bar{\mathbf{X}}_2\bar{\mathbf{X}}_5(2)$ $\bar{\mathbf{X}}_3\bar{\mathbf{X}}_4(2)$	$\bar{\mathbf{S}}_5\bar{\mathbf{S}}_5(4)$

(a) $G_0^A = C_{2v}$ and $G_0 = Pba2$

$G_0^A = C_{2v}$	$G_0 = Pb11$			
Γ	Γ_M	\mathbf{Y}_M	\mathbf{X}_M	\mathbf{S}_M
$\mathbf{\Delta}\Gamma_1$	Γ_1	$\mathbf{Y}_1 \oplus \mathbf{Y}_2$	$\mathbf{X}_1\mathbf{X}_2(2)$	$2\mathbf{S}_1\mathbf{S}_2(2)$
$\mathbf{\Delta}\Gamma_2$	Γ_1	$\mathbf{Y}_1 \oplus \mathbf{Y}_2$	$\mathbf{X}_1\mathbf{X}_2(2)$	$2\mathbf{S}_1\mathbf{S}_2(2)$
$\mathbf{\Delta}\Gamma_3$	Γ_2	$\mathbf{Y}_1 \oplus \mathbf{Y}_2$	$\mathbf{X}_1\mathbf{X}_2(2)$	$2\mathbf{S}_1\mathbf{S}_2(2)$
$\mathbf{\Delta}\Gamma_4$	Γ_2	$\mathbf{Y}_1 \oplus \mathbf{Y}_2$	$\mathbf{X}_1\mathbf{X}_2(2)$	$2\mathbf{S}_1\mathbf{S}_2(2)$
$\mathbf{\Delta}\bar{\Gamma}_5(2)$	$\bar{\Gamma}_3\bar{\Gamma}_4(2)$	$\bar{\mathbf{Y}}_3\bar{\mathbf{Y}}_4(2)$	$\bar{\mathbf{X}}_3\bar{\mathbf{X}}_3(2)$ $\bar{\mathbf{X}}_4\bar{\mathbf{X}}_4(2)$	$\bar{\mathbf{S}}_3\bar{\mathbf{S}}_3(2) \oplus \bar{\mathbf{S}}_4\bar{\mathbf{S}}_4(2)$

(c) $G_0^A = C_{2v}$ and $G_0 = Pb11$

$G_0^A = C_{2v}$	$G_0 = Pma2$			
Γ	Γ_M	\mathbf{Y}_M	\mathbf{X}_M	\mathbf{S}_M
$\mathbf{\Delta}\Gamma_1$	Γ_1	$\mathbf{Y}_1 \oplus \mathbf{Y}_3$	$\mathbf{X}_1(2)$	$2\mathbf{S}_1(2)$
$\mathbf{\Delta}\Gamma_2$	Γ_2	$\mathbf{Y}_2 \oplus \mathbf{Y}_4$	$\mathbf{X}_1(2)$	$2\mathbf{S}_1(2)$
$\mathbf{\Delta}\Gamma_3$	Γ_3	$\mathbf{Y}_1 \oplus \mathbf{Y}_3$	$\mathbf{X}_1(2)$	$2\mathbf{S}_1(2)$
$\mathbf{\Delta}\Gamma_4$	Γ_4	$\mathbf{Y}_2 \oplus \mathbf{Y}_4$	$\mathbf{X}_1(2)$	$2\mathbf{S}_1(2)$
$\mathbf{\Delta}\bar{\Gamma}_5(2)$	$\bar{\Gamma}_5(2)$	$\bar{\mathbf{Y}}_5(2)$	$\bar{\mathbf{X}}_2\bar{\mathbf{X}}_5(2)$ $\bar{\mathbf{X}}_3\bar{\mathbf{X}}_4(2)$	$\bar{\mathbf{S}}_2\bar{\mathbf{S}}_5(2) \oplus \bar{\mathbf{S}}_3\bar{\mathbf{S}}_4(2)$

(b) $G_0^A = C_{2v}$ and $G_0 = Pma2$

TABLE SXI: With TR and $G_0^A = C_{2v}$, for the nonsymmorphic space groups G_0 listed above, there exists at least one irrep for which the low-energy moiré bands are necessarily symmetry-enforced semimetallic.

$G_0^A = C_s$	$G_0 = Pb11$			
Γ	Γ_M	\mathbf{Y}_M	\mathbf{X}_M	\mathbf{S}_M
$\mathbf{\Delta}\Gamma_1$	Γ_1	$\mathbf{Y}_1 \oplus \mathbf{Y}_2$	$\mathbf{X}_1\mathbf{X}_2(2)$	$2\mathbf{S}_1\mathbf{S}_2(2)$
$\mathbf{\Delta}\Gamma_2$	Γ_2	$\mathbf{Y}_1 \oplus \mathbf{Y}_2$	$\mathbf{X}_1\mathbf{X}_2(2)$	$2\mathbf{S}_1\mathbf{S}_2(2)$
$\mathbf{\Delta}\bar{\Gamma}_3\bar{\Gamma}_4(2)$	$\bar{\Gamma}_3\bar{\Gamma}_4(2)$	$\bar{\mathbf{Y}}_3\bar{\mathbf{Y}}_4(2)$	$\bar{\mathbf{X}}_3\bar{\mathbf{X}}_3(2)$ $\bar{\mathbf{X}}_4\bar{\mathbf{X}}_4(2)$	$\bar{\mathbf{S}}_3\bar{\mathbf{S}}_3(2) \oplus \bar{\mathbf{S}}_4\bar{\mathbf{S}}_4(2)$

TABLE SXII: With TR and $G_0^A = C_s$, for the space groups $Pb11$, there exists at least one irrep for which the low-energy moiré bands are necessarily symmetry-enforced semimetallic.

$G_0^A = C_6$	$G_0 = P6$		
Γ	Γ_M	M_M	K_M
Γ_1	Γ_1	$M_1 \oplus M_2$	$K_1 \oplus K_2 \oplus K_3$
Γ_2	Γ_2	$M_1 \oplus M_2$	$K_1 \oplus K_2 \oplus K_3$
$\blacktriangle \Gamma_3 \Gamma_5(2)$	$\Gamma_3 \Gamma_5(2)$	$M_1 \oplus M_2$	$K_1 \oplus K_2 \oplus K_3$
$\blacktriangle \Gamma_4 \Gamma_6(2)$	$\Gamma_4 \Gamma_6(2)$	$M_1 \oplus M_2$	$K_1 \oplus K_2 \oplus K_3$
$\star \bar{\Gamma}_7 \bar{\Gamma}_8(2)$	$\bar{\Gamma}_7 \bar{\Gamma}_8(2)$	$\bar{M}_3 \bar{M}_4(2)$	$\bar{K}_4 \oplus \bar{K}_5 \oplus \bar{K}_6$
$\bar{\Gamma}_{10} \bar{\Gamma}_{11}(2)$	$\bar{\Gamma}_{10} \bar{\Gamma}_{11}(2)$	$\bar{M}_3 \bar{M}_4(2)$	$\bar{K}_4 \oplus \bar{K}_5 \oplus \bar{K}_6$
$\bar{\Gamma}_9 \bar{\Gamma}_{12}(2)$	$\bar{\Gamma}_9 \bar{\Gamma}_{12}(2)$	$\bar{M}_3 \bar{M}_4(2)$	$\bar{K}_4 \oplus \bar{K}_5 \oplus \bar{K}_6$

(a) $G_0^A = C_6$ and $G_0 = P6$

$G_0^A = C_6$	$G_0 = P2$			
Γ	Γ_M	Y_M	A_M	B_M
Γ_1	Γ_1	$Y_1 \oplus Y_2$	$A_1 \oplus A_2$	$B_1 \oplus B_2$
Γ_2	Γ_1	$Y_1 \oplus Y_2$	$A_1 \oplus A_2$	$B_1 \oplus B_2$
$\blacktriangle \Gamma_3 \Gamma_5(2)$	$2\Gamma_1$	$Y_1 \oplus Y_2$	$A_1 \oplus A_2$	$B_1 \oplus B_2$
$\blacktriangle \Gamma_4 \Gamma_6(2)$	$2\Gamma_2$	$Y_1 \oplus Y_2$	$A_1 \oplus A_2$	$B_1 \oplus B_2$
$\bar{\Gamma}_7 \bar{\Gamma}_8(2)$	$\bar{\Gamma}_3 \oplus \bar{\Gamma}_4$	$\bar{Y}_3 \oplus \bar{Y}_4$	$\bar{A}_3 \oplus \bar{A}_4$	$\bar{B}_3 \oplus \bar{B}_4$
$\bar{\Gamma}_{10} \bar{\Gamma}_{11}(2)$	$\bar{\Gamma}_3 \oplus \bar{\Gamma}_4$	$\bar{Y}_3 \oplus \bar{Y}_4$	$\bar{A}_3 \oplus \bar{A}_4$	$\bar{B}_3 \oplus \bar{B}_4$
$\bar{\Gamma}_9 \bar{\Gamma}_{12}(2)$	$\bar{\Gamma}_3 \oplus \bar{\Gamma}_4$	$\bar{Y}_3 \oplus \bar{Y}_4$	$\bar{A}_3 \oplus \bar{A}_4$	$\bar{B}_3 \oplus \bar{B}_4$

(b) $G_0^A = C_6$ and $G_0 = P2$

$G_0^A = C_6$	$G_0 = P3$		
Γ	Γ_M	M_M	$K_M(KA)_M$
Γ_1	Γ_1	$2M_1$	$K_1 \oplus K_2 \oplus K_3 (KA_1 \oplus KA_2 \oplus KA_3)$
Γ_2	Γ_1	$2M_1$	$K_1 \oplus K_2 \oplus K_3 (KA_1 \oplus KA_2 \oplus KA_3)$
$\Gamma_3 \Gamma_5(2)$	$\Gamma_2 \Gamma_3(2)$	$2M_1$	$K_1 \oplus K_2 \oplus K_3 (KA_1 \oplus KA_2 \oplus KA_3)$
$\Gamma_4 \Gamma_6(2)$	$\Gamma_2 \Gamma_3(2)$	$2M_1$	$K_1 \oplus K_2 \oplus K_3 (KA_1 \oplus KA_2 \oplus KA_3)$
$\star \bar{\Gamma}_7 \bar{\Gamma}_8(2)$	$\bar{\Gamma}_4 \bar{\Gamma}_4(2)$	$\bar{M}_2 \bar{M}_2(2)$	$\bar{K}_4 \oplus \bar{K}_5 \oplus \bar{K}_6 (\bar{KA}_4 \oplus \bar{KA}_5 \oplus \bar{KA}_6)$
$\bar{\Gamma}_{10} \bar{\Gamma}_{11}(2)$	$\bar{\Gamma}_5 \bar{\Gamma}_6(2)$	$\bar{M}_2 \bar{M}_2(2)$	$\bar{K}_4 \oplus \bar{K}_5 \oplus \bar{K}_6 (\bar{KA}_4 \oplus \bar{KA}_5 \oplus \bar{KA}_6)$
$\bar{\Gamma}_9 \bar{\Gamma}_{12}(2)$	$\bar{\Gamma}_5 \bar{\Gamma}_6(2)$	$\bar{M}_2 \bar{M}_2(2)$	$\bar{K}_4 \oplus \bar{K}_5 \oplus \bar{K}_6 (\bar{KA}_4 \oplus \bar{KA}_5 \oplus \bar{KA}_6)$

(c) $G_0^A = C_6$ and $G_0 = P3$ TABLE SXIII: With TR and $G_0^A = C_6$, for the space groups G_0 listed above, there exists at least one irrep for symmetry-enforced topologically insulating or semimetallic moiré bands.

$G_0^A = C_4$	$G_0 = P2$			
Γ	Γ_M	Y_M	A_M	B_M
Γ_1	Γ_1	$Y_1 \oplus Y_2$	$A_1 \oplus A_2$	$B_1 \oplus B_2$
Γ_2	Γ_1	$Y_1 \oplus Y_2$	$A_1 \oplus A_2$	$B_1 \oplus B_2$
$\blacktriangle \Gamma_3 \Gamma_4(2)$	$2\Gamma_2$	$Y_1 \oplus Y_2$	$A_1 \oplus A_2$	$B_1 \oplus B_2$
$\bar{\Gamma}_5 \bar{\Gamma}_7(2)$	$\bar{\Gamma}_3 \oplus \bar{\Gamma}_4$	$\bar{Y}_3 \oplus \bar{Y}_4$	$\bar{A}_3 \oplus \bar{A}_4$	$\bar{B}_3 \oplus \bar{B}_4$
$\bar{\Gamma}_6 \bar{\Gamma}_8(2)$	$\bar{\Gamma}_3 \oplus \bar{\Gamma}_4$	$\bar{Y}_3 \oplus \bar{Y}_4$	$\bar{A}_3 \oplus \bar{A}_4$	$\bar{B}_3 \oplus \bar{B}_4$

TABLE SXIV: With TR and $G_0^A = C_4$, for the space groups $P2$, there exists at least one irrep for which the low-energy moiré bands are necessarily symmetry-enforced semimetallic.

$G_0^A = C_3$	$G_0 = P3$		
	Γ_M	M_M	$K_M(KA)_M$
Γ_1	Γ_1	$2M_1$	$K_1 \oplus K_2 \oplus K_3 (KA_1 \oplus KA_2 \oplus KA_3)$
$\Gamma_2 \Gamma_3(2)$	$\Gamma_2 \Gamma_3(2)$	$2M_1$	$K_1 \oplus K_2 \oplus K_3 (KA_1 \oplus KA_2 \oplus KA_3)$
$\star \bar{\Gamma}_4 \bar{\Gamma}_4(2)$	$\bar{\Gamma}_4 \bar{\Gamma}_4(2)$	$\bar{M}_2 \bar{M}_2(2)$	$\bar{K}_4 \oplus \bar{K}_5 \oplus \bar{K}_6 (\bar{KA}_4 \oplus \bar{KA}_5 \oplus \bar{KA}_6)$
$\bar{\Gamma}_5 \bar{\Gamma}_6(2)$	$\bar{\Gamma}_5 \bar{\Gamma}_6(2)$	$\bar{M}_2 \bar{M}_2(2)$	$\bar{K}_4 \oplus \bar{K}_5 \oplus \bar{K}_6 (\bar{KA}_4 \oplus \bar{KA}_5 \oplus \bar{KA}_6)$

TABLE SXV: With TR and $G_0^A = C_3$, for the space group $P3$, there exists at least one irrep for symmetry-enforced topologically insulating moiré bands.

C_{6v}	\mathcal{E}	C_{3z}, C_{3z}^{-1}	C_{2z}	C_{6z}, C_{6z}^{-1}	$C_{3z}M_xC_{3z}^{-1}, M_x, C_{3z}^{-1}M_xC_{3z}$	$C_{3z}M_yC_{3z}^{-1}, M_y, C_{3z}^{-1}M_yC_{3z}$
Γ_1	1	1	1	1	1	1
Γ_2	1	1	1	1	-1	-1
Γ_3	1	1	-1	-1	-1	1
Γ_4	1	1	-1	-1	1	-1
Γ_5	2	-1	2	-1	0	0
Γ_6	2	-1	-2	1	0	0
$\bar{\Gamma}_7$	2	-1	0	0	0	0
$\bar{\Gamma}_8$	2	1	0	$-\sqrt{3}$	0	0
$\bar{\Gamma}_9$	2	1	0	$\sqrt{3}$	0	0

(a) The character table for point group C_{6v} .

C_{4v}	\mathcal{E}	C_{2z}	C_{4z}, C_{4z}^{-1}	M_y, M_x	$C_{4z}M_x, M_xC_{4z}$
Γ_1	1	1	1	1	1
Γ_2	1	1	-1	1	-1
Γ_3	1	1	-1	-1	1
Γ_4	1	1	1	-1	-1
Γ_5	2	-2	0	0	0
$\bar{\Gamma}_6$	2	0	$-\sqrt{2}$	0	0
$\bar{\Gamma}_7$	2	0	$\sqrt{2}$	0	0

(b) The character table for point group C_{4v} .

C_{3v}	\mathcal{E}	C_{3z}, C_{3z}^{-1}	$C_{3z}M_yC_{3z}^{-1}, M_y, C_{3z}^{-1}M_yC_{3z}$
Γ_1	1	1	1
Γ_2	1	1	-1
Γ_3	2	-1	0
$\bar{\Gamma}_4$	1	-1	$-i$
$\bar{\Gamma}_5$	1	-1	$+i$
$\bar{\Gamma}_6$	2	1	0

(c) The character table for point group C_{3v} .

C_{2v}	\mathcal{E}	C_{2z}	M_x	M_y	C_s	\mathcal{E}	M_x
Γ_1	1	1	1	1	Γ_1	1	1
Γ_2	1	1	-1	-1	Γ_2	1	-1
Γ_3	1	-1	-1	1	$\bar{\Gamma}_3$	1	$-i$
Γ_4	1	-1	1	-1	$\bar{\Gamma}_4$	1	i
$\bar{\Gamma}_5$	2	0	0	0			

(d) The character table for point group C_{2v} .(e) The character table for point group C_s , where $C_s = C_{1v}$ TABLE SXVI: The character table for the point group C_{nv} with $n = 1, 2, 3, 4, 6$.

C_6	\mathcal{E}	C_{3z}	C_{3z}^{-1}	C_{2z}	C_{6z}^{-1}	C_{6z}
Γ_1	1	1	1	1	1	1
Γ_2	1	1	1	-1	-1	-1
Γ_3	1	$e^{\frac{i2\pi}{3}}$	$e^{-\frac{i2\pi}{3}}$	1	$e^{\frac{i2\pi}{3}}$	$e^{-\frac{i2\pi}{3}}$
Γ_4	1	$e^{\frac{i2\pi}{3}}$	$e^{-\frac{i2\pi}{3}}$	-1	$e^{-\frac{i\pi}{3}}$	$e^{\frac{i\pi}{3}}$
Γ_5	1	$e^{-\frac{i2\pi}{3}}$	$e^{\frac{i2\pi}{3}}$	1	$e^{-\frac{i2\pi}{3}}$	$e^{\frac{i2\pi}{3}}$
Γ_6	1	$e^{-\frac{i2\pi}{3}}$	$e^{\frac{i2\pi}{3}}$	-1	$e^{\frac{i\pi}{3}}$	$e^{-\frac{i\pi}{3}}$
$\bar{\Gamma}_7$	1	-1	-1	$-i$	i	$-i$
$\bar{\Gamma}_8$	1	-1	-1	i	$-i$	i
$\bar{\Gamma}_9$	1	$e^{-\frac{i\pi}{3}}$	$e^{\frac{i\pi}{3}}$	$-i$	$e^{-\frac{i5\pi}{6}}$	$e^{\frac{i5\pi}{6}}$
$\bar{\Gamma}_{10}$	1	$e^{-\frac{i\pi}{3}}$	$e^{\frac{i\pi}{3}}$	i	$e^{\frac{i\pi}{6}}$	$e^{-\frac{i\pi}{6}}$
$\bar{\Gamma}_{11}$	1	$e^{\frac{i\pi}{3}}$	$e^{-\frac{i\pi}{3}}$	$-i$	$e^{-\frac{i\pi}{6}}$	$e^{\frac{i\pi}{6}}$
$\bar{\Gamma}_{12}$	1	$e^{\frac{i\pi}{3}}$	$e^{-\frac{i\pi}{3}}$	i	$e^{\frac{i5\pi}{6}}$	$e^{-\frac{i5\pi}{6}}$

(a) The character table for point group C_6 .

C_{3v}	\mathcal{E}	C_{3z}	C_{3z}^{-1}
Γ_1	1	1	1
Γ_2	1	$e^{\frac{i2\pi}{3}}$	$e^{-\frac{i2\pi}{3}}$
Γ_3	1	$e^{-\frac{i2\pi}{3}}$	$e^{\frac{i2\pi}{3}}$
$\bar{\Gamma}_4$	1	-1	-1
$\bar{\Gamma}_5$	1	$e^{-\frac{i\pi}{3}}$	$e^{\frac{i\pi}{3}}$
$\bar{\Gamma}_6$	1	$e^{\frac{i\pi}{3}}$	$e^{-\frac{i\pi}{3}}$

(c) The character table for point group C_3 .

C_4	\mathcal{E}	C_{2z}	C_{4z}	C_{4z}^{-1}
Γ_1	1	1	1	1
Γ_2	1	1	-1	-1
Γ_3	1	1	i	$-i$
Γ_4	1	1	$-i$	i
$\bar{\Gamma}_5$	1	$-i$	$e^{\frac{i3\pi}{4}}$	$e^{-\frac{i3\pi}{4}}$
$\bar{\Gamma}_6$	1	$-i$	$e^{-\frac{i\pi}{4}}$	$e^{\frac{i\pi}{4}}$
$\bar{\Gamma}_7$	1	i	$e^{-\frac{i3\pi}{4}}$	$e^{\frac{i3\pi}{4}}$
$\bar{\Gamma}_8$	1	i	$e^{\frac{i\pi}{4}}$	$e^{-\frac{i\pi}{4}}$

(b) The character table for point group C_4 .TABLE SXVII: The character table for the point group C_n with $n = 3, 4, 6$.

C_{6v}	\mathcal{E}	C_{3z}, C_{3z}^{-1}	C_{2z}	C_{6z}, C_{6z}^{-1}	$C_{3z}M_xC_{3z}^{-1}, M_x, C_{3z}^{-1}M_xC_{3z}$	$C_{3z}M_yC_{3z}^{-1}, M_y, C_{3z}^{-1}M_yC_{3z}$
Γ_1	1	1	1	1	1	1
Γ_2	1	1	1	1	-1	-1
Γ_3	1	1	-1	-1	-1	1
Γ_4	1	1	-1	-1	1	-1
Γ_5	2	-1	2	-1	0	0
Γ_6	2	-1	-2	1	0	0
$\bar{\Gamma}_7$	2	-2	0	0	0	0
$\bar{\Gamma}_8$	2	1	0	$-\sqrt{3}$	0	0
$\bar{\Gamma}_9$	2	1	0	$\sqrt{3}$	0	0

(a) The character table for the wave vector group $G_{\Gamma_M} = C_{6v}$.

C_{3v}	\mathcal{E}	C_{3z}, C_{3z}^{-1}	$C_{3z}M_yC_{3z}^{-1}, M_y, C_{3z}^{-1}M_yC_{3z}$
\mathbf{K}_1	1	1	1
\mathbf{K}_2	1	1	-1
\mathbf{K}_3	2	-1	0
$\bar{\mathbf{K}}_4$	1	-1	$-i$
$\bar{\mathbf{K}}_5$	1	-1	$+i$
$\bar{\mathbf{K}}_6$	2	1	0

(b) The character table for the wave vector group $G_{\mathbf{K}_M} = C_{3v}$.

C_{3v}	\mathcal{E}	C_{2z}	M_x	M_y
\mathbf{M}_1	1	1	1	1
\mathbf{M}_2	1	1	-1	-1
\mathbf{M}_3	1	-1	-1	1
\mathbf{M}_4	1	-1	1	-1
$\bar{\mathbf{M}}_5$	2	0	0	0

(c) The character table for the wave vector group $G_{\mathbf{M}_M} = C_{2v}$.TABLE SXVIII: The character table for the little groups of $P6mm$

C_s	\mathcal{E}	\mathbf{M}_x	C_s	\mathcal{E}	\mathbf{M}_y
$\Gamma\mathbf{M}_1$	1	1	$\Gamma\mathbf{K}_1$	1	-1
$\Gamma\mathbf{M}_2$	1	-1	$\Gamma\mathbf{K}_2$	1	-1
$\Gamma\bar{\mathbf{M}}_3$	1	i	$\Gamma\bar{\mathbf{K}}_3$	1	i
$\Gamma\bar{\mathbf{M}}_4$	1	$-i$	$\Gamma\bar{\mathbf{K}}_4$	1	$-i$

TABLE SXIX: The character table for the group $G_{\Gamma_M\mathbf{M}_M}^A = G_{\Gamma_M\mathbf{K}_M}^A = C_s$

Wyckoff position	1a	1a	1a
EBR	$\bar{E}_3 \uparrow G(2)$	$\bar{E}_2 \uparrow G(2)$	$\bar{E}_1 \uparrow G(2)$
Γ_M	$\bar{\Gamma}_7(2)$	$\bar{\Gamma}_8(2)$	$\bar{\Gamma}_9(2)$
\mathbf{K}_M	$\bar{\mathbf{K}}_4(1) \oplus \bar{\mathbf{K}}_5(1)$	$\bar{\mathbf{K}}_6(2)$	$\bar{\mathbf{K}}_6(2)$
\mathbf{M}_M	$\bar{\mathbf{M}}_5(2)$	$\bar{\mathbf{M}}_5(2)$	$\bar{\mathbf{M}}_5(2)$

TABLE SXX: 2D spinful EBR table for the $P6mm$ group with TR.

2. Cases without TR symmetry

Table II in the main text summarizes all combinations of G_0^A , Λ_Γ^A , and G_0 that lead to symmetry-enforced moiré topology in a spinless TR-breaking system. Table SXXI summarizes all the combinations of G_0^A , Λ_Γ^A and G_0 that lead to symmetry-enforced moiré topology in a spinful TR-breaking system. Without TR, we find 24 cases for spinful systems, and 66 cases for the spinless systems. Among the 66 spinless cases, we find that there are 5 cases that allow for isolated symmetry-enforced low-energy topological moiré bands, while all other cases only have topological semi-metal phases for the low-energy moiré bands. For an atomic 1D irrep Λ_Γ^A , symmetry-enforced moiré semi-metal phases only appear when G_0 is a non-symmorphic plane group, which is similar to the cases with TR. Tables SXXII–SXXX show the possible representations at high-symmetry momenta in the mBZ for all the non-trivial cases in Table SXXI and Table II in the main text. We organize these tables according to G_0^A , namely, Tables SXXII–SXXIV are for $G_0^A = C_{6v}$, Tables SXXV–SXXVII are for $G_0^A = C_{4v}$, Tables SXXVIII is for $G_0^A = C_{3v}$, Table SXXIX is for $G_0^A = C_{2v}$, and Table SXXX is for $G_0^A = C_s$.

To illustrate the symmetry-enforced moiré topology with a spinless atomic irrep when TR is broken, we consider the case with $\Lambda_\Gamma^A = \Gamma_5$, $G_0^A = C_{4v}$ and $G_0 = P2$ in Table. SXXV. The mBZ is shown in Fig.S2(e), and the band representations in the mBZ of low-energy moiré bands for this case are

$$(2\Gamma_2, \mathbf{Y}_1 \oplus \mathbf{Y}_2, \mathbf{A}_1 \oplus \mathbf{A}_2, \mathbf{B}_1 \oplus \mathbf{B}_2), \quad (\text{S.B1})$$

as listed in Table. SXXV. With a nonzero moiré potential respecting $G_0 = P2$, the little groups at the high-symmetry momenta Γ_M , \mathbf{A}_M , \mathbf{B}_M , and \mathbf{Y}_M are all C_2 . Therefore, the irrep at any of these high-symmetry points is characterized by the C_{2z} eigenvalue, denoted as $\zeta_i(\mathbf{k}_M)$, where i labels the moiré band. According to Ref.[5], the Chern number C of the low-energy two bands is associated with the ζ_i by

$$(-1)^C = \prod_{i=1}^2 \zeta_i(\Gamma_M) \zeta_i(\mathbf{A}_M) \zeta_i(\mathbf{B}_M) \zeta_i(\mathbf{Y}_M). \quad (\text{S.B2})$$

According to Eq.(S.B2) and the band irreps in Eq.(S.B1), we get

$$(-1)^C = -1, \quad (\text{S.B3})$$

which implies that the total Chern number of the two low-energy bands must be odd. We can use the same method to demonstrate the symmetry-enforced topological moiré Chern bands in the combination of $G_0^A = C_{6v}$ and $G_0 = P2$ as well as the combination of $G_0^A = C_{6v}$ and $G_0 = P6$. Without TR, all symmetry-enforced moiré topologically insulating bands have non-zero total Chern number.

$G_0 \backslash G_0^A$	C_{6v}	C_{4v}	C_{3v}	C_{2v}	C_s
$P4bm$		Γ_6, Γ_7			
$Pba2$	$\bar{\Gamma}_7, \bar{\Gamma}_8, \bar{\Gamma}_9$	$\bar{\Gamma}_6, \bar{\Gamma}_7$		$\bar{\Gamma}_5$	
$Pma2$	$\bar{\Gamma}_7, \bar{\Gamma}_8, \bar{\Gamma}_9$	$\bar{\Gamma}_6, \bar{\Gamma}_7$		$\bar{\Gamma}_5$	
$Pb11$	$\bar{\Gamma}_7, \bar{\Gamma}_8, \bar{\Gamma}_9$	$\bar{\Gamma}_6, \bar{\Gamma}_7$	$\bar{\Gamma}_4, \bar{\Gamma}_5$	$\bar{\Gamma}_5$	$\bar{\Gamma}_3, \bar{\Gamma}_4$

TABLE SXXI: **Spinful TR-breaking cases for low-energy moiré topology.** List of combinations of atomic point group G_0^A , atomic Γ irrep, and moiré plane group G_0 that lead to symmetry-enforced nontrivial moiré topology, in the presence of SOC and without TR symmetry. For a given G_0^A and G_0 , the table entry indicates the required atomic Γ irrep to give symmetry-enforced topology. The low-energy bands are semimetallic.

$G_0^A = C_{6v}$	$G_0 = P6$		
Γ	Γ_M	M_M	K_M
Γ_1	Γ_1	$M_1 \oplus M_2$	$K_1 \oplus K_2 \oplus K_3$
Γ_2	Γ_1	$M_1 \oplus M_2$	$K_1 \oplus K_2 \oplus K_3$
Γ_3	Γ_2	$M_1 \oplus M_2$	$K_1 \oplus K_2 \oplus K_3$
Γ_4	Γ_2	$M_1 \oplus M_2$	$K_1 \oplus K_2 \oplus K_3$
$\star\Gamma_5(2)$	$\Gamma_3 \oplus \Gamma_5$	$M_1 \oplus M_2$	$K_1 \oplus K_2 \oplus K_3$
$\star\Gamma_6(2)$	$\Gamma_4 \oplus \Gamma_6$	$M_1 \oplus M_2$	$K_1 \oplus K_2 \oplus K_3$
$\bar{\Gamma}_7(2)$	$\bar{\Gamma}_7 \oplus \bar{\Gamma}_8$	$\bar{M}_3 \oplus \bar{M}_4$	$\bar{K}_4 \oplus \bar{K}_5 \oplus \bar{K}_6$
$\bar{\Gamma}_8(2)$	$\bar{\Gamma}_{10} \oplus \bar{\Gamma}_{11}$	$\bar{M}_3 \oplus \bar{M}_4$	$\bar{K}_4 \oplus \bar{K}_5 \oplus \bar{K}_6$
$\bar{\Gamma}_9(2)$	$\bar{\Gamma}_9 \oplus \bar{\Gamma}_{12}$	$\bar{M}_3 \oplus \bar{M}_4$	$\bar{K}_4 \oplus \bar{K}_5 \oplus \bar{K}_6$

(a) $G_0^A = C_{6v}$ and $G_0 = P6$

$G_0^A = C_{6v}$	$G_0 = P2$			
Γ	Γ_M	Y_M	A_M	B_M
Γ_1	Γ_1	$Y_1 \oplus Y_2$	$A_1 \oplus A_2$	$B_1 \oplus B_2$
Γ_2	Γ_1	$Y_1 \oplus Y_2$	$A_1 \oplus A_2$	$B_1 \oplus B_2$
Γ_3	Γ_2	$Y_1 \oplus Y_2$	$A_1 \oplus A_2$	$B_1 \oplus B_2$
Γ_4	Γ_2	$Y_1 \oplus Y_2$	$A_1 \oplus A_2$	$B_1 \oplus B_2$
$\star\Gamma_5(2)$	$2\Gamma_1$	$Y_1 \oplus Y_2$	$A_1 \oplus A_2$	$B_1 \oplus B_2$
$\star\Gamma_6(2)$	$2\Gamma_2$	$Y_1 \oplus Y_2$	$A_1 \oplus A_2$	$B_1 \oplus B_2$
$\bar{\Gamma}_7(2)$	$\bar{\Gamma}_3 \oplus \bar{\Gamma}_4$	$\bar{Y}_3 \oplus \bar{Y}_4$	$\bar{A}_3 \oplus \bar{A}_4$	$\bar{B}_3 \oplus \bar{B}_4$
$\bar{\Gamma}_8(2)$	$\bar{\Gamma}_3 \oplus \bar{\Gamma}_4$	$\bar{Y}_3 \oplus \bar{Y}_4$	$\bar{A}_3 \oplus \bar{A}_4$	$\bar{B}_3 \oplus \bar{B}_4$
$\bar{\Gamma}_9(2)$	$\bar{\Gamma}_3 \oplus \bar{\Gamma}_4$	$\bar{Y}_3 \oplus \bar{Y}_4$	$\bar{A}_3 \oplus \bar{A}_4$	$\bar{B}_3 \oplus \bar{B}_4$

(b) $G_0^A = C_{6v}$ and $G_0 = P2$

TABLE SXXII: Without TR and $G_0^A = C_{6v}$, for the space groups G_0 listed above, there exists at least one irrep for symmetry-enforced topologically insulating moiré bands.

$G_0^A = C_{6v}$	$G_0 = P6mm$		
Γ	Γ_M	M_M	K_M
Γ_1	Γ_1	$M_1 \oplus M_4$	$K_1 \oplus K_3(2)$
Γ_2	Γ_2	$M_2 \oplus M_3$	$K_2 \oplus K_3(2)$
Γ_3	Γ_3	$M_2 \oplus M_3$	$K_1 \oplus K_3(2)$
Γ_4	Γ_4	$M_1 \oplus M_4$	$K_2 \oplus K_3(2)$
$\blacktriangle\Gamma_5(2)$	$\Gamma_5(2)$	$M_1 \oplus M_4$	$K_1 \oplus K_3(2)$
		$M_2 \oplus M_3$	$K_2 \oplus K_3(2)$
$\blacktriangle\Gamma_6(2)$	$\Gamma_6(2)$	$M_1 \oplus M_4$	$K_1 \oplus K_3(2)$
		$M_2 \oplus M_3$	$K_2 \oplus K_3(2)$
$\bar{\Gamma}_7(2)$	$\bar{\Gamma}_7(2)$	$\bar{M}_5(2)$	$\bar{K}_4 \oplus \bar{K}_6(2)$
$\bar{\Gamma}_8(2)$	$\bar{\Gamma}_8(2)$	$\bar{M}_5(2)$	$\bar{K}_5 \oplus \bar{K}_6(2)$
			$\bar{K}_4 \oplus \bar{K}_6(2)$
$\bar{\Gamma}_9(2)$	$\bar{\Gamma}_9(2)$	$\bar{M}_5(2)$	$\bar{K}_4 \oplus \bar{K}_6(2)$
			$\bar{K}_5 \oplus \bar{K}_6(2)$

(a) $G_0^A = C_{6v}$ and $G_0 = P6mm$

$G_0^A = C_{6v}$	$G_0 = P3m1$		
Γ	Γ_M	M_M	K_M
Γ_1	Γ_1	$2M_1$	$K_1 \oplus K_2 \oplus K_3$
Γ_2	Γ_2	$2M_2$	$K_1 \oplus K_2 \oplus K_3$
Γ_3	Γ_2	$2M_2$	$K_1 \oplus K_2 \oplus K_3$
Γ_4	Γ_1	$2M_1$	$K_1 \oplus K_2 \oplus K_3$
$\blacktriangle\Gamma_5(2)$	Γ_3	$2M_1$	$K_1 \oplus K_2 \oplus K_3$
		$2M_2$	
$\blacktriangle\Gamma_6(2)$	Γ_3	$2M_1$	$K_1 \oplus K_2 \oplus K_3$
		$2M_2$	
$\bar{\Gamma}_7(2)$	$\bar{\Gamma}_4 \oplus \bar{\Gamma}_5$	$\bar{M}_3 \oplus \bar{M}_4$	$\bar{K}_4 \oplus \bar{K}_5 \oplus \bar{K}_6$
$\bar{\Gamma}_8(2)$	$\bar{\Gamma}_6(2)$	$\bar{M}_3 \oplus \bar{M}_4$	$\bar{K}_4 \oplus \bar{K}_5 \oplus \bar{K}_6$
$\bar{\Gamma}_9(2)$	$\bar{\Gamma}_6(2)$	$\bar{M}_3 \oplus \bar{M}_4$	$\bar{K}_4 \oplus \bar{K}_5 \oplus \bar{K}_6$

(b) $G_0^A = C_{6v}$ and $G_0 = P3m1$

$G_0^A = C_{6v}$	$G_0 = Pmm2$			
Γ	Γ_M	Y_M	X_M	S_M
Γ_1	Γ_1	$Y_1 \oplus Y_3$	$X_1 \oplus X_4$	$S_1 \oplus S_2 \oplus S_3 \oplus S_4$
Γ_2	Γ_2	$Y_2 \oplus Y_4$	$X_2 \oplus X_3$	$S_1 \oplus S_2 \oplus S_3 \oplus S_4$
Γ_3	Γ_3	$Y_1 \oplus Y_3$	$X_1 \oplus X_4$	$S_1 \oplus S_2 \oplus S_3 \oplus S_4$
Γ_4	Γ_4	$Y_2 \oplus Y_4$	$X_2 \oplus X_3$	$S_1 \oplus S_2 \oplus S_3 \oplus S_4$
$\blacktriangle\Gamma_5(2)$	$\Gamma_1 \oplus \Gamma_2$	$Y_1 \oplus Y_3$	$X_1 \oplus X_4$	$S_1 \oplus S_2 \oplus S_3 \oplus S_4$
		$Y_2 \oplus Y_4$	$X_2 \oplus X_3$	
$\blacktriangle\Gamma_6(2)$	$\Gamma_3 \oplus \Gamma_4$	$Y_1 \oplus Y_3$	$X_2 \oplus X_3$	$S_1 \oplus S_2 \oplus S_3 \oplus S_4$
		$Y_2 \oplus Y_4$	$X_1 \oplus X_4$	
$\bar{\Gamma}_7(2)$	$\bar{\Gamma}_5(2)$	$\bar{Y}_5(2)$	$\bar{X}_5(2)$	$\bar{S}_5(2) \oplus \bar{S}_5(2)$
$\bar{\Gamma}_8(2)$	$\bar{\Gamma}_5(2)$	$\bar{Y}_5(2)$	$\bar{X}_5(2)$	$\bar{S}_5(2) \oplus \bar{S}_5(2)$
$\bar{\Gamma}_9(2)$	$\bar{\Gamma}_5(2)$	$\bar{Y}_5(2)$	$\bar{X}_5(2)$	$\bar{S}_5(2) \oplus \bar{S}_5(2)$

(c) $G_0^A = C_{6v}$ and $G_0 = Pmm2$

$G_0^A = C_{6v}$	$G_0 = Pm11$			
Γ	Γ_M	Y_M	X_M	S_M
Γ_1	Γ_1	$Y_1 \oplus Y_2$	$2X_1$	$2S_1 \oplus 2S_2$
Γ_2	Γ_2	$Y_1 \oplus Y_2$	$2X_2$	$2S_1 \oplus 2S_2$
Γ_3	Γ_1	$Y_1 \oplus Y_2$	$2X_1$	$2S_1 \oplus 2S_2$
Γ_4	Γ_2	$Y_1 \oplus Y_2$	$2X_2$	$2S_1 \oplus 2S_2$
$\blacktriangle\Gamma_5(2)$	$\Gamma_1 \oplus \Gamma_2$	$Y_1 \oplus Y_2$	$2X_1$	$2S_1 \oplus 2S_2$
			$2X_2$	
$\blacktriangle\Gamma_6(2)$	$\Gamma_1 \oplus \Gamma_2$	$Y_1 \oplus Y_2$	$2X_1$	$2S_1 \oplus 2S_2$
			$2X_2$	
$\bar{\Gamma}_7(2)$	$\bar{\Gamma}_3 \oplus \bar{\Gamma}_4$	$\bar{Y}_3 \oplus \bar{Y}_4$	$\bar{X}_3 \oplus \bar{X}_4$	$\bar{S}_3 \oplus \bar{S}_4 \oplus \bar{S}_3 \oplus \bar{S}_4$
$\bar{\Gamma}_8(2)$	$\bar{\Gamma}_3 \oplus \bar{\Gamma}_4$	$\bar{Y}_3 \oplus \bar{Y}_4$	$\bar{X}_3 \oplus \bar{X}_4$	$\bar{S}_3 \oplus \bar{S}_4 \oplus \bar{S}_3 \oplus \bar{S}_4$
$\bar{\Gamma}_9(2)$	$\bar{\Gamma}_3 \oplus \bar{\Gamma}_4$	$\bar{Y}_3 \oplus \bar{Y}_4$	$\bar{X}_3 \oplus \bar{X}_4$	$\bar{S}_3 \oplus \bar{S}_4 \oplus \bar{S}_3 \oplus \bar{S}_4$

(d) $G_0^A = C_{6v}$ and $G_0 = Pm11$

$G_0^A = C_{6v}$	$G = C2mm$		
Γ	Γ_M	Y_M	S_M
Γ_1	Γ_1	$Y_1 \oplus Y_4$	$S_1 \oplus S_2$
Γ_2	Γ_2	$Y_2 \oplus Y_3$	$S_1 \oplus S_2$
Γ_3	Γ_3	$Y_2 \oplus Y_3$	$S_1 \oplus S_2$
Γ_4	Γ_4	$Y_1 \oplus Y_4$	$S_1 \oplus S_2$
$\blacktriangle\Gamma_5(2)$	$\Gamma_1 \oplus \Gamma_2$	$Y_1 \oplus Y_4$	$S_1 \oplus S_2$
		$Y_2 \oplus Y_3$	
$\blacktriangle\Gamma_6(2)$	$\Gamma_3 \oplus \Gamma_4$	$Y_2 \oplus Y_3$	$S_1 \oplus S_2$
		$Y_1 \oplus Y_4$	
$\bar{\Gamma}_7(2)$	$\bar{\Gamma}_5(2)$	$\bar{Y}_5(2)$	$\bar{S}_3 \oplus \bar{S}_4$
$\bar{\Gamma}_8(2)$	$\bar{\Gamma}_5(2)$	$\bar{Y}_5(2)$	$\bar{S}_3 \oplus \bar{S}_4$
$\bar{\Gamma}_9(2)$	$\bar{\Gamma}_5(2)$	$\bar{Y}_5(2)$	$\bar{S}_3 \oplus \bar{S}_4$

(e) $G_0^A = C_{6v}$ and $G_0 = C2mm$ TABLE SXXIII: Without TR and $G_0^A = C_{6v}$, for the symmorphic space groups G_0 listed above, there exists at least one irrep for which the low-energy moiré bands are necessarily symmetry-enforced semimetallic.

$G_0^A = C_{6v}$	$G_0 = Pba2$			
Γ	Γ_M	Y_M	X_M	S_M
$\Delta\Gamma_1$	Γ_1	$Y_1(2)$	$X_1(2)$	$S_1 \oplus S_2 \oplus S_3 \oplus S_4$
$\Delta\Gamma_2$	Γ_2	$Y_1(2)$	$X_1(2)$	$S_1 \oplus S_2 \oplus S_3 \oplus S_4$
$\Delta\Gamma_3$	Γ_3	$Y_1(2)$	$X_1(2)$	$S_1 \oplus S_2 \oplus S_3 \oplus S_4$
$\Delta\Gamma_4$	Γ_4	$Y_1(2)$	$X_1(2)$	$S_1 \oplus S_2 \oplus S_3 \oplus S_4$
$\Gamma_5(2)$	$\Gamma_1 \oplus \Gamma_2$	$Y_1(2)$	$X_1(2)$	$S_1 \oplus S_2 \oplus S_3 \oplus S_4$
$\Gamma_6(2)$	$\Gamma_3 \oplus \Gamma_4$	$Y_1(2)$	$X_1(2)$	$S_1 \oplus S_2 \oplus S_3 \oplus S_4$
$\Delta\bar{\Gamma}_7(2)$	$\bar{\Gamma}_5(2)$	$\bar{Y}_2 \oplus \bar{Y}_3$ $\bar{Y}_4 \oplus \bar{Y}_5$	$\bar{X}_2 \oplus \bar{X}_5$ $\bar{X}_3 \oplus \bar{X}_4$	$\bar{S}_5(2) \oplus \bar{S}_5(2)$
$\Delta\bar{\Gamma}_8(2)$	$\bar{\Gamma}_5(2)$	$\bar{Y}_2 \oplus \bar{Y}_3$ $\bar{Y}_4 \oplus \bar{Y}_5$	$\bar{X}_2 \oplus \bar{X}_5$ $\bar{X}_3 \oplus \bar{X}_4$	$\bar{S}_5(2) \oplus \bar{S}_5(2)$
$\Delta\bar{\Gamma}_9(2)$	$\bar{\Gamma}_5(2)$	$\bar{Y}_2 \oplus \bar{Y}_3$ $\bar{Y}_4 \oplus \bar{Y}_5$	$\bar{X}_2 \oplus \bar{X}_5$ $\bar{X}_3 \oplus \bar{X}_4$	$\bar{S}_5(2) \oplus \bar{S}_5(2)$

(a) $G_0^A = C_{6v}$ and $G_0 = Pba2$

$G_0^A = C_{6v}$	$G_0 = Pb11$			
Γ	Γ_M	Y_M	X_M	S_M
$\Delta\Gamma_1$	Γ_1	$Y_1 \oplus Y_2$	$X_1 \oplus X_2$	$2S_1 \oplus 2S_2$
$\Delta\Gamma_2$	Γ_2	$Y_1 \oplus Y_2$	$X_1 \oplus X_2$	$2S_1 \oplus 2S_2$
$\Delta\Gamma_3$	Γ_1	$Y_1 \oplus Y_2$	$X_1 \oplus X_2$	$2S_1 \oplus 2S_2$
$\Delta\Gamma_4$	Γ_2	$Y_1 \oplus Y_2$	$X_1 \oplus X_2$	$2S_1 \oplus 2S_2$
$\Gamma_5(2)$	$\Gamma_1 \oplus \Gamma_2$	$Y_1 \oplus Y_2$	$X_1 \oplus X_2$	$2S_1 \oplus 2S_2$
Γ_6	$\Gamma_1 \oplus \Gamma_2$	$Y_1 \oplus Y_2$	$X_1 \oplus X_2$	$2S_1 \oplus 2S_2$
$\Delta\bar{\Gamma}_7(2)$	$\bar{\Gamma}_3 \oplus \bar{\Gamma}_4$	$\bar{Y}_3 \oplus \bar{Y}_4$	$\bar{X}_3 \oplus \bar{X}_4$ $\bar{X}_4 \oplus \bar{X}_4$	$2\bar{S}_3 \oplus 2\bar{S}_4$
$\Delta\bar{\Gamma}_8$	$\bar{\Gamma}_3 \oplus \bar{\Gamma}_4$	$\bar{Y}_3 \oplus \bar{Y}_4$	$\bar{X}_3 \oplus \bar{X}_4$ $\bar{X}_4 \oplus \bar{X}_4$	$2\bar{S}_3 \oplus 2\bar{S}_4$
$\Delta\bar{\Gamma}_9$	$\bar{\Gamma}_3 \oplus \bar{\Gamma}_4$	$\bar{Y}_3 \oplus \bar{Y}_4$	$\bar{X}_3 \oplus \bar{X}_4$ $\bar{X}_4 \oplus \bar{X}_4$	$2\bar{S}_3 \oplus 2\bar{S}_4$

(c) $G_0^A = C_{6v}$ and $G_0 = Pb11$

$G_0^A = C_{6v}$	$G_0 = Pma2$			
Γ	Γ_M	Y_M	X_M	S_M
$\Delta\Gamma_1$	Γ_1	$Y_1 \oplus Y_3$	$X_1(2)$	$2S_1(2)$
$\Delta\Gamma_2$	Γ_2	$Y_2 \oplus Y_4$	$X_1(2)$	$2S_1(2)$
$\Delta\Gamma_3$	Γ_3	$Y_1 \oplus Y_3$	$X_1(2)$	$2S_1(2)$
$\Delta\Gamma_4$	Γ_4	$Y_2 \oplus Y_4$	$X_1(2)$	$2S_1(2)$
$\Delta\Gamma_5(2)$	$\Gamma_1 \oplus \Gamma_2$	$Y_1 \oplus Y_3$ $Y_2 \oplus Y_4$	$X_1(2)$	$2S_1(2)$
$\Delta\Gamma_6(2)$	$\Gamma_3 \oplus \Gamma_4$	$Y_1 \oplus Y_3$ $Y_2 \oplus Y_4$	$X_1(2)$	$2S_1(2)$
$\Delta\bar{\Gamma}_7(2)$	$\bar{\Gamma}_5(2)$	$\bar{Y}_5(2)$	$\bar{X}_2 \oplus \bar{X}_5$ $\bar{X}_3 \oplus \bar{X}_4$	$\bar{S}_2 \oplus \bar{S}_5 \oplus \bar{S}_3 \oplus \bar{S}_4$
$\Delta\bar{\Gamma}_8(2)$	$\bar{\Gamma}_5(2)$	$\bar{Y}_5(2)$	$\bar{X}_2 \oplus \bar{X}_5$ $\bar{X}_3 \oplus \bar{X}_4$	$\bar{S}_2 \oplus \bar{S}_5 \oplus \bar{S}_3 \oplus \bar{S}_4$
$\Delta\bar{\Gamma}_9(2)$	$\bar{\Gamma}_5(2)$	$\bar{Y}_5(2)$	$\bar{X}_2 \oplus \bar{X}_5$ $\bar{X}_3 \oplus \bar{X}_4$	$\bar{S}_2 \oplus \bar{S}_5 \oplus \bar{S}_3 \oplus \bar{S}_4$

(b) $G_0^A = C_{6v}$ and $G_0 = Pma2$ TABLE SXXIV: Without TR and $G_0^A = C_{6v}$, for the nonsymmorphic space groups G_0 listed above, there exists at least one irrep for which the low-energy moiré bands are necessarily symmetry-enforced semimetallic.

$G_0^A = C_{4v}$	$G_0 = P2$			
Γ	Γ_M	Y_M	A_M	B_M
Γ_1	Γ_1	$Y_1 \oplus Y_2$	$A_1 \oplus A_2$	$B_1 \oplus B_2$
Γ_2	Γ_1	$Y_1 \oplus Y_2$	$A_1 \oplus A_2$	$B_1 \oplus B_2$
Γ_3	Γ_2	$Y_1 \oplus Y_2$	$A_1 \oplus A_2$	$B_1 \oplus B_2$
Γ_4	Γ_2	$Y_1 \oplus Y_2$	$A_1 \oplus A_2$	$B_1 \oplus B_2$
$\star\Gamma_5(2)$	$2\Gamma_2$	$Y_1 \oplus Y_2$	$A_1 \oplus A_2$	$B_1 \oplus B_2$
$\bar{\Gamma}_6(2)$	$\bar{\Gamma}_3 \oplus \bar{\Gamma}_4$	$\bar{Y}_3 \oplus \bar{Y}_4$	$\bar{A}_3 \oplus \bar{A}_4$	$\bar{B}_3 \oplus \bar{B}_4$
$\bar{\Gamma}_7(2)$	$\bar{\Gamma}_3 \oplus \bar{\Gamma}_4$	$\bar{Y}_3 \oplus \bar{Y}_4$	$\bar{A}_3 \oplus \bar{A}_4$	$\bar{B}_3 \oplus \bar{B}_4$

TABLE SXXV: Without TR and $G_0^A = C_{4v}$, for the space group $P2$, there exists at least one irrep for symmetry-enforced topologically insulating moiré bands.

$G_0^A = C_{4v}$	$G_0 = P4mm$		
Γ	Γ_M	M_M	X_M
Γ_1	Γ_1	$M_1 \oplus M_3 \oplus M_5(2)$	$X_1 \oplus X_3$
Γ_2	Γ_2	$M_2 \oplus M_4 \oplus M_5(2)$	$X_1 \oplus X_3$
Γ_3	Γ_3	$M_1 \oplus M_3 \oplus M_5(2)$	$X_2 \oplus X_4$
Γ_4	Γ_4	$M_2 \oplus M_4 \oplus M_5(2)$	$X_2 \oplus X_4$
$\blacktriangle\Gamma_5(2)$	$\Gamma_5(2)$	$M_1 \oplus M_3 \oplus M_5(2)$ $M_2 \oplus M_4 \oplus M_5(2)$	$X_1 \oplus X_3$ $X_2 \oplus X_4$
$\bar{\Gamma}_6(2)$	$\bar{\Gamma}_6(2)$	$\bar{M}_6(2) \oplus \bar{M}_7(2)$	$\bar{X}_5(2)$
$\bar{\Gamma}_7(2)$	$\bar{\Gamma}_7(2)$	$\bar{M}_6(2) \oplus \bar{M}_7(2)$	$\bar{X}_5(2)$

(a) $G_0^A = C_{4v}$ and $G_0 = P4mm$

$G_0^A = C_{4v}$	$G_0 = Pm11$			
Γ	Γ	Y	X	S
Γ_1	Γ_1	$Y_1 \oplus Y_2$	$2X_1$	$2S_1 \oplus 2S_2$
Γ_2	Γ_1	$Y_1 \oplus Y_2$	$2X_2$	$2S_1 \oplus 2S_2$
Γ_3	Γ_2	$Y_1 \oplus Y_2$	$2X_1$	$2S_1 \oplus 2S_2$
Γ_4	Γ_2	$Y_1 \oplus Y_2$	$2X_2$	$2S_1 \oplus 2S_2$
$\blacktriangle\Gamma_5(2)$	$\Gamma_1 \oplus \Gamma_2$	$Y_1 \oplus Y_2$ $Y_1 \oplus Y_2$	$2X_1$ $2X_2$	$2S_1 \oplus 2S_2$
$\bar{\Gamma}_6(2)$	$\bar{\Gamma}_3 \oplus \bar{\Gamma}_4$	$\bar{Y}_3 \oplus \bar{Y}_4$	$\bar{X}_3 \oplus \bar{X}_4$	$\bar{S}_3 \oplus \bar{S}_4 \oplus \bar{S}_3 \oplus \bar{S}_4$
$\bar{\Gamma}_7(2)$	$\bar{\Gamma}_3 \oplus \bar{\Gamma}_4$	$\bar{Y}_3 \oplus \bar{Y}_4$	$\bar{X}_3 \oplus \bar{X}_4$	$\bar{S}_3 \oplus \bar{S}_4 \oplus \bar{S}_3 \oplus \bar{S}_4$

(c) $G_0^A = C_{4v}$ and $G_0 = Pm11$

$G_0^A = C_{4v}$	$G_0 = Pmm2$			
Γ	Γ_M	Y_M	X_M	S_M
Γ_1	Γ_1	$Y_1 \oplus Y_3$	$X_1 \oplus X_4$	$S_1 \oplus S_2 \oplus S_3 \oplus S_4$
Γ_2	Γ_1	$Y_1 \oplus Y_3$	$X_2 \oplus X_3$	$S_1 \oplus S_2 \oplus S_3 \oplus S_4$
Γ_3	Γ_2	$Y_2 \oplus Y_4$	$X_2 \oplus X_3$	$S_1 \oplus S_2 \oplus S_3 \oplus S_4$
Γ_4	Γ_2	$Y_2 \oplus Y_4$	$X_1 \oplus X_4$	$S_1 \oplus S_2 \oplus S_3 \oplus S_4$
$\blacktriangle\Gamma_5(2)$	$\Gamma_3 \oplus \Gamma_4$	$Y_1 \oplus Y_3$ $Y_2 \oplus Y_4$	$X_1 \oplus X_4$ $X_2 \oplus X_3$	$S_1 \oplus S_2 \oplus S_3 \oplus S_4$
$\bar{\Gamma}_6(2)$	$\bar{\Gamma}_5(2)$	$\bar{Y}_5(2)$	$\bar{X}_5(2)$	$\bar{S}_5(2) \oplus \bar{S}_5(2)$
$\bar{\Gamma}_7(2)$	$\bar{\Gamma}_5(2)$	$\bar{Y}_5(2)$	$\bar{X}_5(2)$	$\bar{S}_5(2) \oplus \bar{S}_5(2)$

(b) $G_0^A = C_{4v}$ and $G_0 = Pmm2$

$G_0^A = C_{4v}$	$G_0 = C2mm$		
Γ	Γ_M	Y_M	S_M
Γ_1	Γ_1	$Y_1 \oplus Y_4$	$S_1 \oplus S_2$
Γ_2	Γ_1	$Y_1 \oplus Y_4$	$S_1 \oplus S_2$
Γ_3	Γ_2	$Y_2 \oplus Y_3$	$S_1 \oplus S_2$
Γ_4	Γ_2	$Y_2 \oplus Y_3$	$S_1 \oplus S_2$
$\blacktriangle\Gamma_5(2)$	$\Gamma_3 \oplus \Gamma_4$	$Y_2 \oplus Y_3$ $Y_1 \oplus Y_4$	$S_1 \oplus S_2$
$\bar{\Gamma}_6(2)$	$\bar{\Gamma}_5(2)$	$\bar{Y}_5(2)$	$\bar{S}_3 \oplus \bar{S}_4$
$\bar{\Gamma}_7(2)$	$\bar{\Gamma}_5(2)$	$\bar{Y}_5(2)$	$\bar{S}_3 \oplus \bar{S}_4$

(d) $G_0^A = C_{4v}$ and $G_0 = C2mm$

TABLE SXXVI: Without TR and $G_0^A = C_{4v}$, for the symmorphic space groups G_0 listed above, there exists at least one irrep for which the low-energy moiré bands are necessarily symmetry-enforced semimetallic.

$G_0^A = C_{4v}$	$G_0 = P4bm$		
Γ	Γ_M	M_M	X_M
$\blacktriangle\Gamma_1$	Γ_1	$M_1 \oplus M_3 \oplus M_5(2)$	$X_1(2)$
$\blacktriangle\Gamma_2$	Γ_2	$M_2 \oplus M_4 \oplus M_5(2)$	$X_1(2)$
$\blacktriangle\Gamma_3$	Γ_3	$M_1 \oplus M_3 \oplus M_5(2)$	$X_1(2)$
$\blacktriangle\Gamma_4$	Γ_4	$M_2 \oplus M_4 \oplus M_5(2)$	$X_1(2)$
$\Gamma_5(2)$	$\Gamma_5(2)$	$M_1 \oplus M_3 \oplus M_5(2)$ $M_2 \oplus M_4 \oplus M_5(2)$	$X_1(2)$
$\blacktriangle\bar{\Gamma}_6(2)$	$\bar{\Gamma}_6(2)$	$\bar{M}_6(2) \oplus \bar{M}_7(2)$	$\bar{X}_2 \oplus \bar{X}_3$ $\bar{X}_4 \oplus \bar{X}_5$
$\blacktriangle\bar{\Gamma}_7(2)$	$\bar{\Gamma}_7(2)$	$\bar{M}_6(2) \oplus \bar{M}_7(2)$	$\bar{X}_2 \oplus \bar{X}_3$ $\bar{X}_4 \oplus \bar{X}_5$

(a) $G_0^A = C_{4v}$ and $G_0 = P4bm$

$G_0^A = C_{4v}$	$G_0 = Pma2$			
Γ	Γ	Y	X	S
$\blacktriangle\Gamma_1$	Γ_1	$Y_1 \oplus Y_3$	$X_1(2)$	$2S_1(2)$
$\blacktriangle\Gamma_2$	Γ_1	$Y_1 \oplus Y_3$	$X_1(2)$	$2S_1(2)$
$\blacktriangle\Gamma_3$	Γ_2	$Y_2 \oplus Y_4$	$X_1(2)$	$2S_1(2)$
$\blacktriangle\Gamma_4$	Γ_2	$Y_2 \oplus Y_4$	$X_1(2)$	$2S_1(2)$
$\blacktriangle\Gamma_5(2)$	$\Gamma_3 \oplus \Gamma_4$	$Y_1 \oplus Y_3$ $Y_2 \oplus Y_4$	$X_1(2)$	$2S_1(2)$
$\blacktriangle\bar{\Gamma}_6(2)$	$\bar{\Gamma}_5(2)$	$\bar{Y}_5(2)$ $\bar{Y}_5(2)$	$\bar{X}_2 \oplus \bar{X}_5$ $\bar{X}_3 \oplus \bar{X}_4$	$\bar{S}_2 \oplus \bar{S}_5 \oplus \bar{S}_3 \oplus \bar{S}_4$
$\blacktriangle\bar{\Gamma}_7(2)$	$\bar{\Gamma}_5(2)$	$\bar{Y}_5(2)$ $\bar{Y}_5(2)$	$\bar{X}_2 \oplus \bar{X}_5$ $\bar{X}_3 \oplus \bar{X}_4$	$\bar{S}_2 \oplus \bar{S}_5 \oplus \bar{S}_3 \oplus \bar{S}_4$

(c) $G_0^A = C_{4v}$ and $G_0 = Pma2$

$G_0^A = C_{4v}$	$G_0 = Pba2$			
Γ	Γ	Y	X	S
$\blacktriangle\Gamma_1$	Γ_1	$Y_1(2)$	$X_1(2)$	$S_1 \oplus S_2 \oplus S_3 \oplus S_4$
$\blacktriangle\Gamma_2$	Γ_1	$Y_1(2)$	$X_1(2)$	$S_1 \oplus S_2 \oplus S_3 \oplus S_4$
$\blacktriangle\Gamma_3$	Γ_2	$Y_1(2)$	$X_1(2)$	$S_1 \oplus S_2 \oplus S_3 \oplus S_4$
$\blacktriangle\Gamma_4$	Γ_2	$Y_1(2)$	$X_1(2)$	$S_1 \oplus S_2 \oplus S_3 \oplus S_4$
$\Gamma_5(2)$	$\Gamma_3 \oplus \Gamma_4$	$Y_1(2)$	$X_1(2)$	$S_1 \oplus S_2 \oplus S_3 \oplus S_4$
$\blacktriangle\bar{\Gamma}_6(2)$	$\bar{\Gamma}_5(2)$	$\bar{Y}_2 \oplus \bar{Y}_3$ $\bar{Y}_4 \oplus \bar{Y}_5$	$\bar{X}_2 \oplus \bar{X}_5$ $\bar{X}_3 \oplus \bar{X}_4$	$\bar{S}_5(2) \oplus \bar{S}_5(2)$
$\blacktriangle\bar{\Gamma}_7(2)$	$\bar{\Gamma}_5(2)$	$\bar{Y}_2 \oplus \bar{Y}_3$ $\bar{Y}_4 \oplus \bar{Y}_5$	$\bar{X}_2 \oplus \bar{X}_5$ $\bar{X}_3 \oplus \bar{X}_4$	$\bar{S}_5(2) \oplus \bar{S}_5(2)$

(b) $G_0^A = C_{4v}$ and $G_0 = Pba2$

$G_0^A = C_{4v}$	$G_0 = Pb11$			
Γ	Γ_M	Y_M	X_M	S_M
$\blacktriangle\Gamma_1$	Γ_1	$Y_1 \oplus Y_2$	$X_1 \oplus X_2$	$2S_1 \oplus 2S_2$
$\blacktriangle\Gamma_2$	Γ_1	$Y_1 \oplus Y_2$	$X_1 \oplus X_2$	$2S_1 \oplus 2S_2$
$\blacktriangle\Gamma_3$	Γ_2	$Y_1 \oplus Y_2$	$X_1 \oplus X_2$	$2S_1 \oplus 2S_2$
$\blacktriangle\Gamma_4$	Γ_2	$Y_1 \oplus Y_2$	$X_1 \oplus X_2$	$2S_1 \oplus 2S_2$
$\Gamma_5(2)$	$\Gamma_1 \oplus \Gamma_2$	$Y_1 \oplus Y_2$	$X_1 \oplus X_2$	$2S_1 \oplus 2S_2$
$\blacktriangle\bar{\Gamma}_6(2)$	$\bar{\Gamma}_3 \oplus \bar{\Gamma}_4$	$\bar{Y}_3 \oplus \bar{Y}_4$ $\bar{Y}_3 \oplus \bar{Y}_4$	$\bar{X}_3 \oplus \bar{X}_3$ $\bar{X}_4 \oplus \bar{X}_4$	$2\bar{S}_3 \oplus 2\bar{S}_4$
$\blacktriangle\bar{\Gamma}_7(2)$	$\bar{\Gamma}_3 \oplus \bar{\Gamma}_4$	$\bar{Y}_3 \oplus \bar{Y}_4$ $\bar{Y}_3 \oplus \bar{Y}_4$	$\bar{X}_3 \oplus \bar{X}_3$ $\bar{X}_4 \oplus \bar{X}_4$	$2\bar{S}_3 \oplus 2\bar{S}_4$

(d) $G_0^A = C_{4v}$ and $G_0 = Pb11$ TABLE SXXVII: Without TR and $G_0^A = C_{4v}$, for the nonsymmorphic space groups G_0 listed above, there exists at least one irrep for which the low-energy moiré bands are necessarily symmetry-enforced semimetallic.

$G_0^A = C_{3v}$	$G_0 = Pb11$			
Γ	Γ_M	Y_M	X_M	S_M
$\blacktriangle\Gamma_1$	Γ_1	$Y_1 \oplus Y_2$	X_1	$S_1 \oplus S_2$
$\blacktriangle\Gamma_2$	Γ_2	$Y_1 \oplus Y_2$	X_2	$S_1 \oplus S_2$
Γ_3	$\Gamma_1 \oplus \Gamma_2$	$Y_1 \oplus Y_2$	X_1 X_2	$S_1 \oplus S_2$
$\blacktriangle\bar{\Gamma}_4$	$\bar{\Gamma}_3$	$\bar{Y}_3 \oplus \bar{Y}_4$	\bar{X}_3	$\bar{S}_3 \oplus \bar{S}_4$
$\blacktriangle\bar{\Gamma}_5$	$\bar{\Gamma}_4$	$\bar{Y}_3 \oplus \bar{Y}_4$	\bar{X}_4	$\bar{S}_3 \oplus \bar{S}_4$
$\bar{\Gamma}_6(2)$	$\bar{\Gamma}_3 \oplus \bar{\Gamma}_4$	$\bar{Y}_3 \oplus \bar{Y}_4$	\bar{X}_3 \bar{X}_4	$\bar{S}_3 \oplus \bar{S}_4$

TABLE SXXVIII: Without TR and $G_0^A = C_{3v}$, for the space group $Pb11$, there exists at least one irrep for which the low-energy moiré bands are necessarily symmetry-enforced semimetallic.

$G_0^A = C_{2v}$	$G_0 = Pba2$			
Γ	Γ_M	\mathbf{Y}_M	\mathbf{X}_M	\mathbf{S}_M
$\mathbf{\Delta}\Gamma_1$	Γ_1	$\mathbf{Y}_1(2)$	$\mathbf{X}_1(2)$	$\mathbf{S}_1 \oplus \mathbf{S}_2 \oplus \mathbf{S}_3 \oplus \mathbf{S}_4$
$\mathbf{\Delta}\Gamma_2$	Γ_1	$\mathbf{Y}_1(2)$	$\mathbf{X}_1(2)$	$\mathbf{S}_1 \oplus \mathbf{S}_2 \oplus \mathbf{S}_3 \oplus \mathbf{S}_4$
$\mathbf{\Delta}\Gamma_3$	Γ_2	$\mathbf{Y}_1(2)$	$\mathbf{X}_1(2)$	$\mathbf{S}_1 \oplus \mathbf{S}_2 \oplus \mathbf{S}_3 \oplus \mathbf{S}_4$
$\mathbf{\Delta}\Gamma_4$	Γ_2	$\mathbf{Y}_1(2)$	$\mathbf{X}_1(2)$	$\mathbf{S}_1 \oplus \mathbf{S}_2 \oplus \mathbf{S}_3 \oplus \mathbf{S}_4$
$\mathbf{\Delta}\bar{\Gamma}_5(2)$	$\bar{\Gamma}_5(2)$	$\bar{\mathbf{Y}}_2 \oplus \bar{\mathbf{Y}}_3$ $\bar{\mathbf{Y}}_4 \oplus \bar{\mathbf{Y}}_5$	$\bar{\mathbf{X}}_2 \oplus \bar{\mathbf{X}}_5$ $\bar{\mathbf{X}}_3 \oplus \bar{\mathbf{X}}_4$	$\bar{\mathbf{S}}_5(2) \oplus \bar{\mathbf{S}}_5(2)$

(a) $G_0^A = C_{2v}$ and $G_0 = Pba2$

$G_0^A = C_{2v}$	$G_0 = Pb11$			
Γ	Γ_M	\mathbf{Y}_M	\mathbf{X}_M	\mathbf{S}_M
$\mathbf{\Delta}\Gamma_1$	Γ_1	$\mathbf{Y}_1 \oplus \mathbf{Y}_2$	$\mathbf{X}_1 \oplus \mathbf{X}_2$	$2\mathbf{S}_1 \oplus 2\mathbf{S}_2$
$\mathbf{\Delta}\Gamma_2$	Γ_1	$\mathbf{Y}_1 \oplus \mathbf{Y}_2$	$\mathbf{X}_1 \oplus \mathbf{X}_2$	$2\mathbf{S}_1 \oplus 2\mathbf{S}_2$
$\mathbf{\Delta}\Gamma_3$	Γ_2	$\mathbf{Y}_1 \oplus \mathbf{Y}_2$	$\mathbf{X}_1 \oplus \mathbf{X}_2$	$2\mathbf{S}_1 \oplus 2\mathbf{S}_2$
$\mathbf{\Delta}\Gamma_4$	Γ_2	$\mathbf{Y}_1 \oplus \mathbf{Y}_2$	$\mathbf{X}_1 \oplus \mathbf{X}_2$	$2\mathbf{S}_1 \oplus 2\mathbf{S}_2$
$\mathbf{\Delta}\bar{\Gamma}_5(2)$	$\bar{\Gamma}_3 \oplus \bar{\Gamma}_4$	$\bar{\mathbf{Y}}_3 \oplus \bar{\mathbf{Y}}_4$	$\bar{\mathbf{X}}_3 \oplus \bar{\mathbf{X}}_3$ $\bar{\mathbf{X}}_4 \oplus \bar{\mathbf{X}}_4$	$2\bar{\mathbf{S}}_3 \oplus 2\bar{\mathbf{S}}_4$

(c) $G_0^A = C_{2v}$ and $G_0 = Pb11$

$G_0^A = C_{2v}$	$G_0 = Pma2$			
Γ	Γ_M	\mathbf{Y}_M	\mathbf{X}_M	\mathbf{S}_M
$\mathbf{\Delta}\Gamma_1$	Γ_1	$\mathbf{Y}_1 \oplus \mathbf{Y}_3$	$\mathbf{X}_1(2)$	$2\mathbf{S}_1(2)$
$\mathbf{\Delta}\Gamma_2$	Γ_1	$\mathbf{Y}_1 \oplus \mathbf{Y}_3$	$\mathbf{X}_1(2)$	$2\mathbf{S}_1(2)$
$\mathbf{\Delta}\Gamma_3$	Γ_2	$\mathbf{Y}_2 \oplus \mathbf{Y}_4$	$\mathbf{X}_1(2)$	$2\mathbf{S}_1(2)$
$\mathbf{\Delta}\Gamma_4$	Γ_2	$\mathbf{Y}_2 \oplus \mathbf{Y}_4$	$\mathbf{X}_1(2)$	$2\mathbf{S}_1(2)$
$\mathbf{\Delta}\bar{\Gamma}_5(2)$	$\bar{\Gamma}_5(2)$	$\bar{\mathbf{Y}}_5(2)$	$\bar{\mathbf{X}}_2 \oplus \bar{\mathbf{X}}_5$ $\bar{\mathbf{X}}_3 \oplus \bar{\mathbf{X}}_4$	$\bar{\mathbf{S}}_2 \oplus \bar{\mathbf{S}}_5 \oplus \bar{\mathbf{S}}_3 \oplus \bar{\mathbf{S}}_4$

(b) $G_0^A = C_{2v}$ and $G_0 = Pma2$ TABLE SXXIX: Without TR and $G_0^A = C_{2v}$, for the space groups G_0 listed above, there exists at least one irrep for which the low-energy moiré bands are necessarily symmetry-enforced semimetallic.

$G_0^A = C_{3v}$	$G_0 = Pb11$			
Γ	Γ_M	\mathbf{Y}_M	\mathbf{X}_M	\mathbf{S}_M
$\mathbf{\Delta}\Gamma_1$	Γ_1	$\mathbf{Y}_1 \oplus \mathbf{Y}_2$	\mathbf{X}_1	$\mathbf{S}_1 \oplus \mathbf{S}_2$
$\mathbf{\Delta}\Gamma_2$	Γ_2	$\mathbf{Y}_1 \oplus \mathbf{Y}_2$	\mathbf{X}_2	$\mathbf{S}_1 \oplus \mathbf{S}_2$
$\mathbf{\Delta}\bar{\Gamma}_3$	$\bar{\Gamma}_3$	$\bar{\mathbf{Y}}_3 \oplus \bar{\mathbf{Y}}_4$	$\bar{\mathbf{X}}_3$	$\bar{\mathbf{S}}_3 \oplus \bar{\mathbf{S}}_4$
$\mathbf{\Delta}\bar{\Gamma}_4$	$\bar{\Gamma}_4$	$\bar{\mathbf{Y}}_3 \oplus \bar{\mathbf{Y}}_4$	$\bar{\mathbf{X}}_4$	$\bar{\mathbf{S}}_3 \oplus \bar{\mathbf{S}}_4$

TABLE SXXX: Without TR and $G_0^A = C_{3s}$, for the space group $Pb11$, there exists at least one irrep for which the low-energy moiré bands are necessarily symmetry-enforced semimetallic.

C. TWO MODELS FOR SYMMETRY-ENFORCED MOIRÉ TOPOLOGY

In this section, we will present two toy models for the symmetry-enforced moiré topology, namely the moiré cubic Rashba model that preserves TR symmetry and a spinless two-band model that breaks TR symmetry.

1. Moiré cubic Rashba model

We consider a 2D electron model with the cubic Rashba spin-orbit coupling (SOC) [21, 22] and a moiré superlattice potential that belongs to the 2D plane group $P6mm$. The model Hamiltonian is written as

$$\begin{aligned}\hat{H} &= \hat{H}^A + \hat{H}_M, \\ \hat{H}^A &= \sum_{\mathbf{k}} \sum_{n,m=1,2} a_{n\mathbf{k}}^\dagger [H^A(\mathbf{k})]_{nm} a_{m\mathbf{k}}, \\ H^A(\mathbf{k}) &= \begin{pmatrix} \alpha k^2 + \beta k^4 & iR_3 k_+^3 \\ -iR_3 k_-^3 & \alpha k^2 + \beta k^4 \end{pmatrix}, \\ \hat{H}_M &= \sum_{n=1,2} \int d^2r a_{n\mathbf{r}}^\dagger H_M(\mathbf{r}) a_{n\mathbf{r}},\end{aligned}\tag{S.C1}$$

where $k_\pm = k_x \pm ik_y$, $a_{n\mathbf{r}} = \frac{1}{\sqrt{V}} \int d^2k a_{n\mathbf{k}} e^{i\mathbf{k}\cdot\mathbf{r}}$ with the integral over the momentum \mathbf{k} in the ABZ and the system area V . Here we include the k^4 terms in the diagonal part of H^A to ensure that the Hamiltonian is bounded.

We consider the second harmonics approximation for the moiré potential to show that the symmetry-enforced moiré topology does not rely on the form of the moiré potential. $H_M(\mathbf{r})$ can be expressed as $H_M(\mathbf{r}) = \sum_{\mathbf{g} \in \mathbf{G}_M^1} \Delta_1 e^{i\mathbf{g}\cdot\mathbf{r}} + \sum_{\mathbf{g} \in \mathbf{G}_M^2} \Delta_2 e^{i\mathbf{g}\cdot\mathbf{r}}$, where \mathbf{G}_M^1 consists of \mathbf{b}_1^M and its partners under six-fold rotation symmetries, while \mathbf{G}_M^2 consists of $\mathbf{b}_1^M + \mathbf{b}_2^M$ and its partners under six-fold rotation symmetries. $\mathbf{b}_1^M = 2\pi(1, -1/\sqrt{3})/a_M$ and $\mathbf{b}_2^M = 2\pi(1, 1/\sqrt{3})/a_M$ are primitive reciprocal lattice vectors, and a_M is the moiré lattice constant. We rewrite Eq.(S.C1) into the momentum space as

$$\hat{H}^A = \sum_{\mathbf{kg}} \sum_{n,m=1,2} a_{n\mathbf{kg}}^\dagger [H^A(\mathbf{k} + \mathbf{g})]_{nm} c_{m\mathbf{kg}}\tag{S.C2}$$

$$\hat{H}_M = \sum_{\mathbf{kgg}'} \sum_{n=1,2} \left(\Delta_1 \sum_{\mathbf{q} \in \mathbf{G}_M^1} \delta(\mathbf{g}' - \mathbf{g} - \mathbf{q}) + \Delta_2 \sum_{\mathbf{q} \in \mathbf{G}_M^2} \delta(\mathbf{g}' - \mathbf{g} - \mathbf{q}) \right) a_{n\mathbf{kg}}^\dagger a_{n\mathbf{kg}'},\tag{S.C3}$$

where $a_{n\mathbf{kg}} = c_{n,\mathbf{k}+\mathbf{g}}$ with \mathbf{k} to be the momentum in the first mBZ and $\mathbf{g}, \mathbf{g}' \in \mathbf{G}_M$ (\mathbf{G}_M is the group of moiré reciprocal lattice vectors). For the calculation in the main text, $\alpha = -2 \text{ nm}^2 \cdot \text{eV}$, $\beta = -6.1 \text{ nm}^4 \cdot \text{eV}$, $R_3 = 5 \text{ nm}^3 \cdot \text{eV}$ and $a_M = 11.46 \text{ nm}$. Both Δ_1 and Δ_2 are treated as tunable parameters. The calculations in the main text take the same parameters.

1. Perturbation theory at \mathbf{K} point

In the main text, we have demonstrated that the topmost two bands of the moiré cubic Rashba model must be topologically insulating when Δ_1 is negative. In this section, we will implement perturbation theory to support this claim.

We first consider the eigen-energy and eigen-wavefunctions of the Hamiltonian $H^A(\mathbf{k})$ in Eq.(S.C1) for zero Δ_1 and Δ_2 , which are given by

$$E_\pm(k) = \alpha k^2 + \beta k^4 \pm R_3 k^3.\tag{S.C4}$$

and

$$|\mathbf{k}, \pm\rangle = \frac{1}{\sqrt{2}} (\pm i e^{-3i\phi}, 1),\tag{S.C5}$$

where $\phi = \arctan\left(\frac{k_y}{k_x}\right)$ is the momentum angle.

Since $R_3 > 0$ in our numerical calculation, we focus on the eigen-state $|\mathbf{k}, +\rangle$ with a higher energy. Along the $\Gamma_M \mathbf{K}_M$ line, the M_y eigenvalue of $|\mathbf{k}, +\rangle$ is $-i$ and belongs to irrep $\Gamma \mathbf{K}_2$, according to the character table in Table SXIX. Therefore, as discussed in Sec.B1, $|\mathbf{K}_M(\phi=0), +\rangle$, $|C_{3z} \mathbf{K}_M(\phi=\frac{2\pi}{3}), +\rangle$, $|C_{3z}^{-1} \mathbf{K}_M(\phi=\frac{4\pi}{3}), +\rangle$ are folded into \mathbf{K}_M point in the mBZ and form the representation $\bar{\mathbf{K}}_4 \oplus \bar{\mathbf{K}}_6$ with zero moiré potential. The ϕ value for each \mathbf{k} point is indicated in parentheses. The character for $G_{\mathbf{K}_M} = C_{3v}$ is shown in Table. SXVIII(b). In addition, for perturbation theory, we also consider the momenta in the second momentum shell that are folded into \mathbf{K}_M , including three momenta $\mathbf{K}_{M,2}(\phi=\pi) = \mathbf{K}_M - \mathbf{b}_1^M - \mathbf{b}_2^M$, $C_{3z} \mathbf{K}_{M,2}(\phi=\frac{5\pi}{3})$ and $C_{3z}^{-1} \mathbf{K}_{M,2}(\phi=\frac{1\pi}{3})$, because those momenta can be connected to the orbit of \mathbf{K}_M by moiré potential. The momenta that are folded into \mathbf{K}_M in both the orbits of \mathbf{K}_M and $\mathbf{K}_{M,2}$ are depicted by the orange and green dots in Fig.S4, respectively.

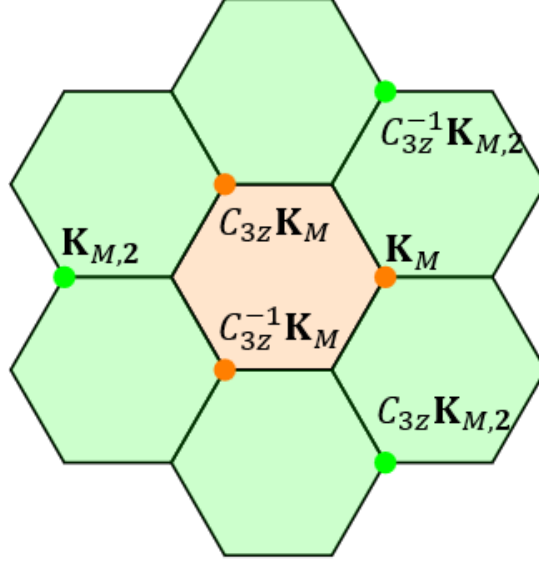


FIG. S4: Extended mBZ with high symmetry \mathbf{K}_M points. Orange and green points are orbits of \mathbf{K}_M and $\mathbf{K}_{M,2}$ respectively

We next treat \hat{H}_M as a perturbation, and project it into the eigen-state basis of $H^A(\mathbf{k})$ discussed above to understand the energy splitting between the $\bar{\mathbf{K}}_4$ state and the $\bar{\mathbf{K}}_6$ states. From the general wavefunction form in Eq.(S.C5), the eigenstate wavefunctions at these six momenta can be explicitly written as

$$|\mathbf{K}_M, +\rangle = |C_{3z} \mathbf{K}_M, +\rangle = |C_{3z}^{-1} \mathbf{K}_M, +\rangle = |\mathbf{K}_{M,2}, -\rangle = |C_{3z} \mathbf{K}_{M,2}, -\rangle = |C_{3z}^{-1} \mathbf{K}_{M,2}, -\rangle = \frac{1}{\sqrt{2}}(i, 1), \quad (\text{S.C6})$$

$$|\mathbf{K}_M, -\rangle = |C_{3z} \mathbf{K}_M, -\rangle = |C_{3z}^{-1} \mathbf{K}_M, -\rangle = |\mathbf{K}_{M,2}, +\rangle = |C_{3z} \mathbf{K}_{M,2}, +\rangle = |C_{3z}^{-1} \mathbf{K}_{M,2}, +\rangle = \frac{1}{\sqrt{2}}(-i, 1). \quad (\text{S.C7})$$

Next, we evaluate the matrix elements of \hat{H} in the basis formed by these 12 eigenstate wavefunctions. We find that

$$\langle \mathbf{K}_M, + | \hat{H} | \mathbf{K}_{M,2}, + \rangle = \langle \mathbf{K}_M, + | \hat{H}^A | \mathbf{K}_{M,2}, + \rangle + \langle \mathbf{K}_M, + | \hat{H}_M | \mathbf{K}_{M,2}, + \rangle = 0, \quad (\text{S.C8})$$

which indicates that $|\mathbf{K}_M, +\rangle$ and $|\mathbf{K}_{M,2}, +\rangle$ are decoupled. Similarly, we find that the matrix elements of \hat{H} between the six eigenstates in Eq. (S.C6) and those in Eq. (S.C7) vanish. Therefore, we only need to consider the basis formed by $|\mathbf{K}_M, +\rangle$, $|C_{3z} \mathbf{K}_M, +\rangle$, $|C_{3z}^{-1} \mathbf{K}_M, +\rangle$, $|\mathbf{K}_{M,2}, -\rangle$, $|C_{3z} \mathbf{K}_{M,2}, -\rangle$, and $|C_{3z}^{-1} \mathbf{K}_{M,2}, -\rangle$, in which the effective Hamiltonian takes the form:

$$H_{eff, \mathbf{K}_M} = \begin{pmatrix} E_0 & \Delta_1 & \Delta_1 & \Delta_2 & \Delta_1 & \Delta_1 \\ \Delta_1 & E_0 & \Delta_1 & \Delta_1 & \Delta_2 & \Delta_1 \\ \Delta_1 & \Delta_1 & E_0 & \Delta_1 & \Delta_1 & \Delta_2 \\ \Delta_2 & \Delta_1 & \Delta_1 & E_1 & 0 & 0 \\ \Delta_1 & \Delta_2 & \Delta_1 & 0 & E_1 & 0 \\ \Delta_1 & \Delta_1 & \Delta_2 & 0 & 0 & E_1 \end{pmatrix}, \quad (\text{S.C9})$$

where $E_0 = E_+(\mathbf{K}_M)$ and $E_1 = E_-(\mathbf{K}_{M,2})$ are given in Eq. (S.C4). We do the second order perturbation theory by

projecting out $|\mathbf{K}_{M,2}, -\rangle$, $|C_{3z}\mathbf{K}_{M,2}, -\rangle$, and $|C_{3z}^{-1}\mathbf{K}_{M,2}, -\rangle$ states,

$$H'_{eff,\mathbf{K}_M} = \begin{pmatrix} E_0 & \Delta_1 & \Delta_1 \\ \Delta_1 & E_0 & \Delta_1 \\ \Delta_1 & \Delta_1 & E_0 \end{pmatrix} + H_{eff,\mathbf{K}_M}^2, \quad (S.C10)$$

$$H_{eff,\mathbf{K}_M}^2 = \sum_{\alpha,\alpha'=1,2,3} \sum_{\beta,\beta'=4,5,6} \frac{\langle\alpha'|H_{eff,\mathbf{K}_M}|\beta'\rangle \langle\beta|H_{eff,\mathbf{K}_M}|\alpha\rangle}{E_0 - E_1},$$

where, $\alpha = 1, 2, 3$ index the basis $|\mathbf{K}_M, +\rangle$, $|C_{3z}\mathbf{K}_M, +\rangle$, and $|C_{3z}^{-1}\mathbf{K}_M, +\rangle$, $\beta = 4, 5, 6$ index the basis $|\mathbf{K}_{M,2}, -\rangle$, $|C_{3z}\mathbf{K}_{M,2}, -\rangle$, and $|C_{3z}^{-1}\mathbf{K}_{M,2}, -\rangle$. The energy eigenvalues of H'_{eff,\mathbf{K}_M} in Eq. (S.C10) are given by

$$E(\bar{\mathbf{K}}_6) = E_0 - \Delta_1 + \frac{\Delta_1^2}{E_0 - E_1} + \frac{\Delta_2^2}{E_0 - E_1} - \frac{2\Delta_1\Delta_2}{E_0 - E_1};$$

$$E(\bar{\mathbf{K}}_4) = E_0 + 2\Delta_1 + \frac{4\Delta_1^2}{E_0 - E_1} + \frac{\Delta_2^2}{E_0 - E_1} + \frac{4\Delta_1\Delta_2}{E_0 - E_1}, \quad (S.C11)$$

where $\bar{\mathbf{K}}_4$ and $\bar{\mathbf{K}}_6$ in the bracket represent the irrep for eigenstates. When $\Delta_1=0$, $E(\bar{\mathbf{K}}_6) = E(\bar{\mathbf{K}}_4)$, so that the band dispersion remains gapless at \mathbf{K}_M . For small Δ_1 and Δ_2 , the leading orders of $E(\bar{\mathbf{K}}_6)$ and $E(\bar{\mathbf{K}}_4)$ are $E_0 - \Delta_1$ and $E_0 + 2\Delta_1$ respectively. Therefore, the 2D irrep $\bar{\mathbf{K}}_6$ has a higher energy when $\Delta_1 < 0$ and the low-energy two moiré bands are topologically insulating. In contrast, if $\Delta_1 > 0$, $\bar{\mathbf{K}}_4$ has a higher energy, and the low-energy moiré bands are semi-metallic.

2. Linear Rashba model with TR

In this section, we consider the moiré linear Rashba model for comparison. The moiré linear Rashba model is given by

$$\hat{H} = \hat{H}_l^A + \hat{H}_M,$$

$$\hat{H}_l^A = \sum_{\mathbf{k}} \sum_{n,m=1,2} a_{n\mathbf{k}}^\dagger [H_l^A(\mathbf{k})]_{nm} a_{m\mathbf{k}},$$

$$H^A(\mathbf{k})_l = \begin{pmatrix} \alpha k^2 + \beta k^4 & iR_1 k_+ \\ -iR_1 k_- & \alpha k^2 + \beta k^4 \end{pmatrix},$$

$$\hat{H}_M = \sum_{n=1,2} \int d^2r a_{n\mathbf{r}}^\dagger H_M(\mathbf{r}) a_{n\mathbf{r}}. \quad (S.C12)$$

We consider the same form for $H_M(\mathbf{r})$ in Eq.(S.C12) as that in Eq.(S.C1) for the moiré cubic Rashba model. The values of α and β take the same value as those in the cubic Rashba model, and $R_1 = 0.4 \text{ nm}\cdot\text{eV}$. The direct band gap between the second top and the third top band as a function of Δ_1 and Δ_2 is shown in Fig. S5(a). When $\Delta_1 > 0$, the low-energy two bands are isolated trivial, while $\Delta_1 < 0$, the low-energy moiré bands connect to the third low-energy band. In contrast to the cubic Rashba model with moiré potential, the low-energy two bands in the linear Rashba model with moiré potential can be isolated trivial—the irreps of the isolated low-energy two bands are $(\bar{\Gamma}_9, \bar{\mathbf{K}}_6, \bar{\mathbf{M}}_5)$ in the trivial phase, which is the EBR $\bar{E}_1 \uparrow G(2)$ at the Wyckoff position 1a (the center of the honeycomb moiré unit cell).

The difference between linear and cubic Rashba model lies in the atomic irrep at Γ , Λ_Γ^A . Λ_Γ^A is $\bar{\Gamma}_9$ for the linear Rashba, while it is $\bar{\Gamma}_7$ for the cubic Rashba. This change in atomic Λ_Γ^A leads to the change of irrep for the low-energy moiré bands at Γ_M , leading to the difference in the symmetry-enforced moiré topology.

2. Spinless two-band model without TR

In Sec.B2, we show that the combination of $G_0^A = C_{4v}$ and $G_0 = P2$ can yield symmetry-enforced moiré topology for $\Lambda_\Gamma^A = \Gamma_5$. In this section, we will verify this statement in a spinless two-band model.

The 2×2 effective Hamiltonian has a general form:

$$H_2^A(\mathbf{k}) = \sum_{i=0}^3 F^i(\mathbf{k}) \sigma_i, \quad (S.C13)$$

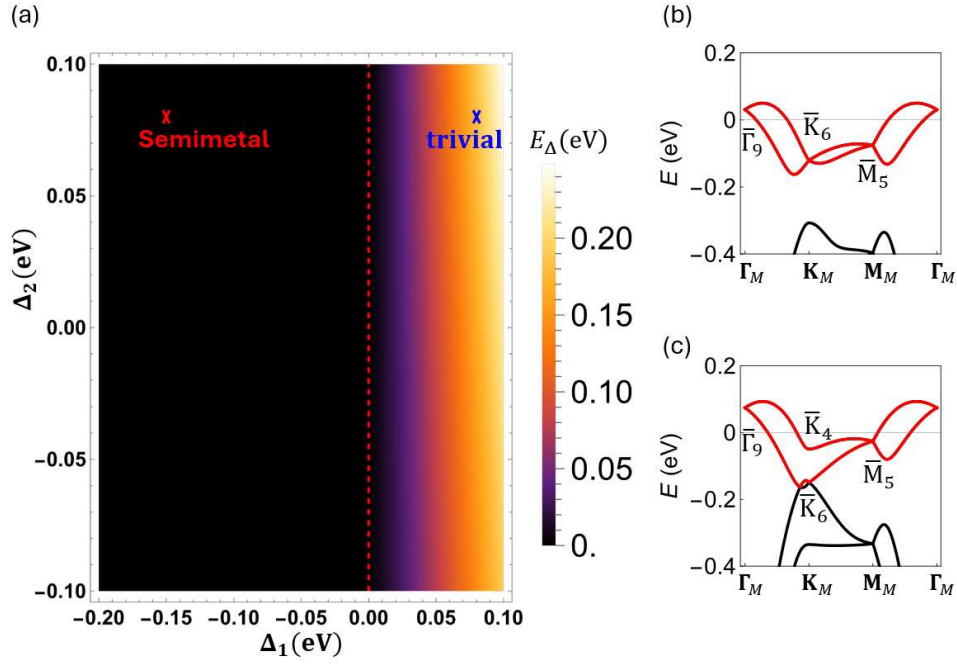


FIG. S5: (a) Phase diagram of the low-energy two bands. E_Δ denotes the direct band gap between the second and third low-energy bands. The red dashed lines separate the insulator region and semimetal regions. (b) The Band dispersions with parameters labeled by the blue cross in the (a). The topomost bands are trivial. (c) The Band dispersions with parameters labeled by the red cross in the (a). The topomost bands connect to the third low-energy band.

where the expansion coefficients $F^i(\mathbf{k})$ are the polynomials of \mathbf{k} , σ_0 and $\sigma_{1,2,3}$ are the 2×2 identity and Pauli matrices. The C_{4v} group is generated by the four-fold rotation along the out-of-plane direction C_{4z} and M_y . The σ matrices transform as

$$D(C_{4z})\sigma_i D^{-1}(C_{4z}) = \sum_j \mathcal{D}^{ji}(C_{4z})\sigma_j; \quad D(M_y)\sigma_i D^{-1}(M_y) = \sum_j \mathcal{D}^{ji}(M_y)\sigma_j, \quad (\text{S.C14})$$

where $D(C_{4z})$ and $D(M_y)$ are representation matrices of C_{4z} and M_y , respectively, given by

$$D(C_{4z}) = i\sigma_3; \quad D(M_y) = \sigma_1 \quad (\text{S.C15})$$

Using these representation matrices of C_{4z} and M_y , we can classify the σ matrices into the irrep table of the C_{4v} group, as shown in Table. SXXXI.

In the Table. SXXXI, the first column shows the irrep, the second and third columns show the construction of representations using σ matrices and k -polynomials up to the k^4 order, respectively. The + (-) sign in parentheses after the representation matrices and k -polynomials shows their even (odd) parity under TR. According to Table SXXXI, we need to keep the fourth-order term $(k_x k_y (k_x^2 - k_y^2))\sigma_3$ to break TR symmetry, and can write down an effective model,

$$H_2^A(\mathbf{k}) = (-k^2 - Ak^4)\sigma_0 + B(k_x k_y (k_x^2 - k_y^2))\sigma_3 + (k_x^2 - k_y^2)\sigma_1 - (2k_x k_y)\sigma_2. \quad (\text{S.C16})$$

The $-Ak^4$ term in Eq.(S.C16), where $A > 0$, plays a similar role to βk^4 in Eq.(S.C1), ensuring boundedness of $H_2(\mathbf{k})$. To obtain $G_0 = P2$, the moiré potential term needs to keep C_2 symmetry and break other symmetries. Similar to the previous sections, the moiré potential is kept up to the second harmonics and written as

$$H_{M,2}(\mathbf{r}) = \frac{\Delta_{1,1}}{2} \cos(\mathbf{b}_1^M \cdot \mathbf{r}) + \frac{\Delta_{1,2}}{2} \cos(C_{3z} \mathbf{b}_1^M \cdot \mathbf{r}) + \frac{\Delta_{1,3}}{2} \cos(C_{3z}^{-1} \mathbf{b}_1^M \cdot \mathbf{r}) \\ + \frac{\Delta_{2,1}}{2} \cos((\mathbf{b}_1^M + \mathbf{b}_2^M) \cdot \mathbf{r}) + \frac{\Delta_{2,2}}{2} \cos(C_{3z}(\mathbf{b}_1^M + \mathbf{b}_2^M) \cdot \mathbf{r}) + \frac{\Delta_{2,3}}{2} \cos(C_{3z}^{-1}(\mathbf{b}_1^M + \mathbf{b}_2^M) \cdot \mathbf{r}). \quad (\text{S.C17})$$

The first three terms correspond to the first harmonic components, while the remaining three terms are for the second harmonic components. All moiré potential parameters $\Delta_{i,j}$ are independent. It should be noted that the form of

moiré potential is not unique, and the example provided is merely illustrative. The Hamiltonian with moiré potential can be rewritten in the second quantization form,

$$\begin{aligned}\hat{H}_2 &= \hat{H}_2^A + \hat{H}_{M,2} = \sum_{\mathbf{k}\mathbf{g}\mathbf{g}'} \sum_{n,m=1,2} c_{n\mathbf{k}\mathbf{g}'}^\dagger [H_2(\mathbf{k})]_{n\mathbf{g}',m\mathbf{g}} c_{m\mathbf{k}\mathbf{g}}, \\ \hat{H}_2^A &= \sum_{\mathbf{k}} \sum_{n,m=1,2} a_{n\mathbf{k}}^\dagger [H_2^A(\mathbf{k})]_{nm} a_{m\mathbf{k}}, \\ \hat{H}_{M,2} &= \sum_{n=1,2} \int d^2r a_{n\mathbf{r}}^\dagger H_{M,2}(\mathbf{r}) a_{n\mathbf{r}}.\end{aligned}\tag{S.C18}$$

C_{3v}	σ	k
$\Gamma_1(A_1)$	$\sigma_0(+)$	$k_x^2 + k_y^2(+), (k_x^4 + k_y^4)(+), k_x^2 k_y^2(+), C(+)$
$\Gamma_2(B_1)$	$\sigma_1(+)$	$k_x^2 - k_y^2(+), k_x^4 - k_y^4(+)$
$\Gamma_3(B_2)$	$\sigma_2(+)$	$k_x k_y(+)$
$\Gamma_3(A_2)$	$\sigma_3(-)$	$k_x k_y (k_x^2 - k_y^2)(+)$

TABLE SXXXI: The classification of the representation matrices and k -polynomials for the C_{4v} group. The + or - in the bracket indicates how the matrices transform under TR (even or odd). The symbol C in the column of k -polynomial is for a constant.

The symmetry group of \hat{H}_2 in Eq.(S.C18) is described by the space group $P2$, with the little groups at high symmetry momenta $\Gamma_M, \mathbf{Y}_M, \mathbf{A}_M$, and \mathbf{B}_M to be the point groups C_2 . In Sec. B2, we have shown that the irreps of the two low-energy bands are always $(2\Gamma_2, \mathbf{Y}_1 \oplus \mathbf{Y}_2, \mathbf{A}_1 \oplus \mathbf{A}_2, \mathbf{B}_1 \oplus \mathbf{B}_2)$, and that these two bands carry a total odd Chern number in the weak moiré potential limit, regardless of the specific form of the potential. To verify this, we choose $A = 8 \text{ nm}^4 \cdot \text{eV}$, $B = 32 \text{ nm}^4 \cdot \text{eV}$, $a_0^M = 11.46 \text{ nm}$ and set the moiré potential strengths as tunable parameter. Here, we choose the parameters as $\Delta_{1,1} = -4\Delta_{1,0}$, $\Delta_{1,2} = \Delta_{1,0}$, $\Delta_{1,3} = 3\Delta_{1,0}$, $\Delta_{2,1} = 3\Delta_{2,0}$, $\Delta_{2,2} = \Delta_{2,0}$, and $\Delta_{2,3} = -4\Delta_{2,0}$, such that the moiré potential preserves only C_{2z} symmetry. This choice is made for illustrative purposes. The direct band gap between the second and third topmost bands as a function of $\Delta_{1,0}$ and $\Delta_{2,0}$ is shown in Fig. S6(a). The red dashed lines separate the semimetallic phase, where the low-energy two bands connect to other bands at generic (non-high-symmetry) momenta, from the Chern insulator phase, where the low-energy two bands carry a total Chern number of -1 . Figure S6(b) and (c) show the band dispersions for $\Delta_{1,0} = 10 \text{ meV}$ and $\Delta_{1,0} = -10 \text{ meV}$, respectively, with $\Delta_{2,0} = 0 \text{ meV}$ in both cases. We can see that the top two bands have a total Chern number -1 for both parameters.

We can go one step further, and determine the irreps and Chern number of each individual band among the low-energy two bands. The two-fold rotation C_{2z} acts on fermion operators as

$$C_{2z} a_{n,\mathbf{k},\mathbf{g}}^\dagger C_{2z}^{-1} = \sum_{m\mathbf{g}'} a_{m,C_{2z}\mathbf{k},\mathbf{g}'}^\dagger D_{m\mathbf{g}',n\mathbf{g}}(C_{2z}).\tag{S.C19}$$

with

$$D_{m\mathbf{g}',n\mathbf{g}}(C_{2z}) = -\delta_{\mathbf{g}',C_{2z}\mathbf{g}} \delta_{m,n}.\tag{S.C20}$$

Under C_{2z} , $H_2(\mathbf{k})$ is invariant

$$D(C_{2z}) H_2(\mathbf{k}) D^{-1}(C_{2z}) = H_2(C_{2z}\mathbf{k}).\tag{S.C21}$$

The irreps at all high symmetry momenta can be determined from the eigenvalues of C_{2z} . In Fig.S6(b), the highest-energy band has the irreps $(\Gamma_2, \mathbf{Y}_1, \mathbf{A}_2, \mathbf{B}_2)$ and a Chern number $C = -1$ while the second highest energy band has the irreps $(\Gamma_2, \mathbf{Y}_2, \mathbf{A}_1, \mathbf{B}_1)$ and a Chern number $C = 0$. In Fig.S6(c), the top band has the irreps $(\Gamma_2, \mathbf{Y}_2, \mathbf{A}_1, \mathbf{B}_1)$ and a Chern number $C = -2$. Meanwhile, the second top band has the irreps $(\Gamma_2, \mathbf{Y}_1, \mathbf{A}_2, \mathbf{B}_2)$ and a Chern number $C = 1$.

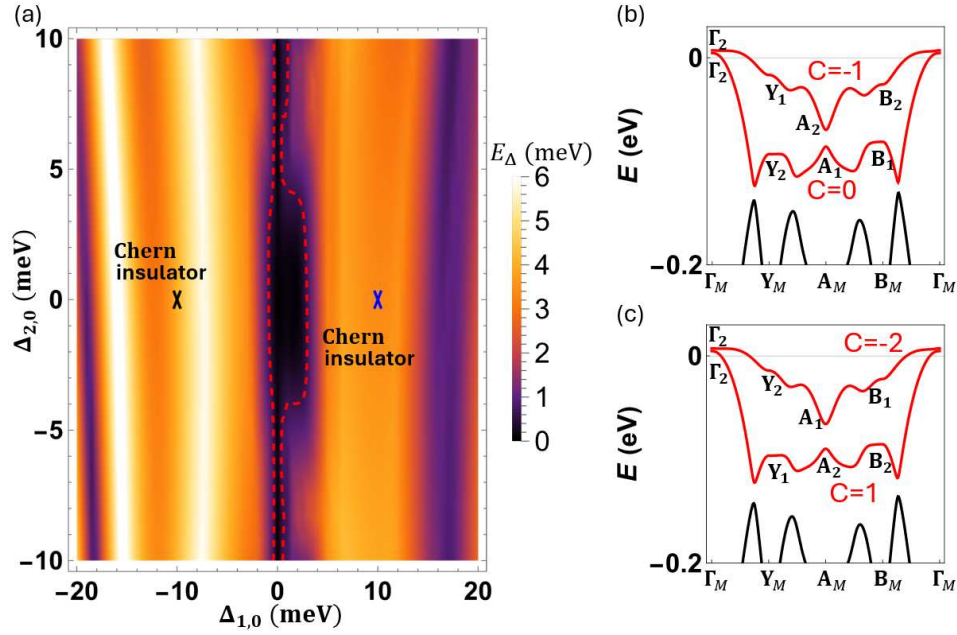


FIG. S6: (a) Phase diagram of the low-energy two bands. E_{Δ} denotes the direct band gap between the second and third low-energy bands. The red dashed lines separate the Chern insulator region and semimetal regions. (b) The Band dispersions with parameters labeled by the blue cross in (a). (c) The Band dispersions with parameters labeled by the black cross in (a).

D. ESTIMATION OF k^3 BAND SPLITTING

In the cubic Rashba model, the atomic band splitting is given by the k^3 term. One may question whether the weak moiré condition is unrealistic given that the atomic band splitting comes from a high-order k^3 term. In this section, we show that the weak moiré condition can still be realistic even if the atomic band splitting is given by a high-order k^3 term. For this purpose, we will look at twisted bilayer MoTe_2 . In monolayer MoTe_2 the little group at Γ is C_{3V} [23]. The irrep of the second top pair of valence bands is $\bar{\Gamma}_4\bar{\Gamma}_5$ ($J_z = \pm\frac{3}{2}$), as shown in Fig. S7(a). The low-energy $\bar{\Gamma}_4\bar{\Gamma}_5$ doublet at Γ also has k^3 band splitting term to the leading order. We will estimate the k^3 order atomic band splitting.

Figure S7(b) shows a zoom-in of the band dispersion. For twist angles between 3.5° and 4.0° , the \mathbf{M}_M point lies within the dashed region, where the atomic band splitting at the edge of mBZ is approximately 7–11 meV. In contrast, the Γ -valley moiré band gap is about 3 meV [24]. Therefore, the moiré potential strength, measured by the moiré band gap, is smaller than the atomic band splitting at the edge of mBZ, naturally satisfying the weak moiré condition.

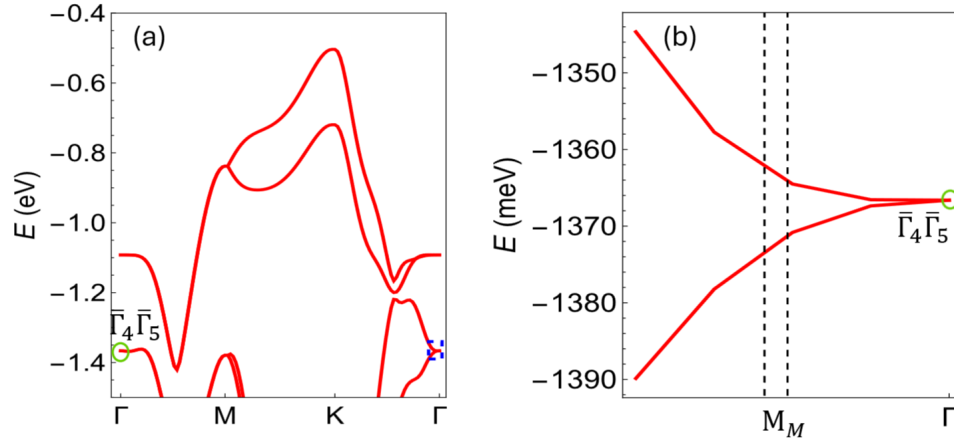


FIG. S7: (a) DFT calculation of monolayer MoTe₂ (b) Zoom-in of the band dispersion in the blue box in (a). When the twist angle of twisted bilayer MoTe₂ varies from 3.5° to 4.5°, the \mathbf{M}_M point lies within the dashed region. Atomic band splitting at \mathbf{M}_M is approximately 7–11 meV for the twist angle range.

-
- ¹ Barry Bradlyn, Luis Elcoro, Jennifer Cano, Maia G Vergniory, Zhijun Wang, Claudia Felser, Mois I Aroyo, and B Andrei Bernevig. Topological quantum chemistry. *Nature*, 547(7663):298–305, 2017.
 - ² Jennifer Cano and Barry Bradlyn. Band representations and topological quantum chemistry. *Annual Review of Condensed Matter Physics*, 12(1):225–246, 2021.
 - ³ Luis Elcoro, Benjamin J Wieder, Zhida Song, Yuanfeng Xu, Barry Bradlyn, and B Andrei Bernevig. Magnetic topological quantum chemistry. *Nature communications*, 12(1):5965, 2021.
 - ⁴ Liang Fu and Charles L Kane. Topological insulators with inversion symmetry. *Physical Review B—Condensed Matter and Materials Physics*, 76(4):045302, 2007.
 - ⁵ Chen Fang, Matthew J Gilbert, and B Andrei Bernevig. Bulk topological invariants in noninteracting point group symmetric insulators. *Physical Review B—Condensed Matter and Materials Physics*, 86(11):115112, 2012.
 - ⁶ Jorrit Kruthoff, Jan De Boer, Jasper Van Wezel, Charles L Kane, and Robert-Jan Slager. Topological classification of crystalline insulators through band structure combinatorics. *Physical Review X*, 7(4):041069, 2017.
 - ⁷ Hoi Chun Po, Ashvin Vishwanath, and Haruki Watanabe. Symmetry-based indicators of band topology in the 230 space groups. *Nature communications*, 8(1):50, 2017.
 - ⁸ Hoi Chun Po. Symmetry indicators of band topology. *Journal of Physics: Condensed Matter*, 32(26):263001, 2020.
 - ⁹ Patrick M Lenggenger, Xiaoxiong Liu, Titus Neupert, and Tomáš Bzdušek. Universal higher-order bulk-boundary correspondence of triple nodal points. *Physical Review B*, 106(8):085129, 2022.
 - ¹⁰ Jingheng Fu, Mikael Kuisma, Ask Hjorth Larsen, Kohei Shinohara, Atsushi Togo, and Kristian S Thygesen. Symmetry classification of 2d materials: layer groups versus space groups. *2D Materials*, 11(3):035009, 2024.
 - ¹¹ Mildred S Dresselhaus, Gene Dresselhaus, and Ado Jorio. *Group theory: application to the physics of condensed matter*. Springer Science & Business Media, 2007.
 - ¹² Robert A Evarestov and Vyacheslav P Smirnov. *Site symmetry in crystals: theory and applications*, volume 108. Springer Science & Business Media, 2012.
 - ¹³ Mois I Aroyo, Juan Manuel Perez-Mato, Danel Orobengoa, EMRE Tasci, Gemma de la Flor, and Asel Kirov. Crystallography online: Bilbao crystallographic server. *Bulg. Chem. Commun*, 43(2):183–197, 2011.
 - ¹⁴ Mois I Aroyo, Asen Kirov, Cesar Capillas, JM Perez-Mato, and Hans Wondratschek. Bilbao crystallographic server. ii. representations of crystallographic point groups and space groups. *Acta Crystallographica Section A: Foundations of Crystallography*, 62(2):115–128, 2006.
 - ¹⁵ Mois Ilia Aroyo, Juan Manuel Perez-Mato, Cesar Capillas, Eli Kroumova, Svetoslav Ivantchev, Gotzon Madariaga, Asen Kirov, and Hans Wondratschek. Bilbao crystallographic server: I. databases and crystallographic computing programs. *Zeitschrift für Kristallographie-Crystalline Materials*, 221(1):15–27, 2006.
 - ¹⁶ L Michel and J Zak. Connectivity of energy bands in crystals. *Physical Review B*, 59(9):5998, 1999.
 - ¹⁷ L Michel and J Zak. Elementary energy bands in crystals are connected. *Physics Reports*, 341(1-6):377–395, 2001.
 - ¹⁸ Haruki Watanabe, Hoi Chun Po, Ashvin Vishwanath, and Michael Zaletel. Filling constraints for spin-orbit coupled insulators in symmorphic and nonsymmorphic crystals. *Proceedings of the National Academy of Sciences*, 112(47):14551–14556, 2015.
 - ¹⁹ MG Vergniory, L Elcoro, Zhijun Wang, Jennifer Cano, C Felser, MI Aroyo, B Andrei Bernevig, and Barry Bradlyn. Graph theory data for topological quantum chemistry. *Physical Review E*, 96(2):023310, 2017.
 - ²⁰ Haruki Watanabe, Hoi Chun Po, Michael P Zaletel, and Ashvin Vishwanath. Filling-enforced gaplessness in band structures of the 230 space groups. *Physical review letters*, 117(9):096404, 2016.
 - ²¹ Hiroyuki Nakamura, Takaaki Koga, and Tsuyoshi Kimura. Experimental evidence of cubic rashba effect in an inversion-symmetric oxide. *Physical Review Letters*, 108(20):206601, 2012.
 - ²² Roland Winkler. Spin-orbit coupling effects in two-dimensional electron and hole systems. (*No Title*), 2003.
 - ²³ Aamir Shafique and Young-Han Shin. Strain engineering of phonon thermal transport properties in monolayer 2h-mote2. *Physical Chemistry Chemical Physics*, 19(47):32072–32078, 2017.
 - ²⁴ Yujin Jia, Jiabin Yu, Jiakuan Liu, Jonah Herzog-Arbeitman, Ziyue Qi, Hanqi Pi, Nicolas Regnault, Hongming Weng, B Andrei Bernevig, and Quansheng Wu. Moiré fractional chern insulators. i. first-principles calculations and continuum models of twisted bilayer mote 2. *Physical Review B*, 109(20):205121, 2024.